THE INFLUENCE OF SOIL SUCTION ON THE COLLAPSE SETTLEMENT OF DIFFERENT SOILS IN SOUTH AFRICA

by

GE Brink

2011

THE INFLUENCE OF SOIL SUCTION ON THE COLLAPSE SETTLEMENT OF DIFFERENT SOILS IN SOUTH AFRICA

by

GE Brink

Submitted in fulfilment of the requirements for the degree

Magister Scientiae in Engineering and Environmental Geology

in the Faculty of Natural and Agricultural Sciences

University of Pretoria
Pretoria

2011

ABSTRACT

Partially saturated soils are often dense with a high bearing capacity and will subsequently only suffer small amounts of compression under normal foundation loads. However, when wetted under load many such soils undergo a marked and sudden increase in settlement, the phenomenon which is known as collapse settlement.

Prodigious development have taken place on potentially collapsible soils in South Africa, especially on the Berea Red Sands, the granitic soils of the Highveld, residual Basement Granite soils in the Lowveld (markedly the Witrivier, Tzaneen and Bushbuck Ridge areas) as well as recently on the Kalahari Aeolian Sands in the Lephalale area.

Even though levels of development have been intense in such areas, the subject of collapsible soils has not received much attention in South Africa in recent years, with very little being published on the subject since Schwartz's state of the art paper on collapsible soils in 1985.

Soil suction can be considered one of the most important parameters describing the stress state at different moisture conditions in an unsaturated soil. Generally, porous materials have the ability to attract and retain water. This ability is described as suction, and can thus be seen as the attraction the soil exerts on the moisture.

The collapse process in partly saturated soils is best considered in terms of two separate components of effective stress; the applied stress and the suction. During this research the collapse phenomenon in South African soils was investigated by focussing on the collapse mechanism of dry or partially saturated collapsible soils during the incremental increase in soil moisture content under constant load. Samples were collected from both typically collapsible residual and collapsible transported soils in an effort to relate the collapse behaviour of the material to its geological origin. The change in suction pressure with change in moisture content for the same materials was monitored and related back to the collapse process. Subsequently the influence of the applied stress and suction pressures on the collapse behaviour could be compared for each material.

THE INFLUENCE OF SOIL SUCTION ON THE COLLAPSE SETTLEMENT OF DIFFERENT SOILS IN SOUTH AFRICA

Page

TABLE OF CONTENTS

LIST OF TABLES

LIST OF FIGURES

THE INFLUENCE OF SOIL SUCTION ON THE COLLAPSE SETTLEMENT OF DIFFERENT SOILS IN SOUTH AFRICA

1. INTRODUCTION

Partially saturated soils are often dense with a high bearing capacity and will subsequently only suffer small amounts of compression under normal foundation loads. However, when wetted under load many such soils undergo a marked and sudden increase in settlement, the phenomenon which is known as collapse settlement (Barden *et al.*, 1973). It is important to understand that in this context and throughout this dissertation the term "dense" refers to the **overall consistency of a non-cohesive soil** (i.e. the resistance of the material to penetration of the sharp end of the geological pick), and **not** to the particle arrangement of the material.

The collapse mechanism in partly saturated soils is best considered in terms of two separate components of effective stress, namely the applied stress and the soil suction which develop intergranular stress through different mechanisms. The applied stress develops shear stresses and thus potential instability at intergranular contacts, while suction is strictly a normal stress and hence increases the stability at intergranular contacts (Barden *et al.*, 1973).

Different types of collapsible soils are identified which collapse under different conditions. According to Fredlund and Gan (1995) these can broadly be divided into two groups; namely wet collapsible soils and dry collapsible soils. Wet collapsible soils, such as quick clays, can exist in a stable condition under high *in-situ* water content. Naturally occurring dry collapsible soils may be cemented or uncemented. This focus of this dissertation is restricted to dry, largely uncemented collapsible soils that commonly occur in southern Africa.

The triggering mechanism in an uncemented, dry-collapsible soil is largely attributed to the loss of strength due to a reduction in matrix suction with an increase in moisture content. This means that an uncemented, dry collapsible soil collapses when there is a change in the stress state of the soil as it changes from an unsaturated condition towards a saturated condition (Fredlund and Gan, 1995).

Dry collapsible soils can further be subdivided into transported and residual soils. The distribution of transported collapsible soils is virtually unrestricted, whereas the distribution of residual collapsible soils largely correlates with those areas where past wet climates caused leaching of the soil and are presently located within areas of annual water surplus.

Much development has taken place on potentially collapsible soils in South Africa, especially on the Berea Red Sands, the granitic soils of the Highveld (Rust *et al.*, 2010), residual Basement Granite soils in the Lowveld (markedly the Witrivier, Tzaneen and Bushbuck Ridge areas) as well as recently on the Kalahari Aeolian Sands in the Lephalale area.

Even though levels of development have been intense in such areas, the subject of collapsible soils has not received much attention in South Africa in recent years, with very little being published on the subject since Schwartz's state of the art paper on collapsible soils in 1985 (Schwartz, 1985).

2. AIM

Schwartz (1985) points out that the degree of saturation is a vital parameter in assessing the collapse potential of a material and that a critical degree of saturation exists above which collapse will not occur.

The aim of this research is to investigate the collapse phenomenon in South African soils by focussing on the collapse mechanism of dry or partially saturated collapsible soils during the incremental increase in soil moisture content under constant load and subsequently evaluate the influence of the soil moisture content on the collapse process.

In the process the effect of the increase in soil moisture on the soil suction in the collapsible materials is investigated in an effort to determine the relationship between the change in soil suction and the settlement behaviour of the test materials. This can then be related back to the effective stress state of the material in an effort to determine the relationship between a change in the effective stress of the material and its collapse behaviour.

3. DEFINITIONS AND PROPERTIES OF COLLAPSIBLE SOILS

3.1 General

Numerous definitions describing potentially collapsible soils or the collapse phenomenon exist. Rogers (1995) discusses a number of definitions appearing randomly in the literature, which is included below.

"...a soil that undergoes an appreciable amount of volume change upon wetting, load application or a combination of both" (Sultan, 1969).

"...any unsaturated soil that goes through a radical rearrangement of particles and a great loss of volume upon wetting with or without additional loading" (Dudley, 1970).

"...additional settlement...due to the wetting of a partially saturated soil, normally without any increase in applied pressure" (Jennings and Knight, 1975).

"...settlement in partially saturated soil due to an increase in the degree of consolidation" (Booth, 1977).

"...a state of underconsolidation related to apparent cohesive strength of unsaturated soils" (Handy, 1973)

Schwartz (1985) defines a collapsible soil as "...a soil which can withstand relatively large imposed stresses with small settlements at a low *in situ* moisture content but will exhibit a decrease in volume and associated settlement with no increase in the applied stress if wetting up occurs."

Barden *et.al* (1973) state that for appreciable collapse to occur, the material should have an open, potentially unstable partly saturated structure; a high enough value of applied stress to develop

a metastable condition and a high enough value of soil suction to stabilize intergranular contacts and whose reduction on wetting will lead to collapse.

Thus, in its simplest form the collapse phenomenon may be expressed as the existence of certain conditions in the subsoil structures that may exist where structures have stood satisfactorily for some time and then suddenly experience additional settlement (Jennings and Knight, 1975).

It is clear from these and other definitions that partially saturated soils are the predominant source of collapsible soils, but that no clear-cut definition for collapsible soils exists. Rogers (1995) therefore argues that a better approach might be to list the features most commonly associated with collapsible soils. These include:

- An open soil structure;
- A high void ratio;
- A low dry density;
- A high porosity;
- Geologically young or recently altered deposit;
- High sensitivity and
- Low interparticle bond strength.

The first four features can be considered to be interrelated and provides the material with the ability to structurally rearrange itself, for volume reduction and fluid transmission. The requirement for the material to be geologically young or recently altered derives from the likelihood and probability that collapse of the material would have already occurred at some point in the material's geological history.

The requirement for the material to have a high sensitivity is to provide a link with the undisturbed and remoulded strength of the material relating to the time before the collapse trigger mechanism, and thus allows for quick clays to be included in the broad term of "collapsible soil". The final feature of low interparticle bond strength refers to particles that exhibit weak, short-range bonds so as to exclude classic clay soils from being included as a typical collapsible soil (Rogers, 1995).

For the purpose of this dissertation the abovementioned typical features are adequate descriptors of the term "collapsible soil" and were used as the identification criteria during the process of collecting representative samples for the laboratory testing process. It should be emphasised once again that focus in this dissertation is only placed on the behaviour of *dry* collapsible soils.

3.2 Recognition of collapse potential using southern African criteria

According to Brink *et. al.* (1982) and Schwartz and Yates (1980), the typical dry densities that could be expected for collapsible soils in South Africa range from 900 to 1 600 kg/m^3, even though collapse in materials with dry densities outside this range cannot be completely excluded (Rust *et.al*, 2005).

Brink (1985) proposes that a relationship exists between collapse potential and dry density for different materials which can be represented by the following equations and correlation coefficients:

Aeolian Sands (correlation coefficient = 0.73):

$$CP = \frac{1672 - \Upsilon d}{22} \quad (1)$$

Mixed origin (correlation coefficient = 0.77):

$$CP = \frac{1590 - \Upsilon d}{18.9} \quad (2)$$

From these equations it is evident that aeolian sands with dry densities greater than 1672 kg/m^3 and mixed soils with dry densities greater than 1590 kg/m^3 are generally not regarded as collapsible.

3.3 Collapse mechanism

For collapse to take place, the following conditions must be met (Schwartz, 1985):

- The soil must have a collapsible fabric (as discussed in 3.1 before);
- A condition of partial saturation is required (collapse will not occur in soils below the water table, see Section 3.5);
- There must be an increase in moisture content, which can be considered as the triggering mechanism for collapse to occur;
- The soil needs to be subjected to an applied pressure greater than the overburden pressure before collapse will take place.

Once the conditions for collapse to occur have been attained, the collapse process can be divided into three phases, with all three phases taking place simultaneously (Klukanova and Frankovska, 1995):

- Phase I: This phase represents the initial stage of destruction of the original microstructure due to an increase in moisture and applied stress. Clay films, bridges and buttresses start to break, aggregates and micro-aggregates disintegrate and the intensity of the dissolution of carbonates and their migration in the soil increases.

- Phase II: Disintegration of the microstructure continues, the content of carbonates decreases, other fabric elements compress and the total volume of the soil decreases.

- Phase III: At this point a new microstructure develops after collapsing, basic structural units disintegrate, clay particle coatings are destroyed or removed completely and clay particles are aggregated.

Figure 1 below depicts the collapse mechanism for collapsing sand effectively illustrating the process as discussed above.

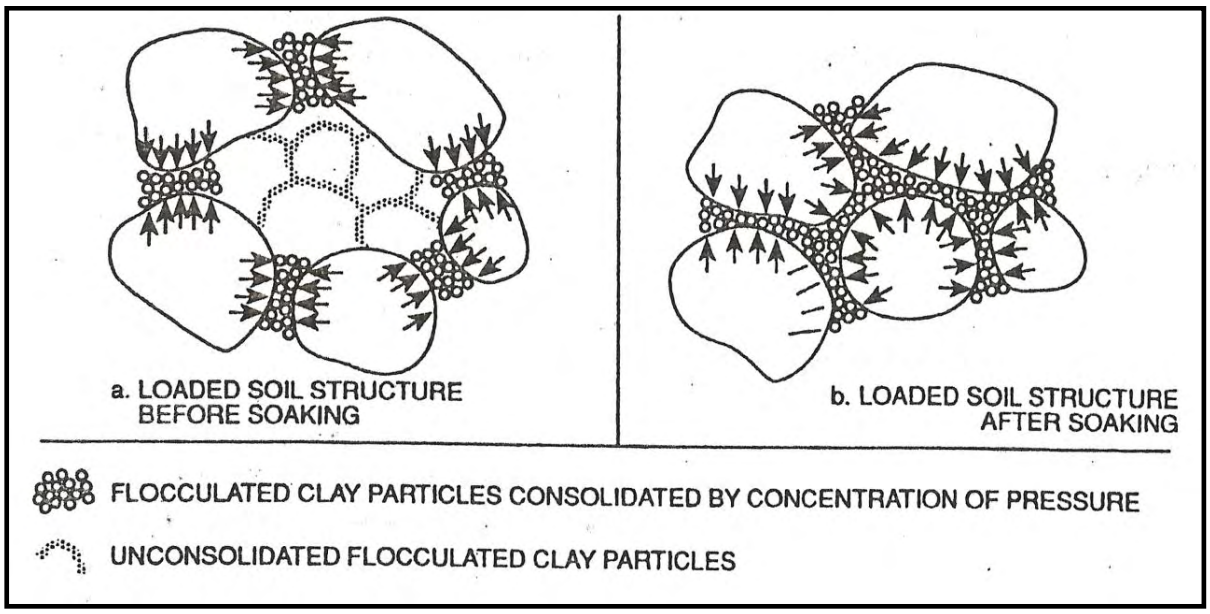

Figure 1: Mechanism of collapse for collapsing sand (Jennings and Knight, 1975 in Rogers, 1995)

3.4 Distribution of collapsible soils in South Africa

According to Schwartz (1985), it was originally assumed that the collapse phenomenon is largely restricted to loose aeolian deposits, with the result that most of the research and work dealt almost exclusively with such deposits. However, the collapse phenomenon has since been identified in a number of different transported soils as well as residual soils.

The vast majority of occurrences of collapsing soils, either transported or residual, are largely restricted to environments of climatic N-values (Weinert, 1980) between 2 and 5 (See Figure 2 below), with very few occurrences of collapse been observed where $N < 2$ and $N > 5$. However, Weinert (1980) attributes this largely to the fact that rates of development have been substantially higher in areas where $2 < N < 5$ than in other areas, and therefore more cases of collapse settlement have been reported.

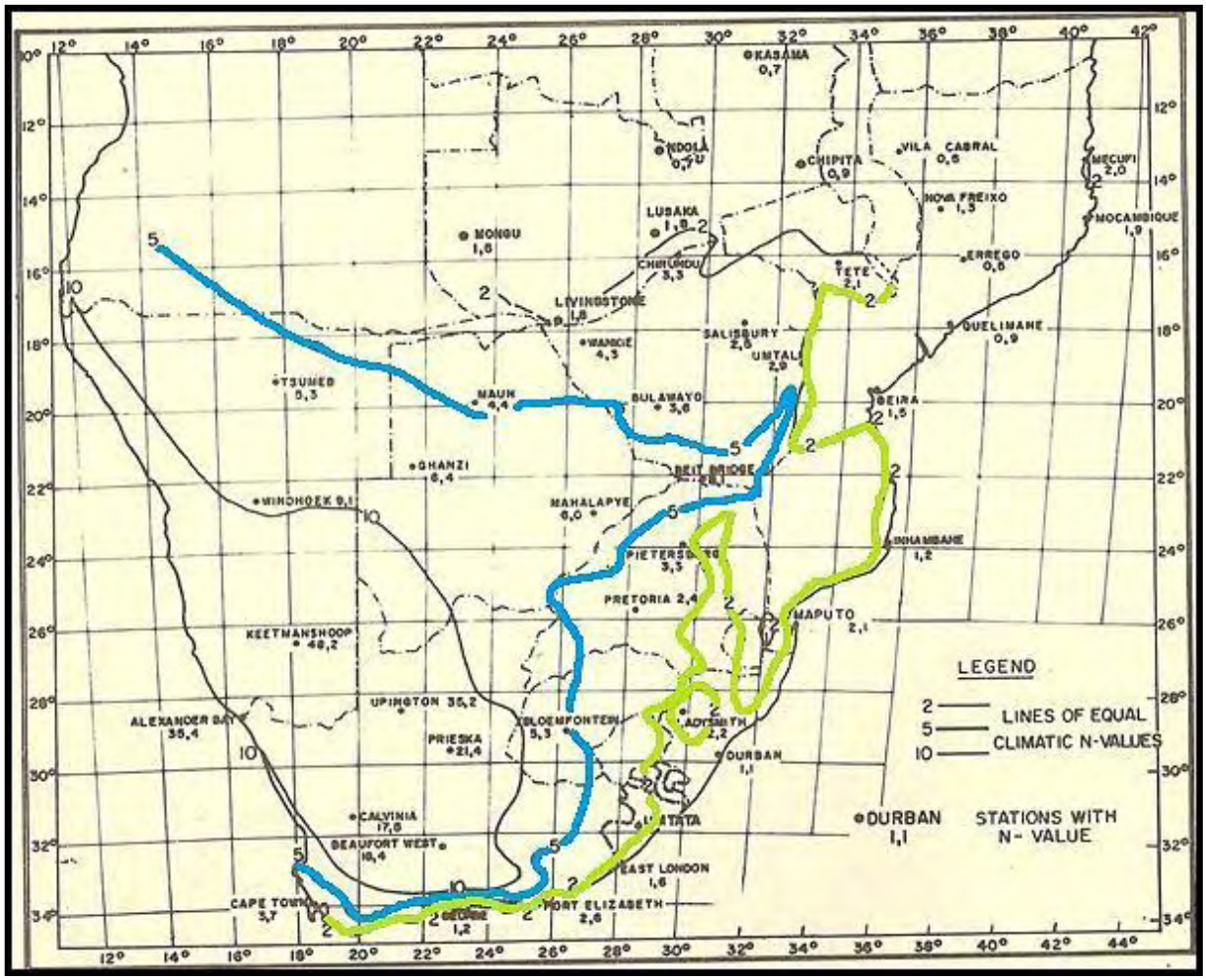

Figure 2: Climatic N-value contours of N=2, N=5 and N=10 (Adapted from Weinert, 1980)

In his discussion of the distribution of collapsible soils, Schwartz (1985) distinguishes between the collapse phenomenon in transported and residual soils, an approach which is supported in this dissertation.

3.4.1 Transported soils

Transported soils can be defined as soils which have been moved by a natural agency in recent geological times. Table 1, adapted from Jennings and Brink (1978) lists the origins and transportation agency of various transported soils that are typically prone to exhibit collapse settlement.

Table 1: Transported soils and commonly associated engineering problems (adapted from Jennings and Brink, 1978 in Schwartz, 1985)

Transported Soil Type	Agency of Transportation	Source	Soil Type	Problems to Anticipate
Hillwash (fine colluvium)	Sheetwash	Acid crystalline rock	Clayey sand	Collapsible grain structure
		Arenaceous sedimentary rock	Sand	Collapsible grain structure
Gulleywash	Gulleywash	Local catchment	Gravels, sands, silts or clays	All possible problems
Aeolian Deposit	Wind	Usually mixed source	Sand	Collapsible grain structure Compressibility
Littoral Deposit	Waves	Mixed	Beach sand	Collapsible grain structure
Biotic Soils	Termites	Underlying soil	Often clayey or silty sand	Collapsible grain structure

It is obvious that the abovementioned types of transported soils and associated problems can occur almost anywhere in South Africa (Schwartz, 1985).

3.4.2 Residual soils

3.4.2.1 Residual granites

In South Africa, the term “collapsible soil” is most often associated with the residual granitic soils of the Basement Complex (Schwartz, 1985). Extensive foundation problems have been encountered with these soils, both in the Highveld and Lowveld of South Africa.

The collapsible nature of the residual soils derived from these granites is associated with the deeply weathered soil profiles encountered in the humid eastern parts of South Africa, typically known as areas of annual water surplus (Figure 3). During the weathering process, quartz remains unaltered in the form of sand grains, mica particles remain partially unaltered but the feldspars are thoroughly kaolinized through the chemical interaction with water charged with carbon dioxide (Schwartz, 1985), forming what is commonly known as ferralitic soils (Brink, 1979).

As the name suggests, ferralitic soils are rich in iron and aluminium hydroxides. Due to the duration of the weathering cycle and the moist nature of the climate, these ferralitic soils have a very low base status and are characterized by a friable and porous structure and the presence of 1:1 lattice kaolinitic clays (Brink, 1979).

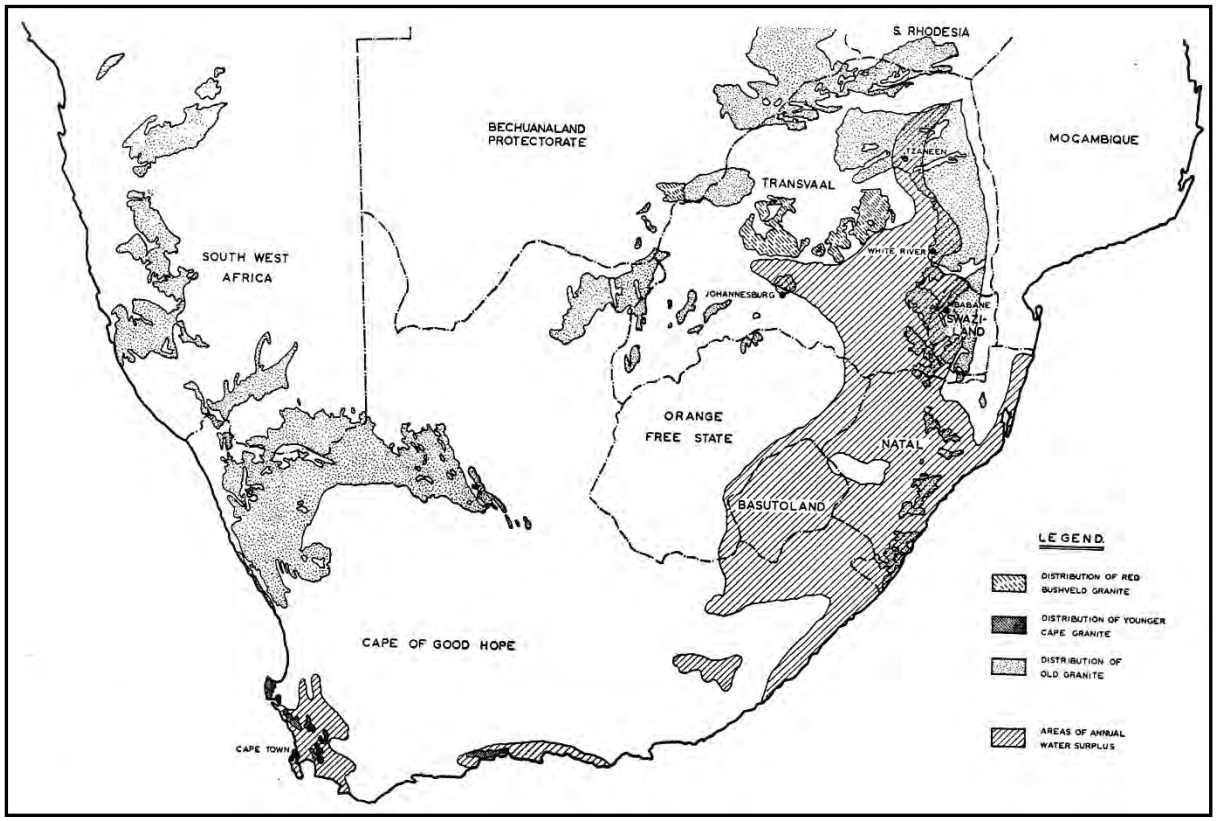

Figure 3: Map of Southern Africa showing the distribution of granite in relation to areas of annual water surplus (Brink and Kantey, 1961)

In areas of relatively high rainfall and conducive to leaching, the colloidal kaolinite is largely removed in suspension by circulating groundwater, resulting in a soil with a collapsible fabric (Schwartz, 1985).

Where these soils occur on the Highveld they appear to be confined to old erosion surfaces which have been preserved from denudation during subsequent erosion cycles (Brink, 1979). As a result it is assumed that residual granite soils on the Highveld, located at 1 500 metres and higher above mean sea-level, are likely to possess a collapsible grain structure. In the Lowveld region, all cases of collapsible residual granite soils fall within or close to the areas of annual water surplus, indicating the importance of the role that climate plays in the distribution of these soils (Schwartz, 1985).

3.4.2.2 Other residual soils

A summary of the reported occurrences of collapsing grain structure in residual soils other than the residual granite soils is presented in Table 2.

Table 2: Reported occurrences of collapsible fabric of residual soils other than residual granite soils in South Africa (adapted from Schwartz, 1985)

Stratigraphic Unit	Location	Soil Properties	Reference
Magaliesberg Quarzite Formation	Boschdal – South of Rustenburg	Moist, reddish brown, very loose, intact micaceous silty medium and fine sand.	Brink (1979)
Rooiberg Group	Witbank	Thin layer (1m) of residual felsite of low dry density (1430kg/m^3)	Brink (1979)
Sibasa and Nzhelele Formations	-	Deeply weathered residual basalt of low dry density	Brink (1983)
Cape Granite Suite	Near Stellenboch and Constantia	Slightly moist, grey mottled reddish brown, stiff, intact clayey silt.	Brink (1983) and Errera (1977)
Clarens and Elliot Formations and Ecca Group	Mainly Free State and Kwazulu Natal	Residual feldspathic sandstones	Weston (1980) and Brink (1983)
Diabase sill intrusive into shales of the Pretoria Group	West Rand	Dry, orange, loose clayey and sandy silt with a low dry density (1000 to 1300kg/m^3)	Wagener (1979)
Berea red sands	Durban area	Red or orange silty sand	Walsh Sparks (1963) and Errera (1977)

As is the case with the residual granites, the majority of the abovementioned cases fall within or close to areas of annual water surplus, hinting towards the importance of decomposition and leaching in the formation of collapsible residual soils.

3.5 Critical moisture contents

Jennings and Knight (1975) propose that there appears to exist a critical value for the degree of saturation above which collapse will not occur. Typical values for the critical degree of saturation are given in Table 3.

Table 3: Typical values for the critical degree of saturation above which collapse will not occur (adapted from Schwartz, 1985)

Soil Type	Critical degree of saturation
Transported clayey sand, 35% finer than 0.075mm.	46-51%
Transported silty sand, 40% finer than 0.075mm.	61%
Fine gravels	6-10%
Fine silty sands	50-60%
Clayey silts	90-95%
Berea red sands, 25% finer than 0.075mm.	69%
Residual granite, 15% finer than 0.075mm.	52%
Transported sand, 10% finer than 0.075mm.	21%

3.6 The concept of soil suction

The collapse process in partly saturated soils is best considered in terms of two separate components of effective stress (Equation 3); the applied stress and the suction. These two components develop intergranular stress through different mechanisms, with the applied stress developing shear stresses and potential instability at the grain contacts while suction is strictly a normal stress and hence increases the stability at grain contacts (Barden *et al.*, 1973).

$$\sigma' = \sigma - u \tag{3}$$

Soil suction is one of the most important parameters describing the stress state at different moisture conditions in an unsaturated soil. Generally, porous materials have the ability to attract and retain water. This ability is described as suction (Bulut *et.al*, 2001), and can thus be seen as the attraction the soil exerts on the moisture.

In engineering practice, the total soil suction is the sum of two components (Equation 4): matrix and osmotic suction (Fredlund and Rahardjo, 1993 in Bulut *et.al*, 2001). Matrix suction is the result of the capillary, texture and surface adsorptive forces whereas osmotic suction arises from the dissolved salts contained in the soil water (Bulut *et.al*, 2001).

$$h_t = h_m + h_\Pi \quad (4)$$

Where:

h_t – Total soil suction (kPa)

h_m – Matrix suction (kPa)

h_Π – Osmotic suction (kPa)

The decrease in effective stress due to a decrease in soil suction with an increase in soil moisture content is also discussed by Rust *et.al* (2005) in their study of the partly saturated sandy soils at the Mozal smelter site in Mozambique. During their studies, the authors found that a moisture content exists where the density of the soil suddenly dramatically decreases with an increase in moisture, and that there exists a critical moisture content above which suction forces are negligible.

The relationship between the soil moisture content and pore water suction pressures can be represented by a soil-water characteristic curve (SWCC). The SWCC essentially indicates the ability of the unsaturated soil to retain water under various matrix suctions (Mohamed *et al.*, 2006).

During their study of the SWCC of an unsaturated residual granitic soil, Mohamed *et al.* (2006) observed that the failure envelope of the unsaturated soil is non-linear due to the non-linear nature of the SWCC. At low matrix suctions, where suction is lower than the air-entry value of the soil, the soil is at or near saturation conditions and behaves as though it is saturated. An increase in matrix suction pressures produces the same increase in shear strength as does an increase in the net normal or applied stress.

4. METHODOLOGY

The methodology refers to the process through which representative data were collected and analysed in an effort to gain a better understanding of the behaviour of dry collapsible soils during wetting and the effect suction pressures have on the collapse behaviour. Undisturbed samples were collected from residual and transported soils that are known to exhibit collapse settlement. The samples were tested in a modified consolidometer that allows the addition of water during testing in a controlled manner.

Smaller samples were cut from the same undisturbed block samples used in the consolidometer testing procedure to determine the soil suctions of the different materials using the filter paper method described by Chandler and Gutierrez (1986).

4.1 Sampling

A number of undisturbed samples of soils that are expected to exhibit collapse behaviour were collected from four localities based on the typical distribution of collapsible soils in South Africa (as discussed in Section 3).

The undisturbed samples were cut from existing road cuttings and construction sites using a geological pick and spade, and then tightly wrapped in cling film to prevent the block samples from disintegrating, as well as to preserve the natural moisture content to some degree. As a rule, undisturbed samples will be wrapped in cling film and tinfoil as well as covered in wax to preserve the natural moisture content of the material. For the purpose of this investigation however the natural moisture content is not critical and is simply seen as the "original moisture content" which is further altered during testing in the modified consolidometer (Discussed in Section 4.2).

The size of the undisturbed block samples cut in the field varied depending on the material characteristics and the ease with which an intact block of material could be cut and removed without breaking. The retrieved block of undisturbed material simply needed to be sufficient to cut a number of undisturbed consolidometer ring specimens to use in the consolidometer, as well as for suction measurements (Discussed in Section 4.2).

Figure 4: Undisturbed block sample retrieved from road cutting in Bushbuck Ridge

Figure 5: Undisturbed block sample

The localities and local geology of the collected samples are summarised and described below.

Table 4: Localities of collected undisturbed samples (coordinate system: WGS 84)

Material Type	Area	Material Description	Latitude	Longitude
Residual Granite (Nelspruit Suite)	Bushbuck Ridge	Slightly moist, dark pink stained orange, medium dense to dense, pinholed gravelly sand.	25º 07' 58.8"S	31º 08' 03.4"E
Residual Vaalian Granite	Tzaneen	Moist, greyish white streaked and banded greenish grey, very loose, slightly pinholed silty sand.	23º 50' 39.1"S	30º 09' 06.7"E
Aeolian Sand	Lephalale	Slightly moist, orange brown, medium dense, pinholed silty sand.	23º 41' 23.8"S	27º 42' 09.8"E
Colluvium on the Magaliesberg Formation	Pretoria	Dry, yellow brown stained orange, medium dense, pinholed silty sand	25º 47' 35.1"S	28º 21' 15.1"E

4.1.1 Bushbuck Ridge residual granite

The residual granite sample collected from the Bushbuck Ridge area represents the product of *in-situ* weathered and decomposed granite from the Nelspruit Granite Suite. The Nelspruit Granite Suite forms part of the Archean Granitoid intrusions comprising the eastern and south-eastern Kaapvaal Craton and predominantly consists of potassic coarse-grained, porphyritic granitiod rocks (Robb *et al.*, 2006). The locality map and the local geology of the area where the material was sampled are indicated in Figures 6 and 7 below.

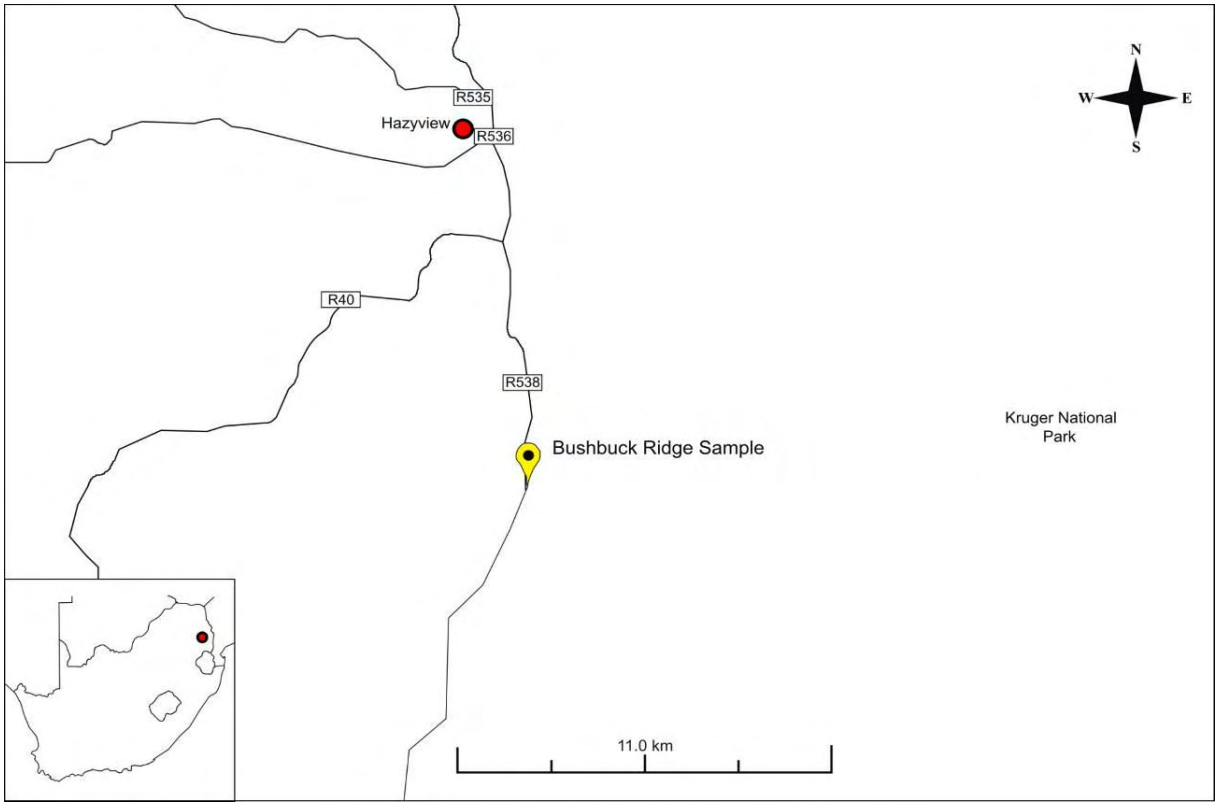

Figure 6: Locality Map – Bushbuck Ridge residual granite

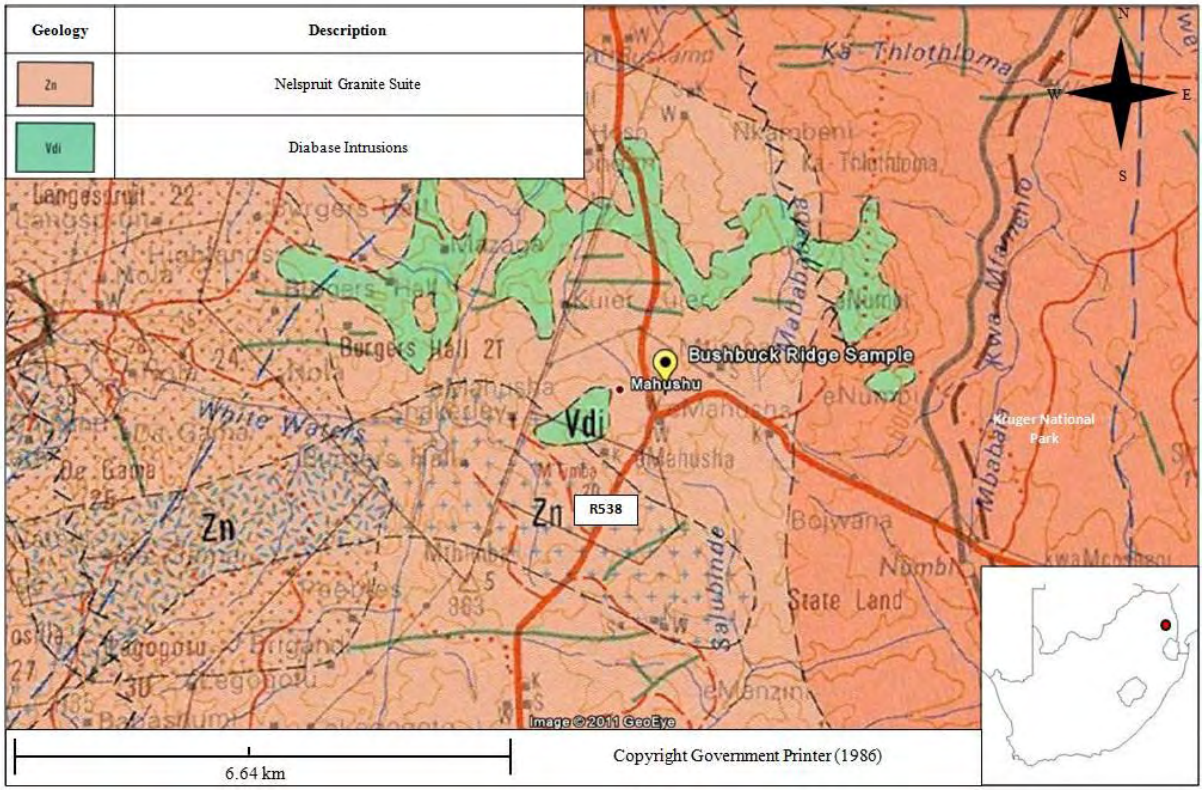

Figure 7: Geology Map – Bushbuck Ridge residual granite (DME, 1986)

The material in its natural state was described as being slightly moist, dark pink with orange stains gravelly sand with a medium dense to dense consistency and pinholed structure.

Figure 8: Dark pink *in-situ* residual granite in road-cutting in Bushbuck Ridge

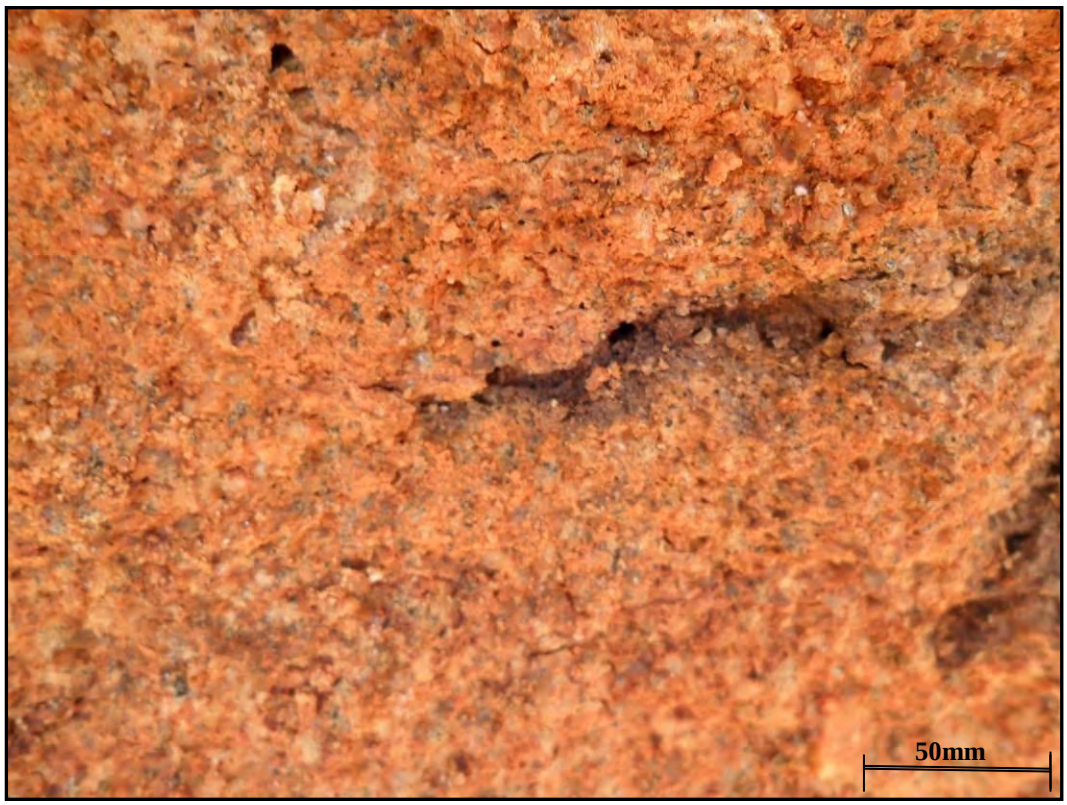

Figure 9: Pinholed structure of *in-situ* residual granite in road-cutting in Bushbuck Ridge

4.1.2 Tzaneen residual leucocratic biotite granite

The residual leucocratic biotite granite sample collected from Tzaneen represents the product of *in-situ* weathered and decomposed granite of Vaalian age. The locality map and the local geology of the area where the material has been sampled are indicated in Figures 10 and 11 below.

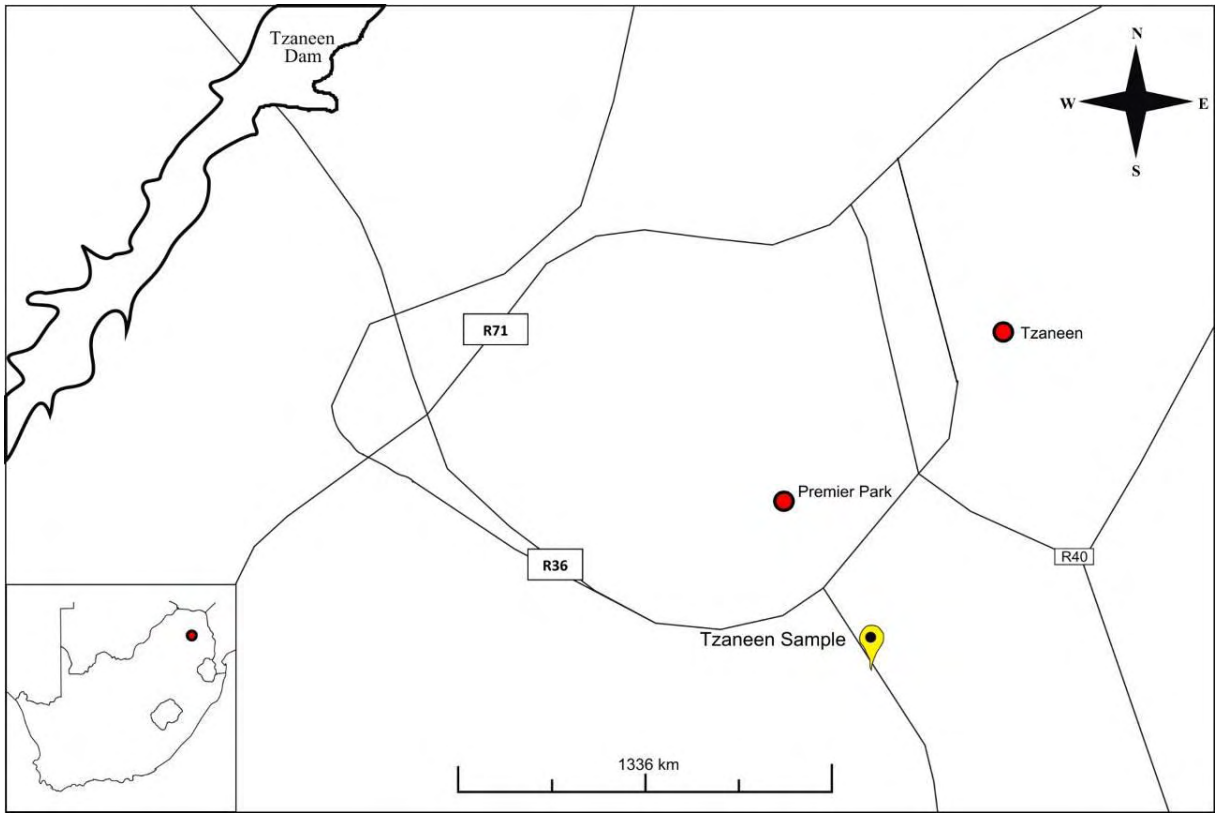

Figure 10: Locality Map – Tzaneen residual granite

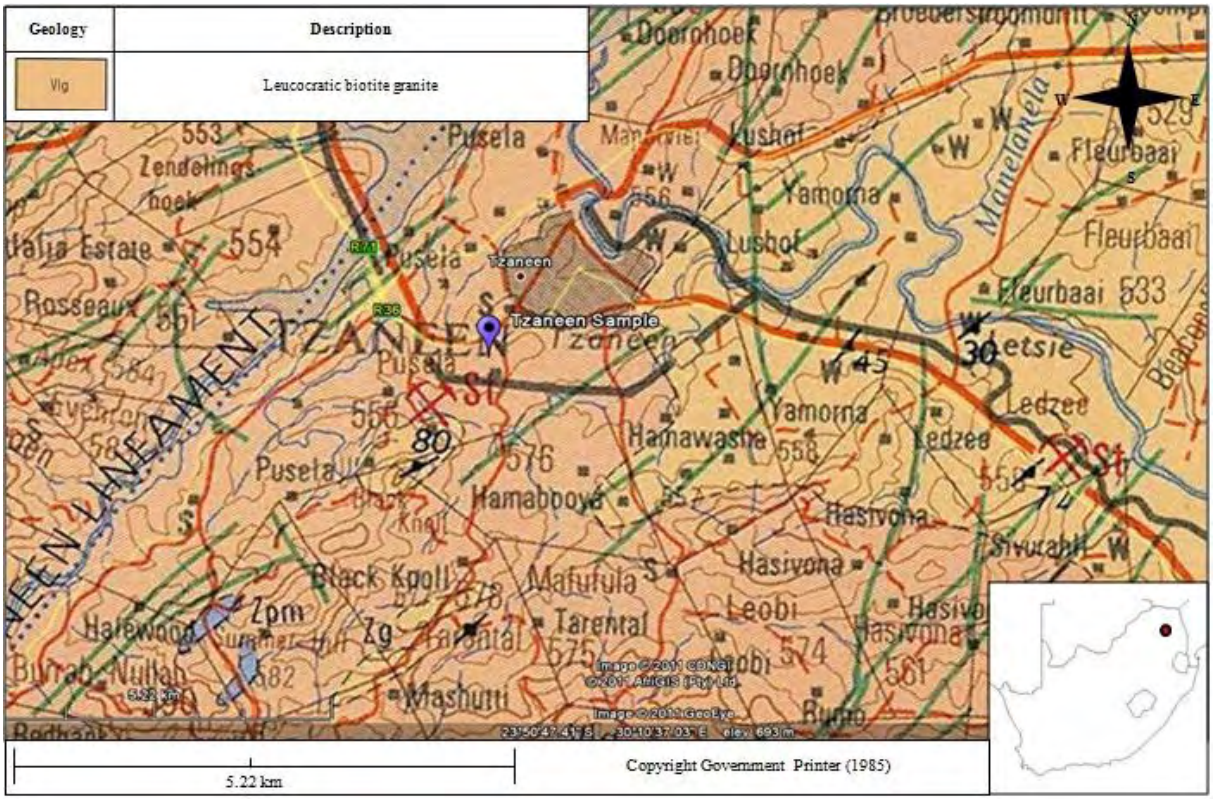

Figure 11: Geology Map – Tzaneen residual granite (DME, 1985)

The material was described in its natural state as being moist, greyish white with green and grey streaks and bands of silty sand with a very loose consistency and a slightly pinholed structure.

Figure 12: Very soft residual granite

Figure 13: Green and grey bands

4.1.3 Lephalale aeolian sand

The sample of aeolian sand collected from a construction site in Lephalale represents material of predominantly sand-sized particles transported and deposited through wind energy. Sandy soils which have undergone redistribution by wind cover almost half of southern Africa, and according to Brink (1985) all of the inland deposits belong to, or are derived from, the uppermost formation of the Kalahari group.

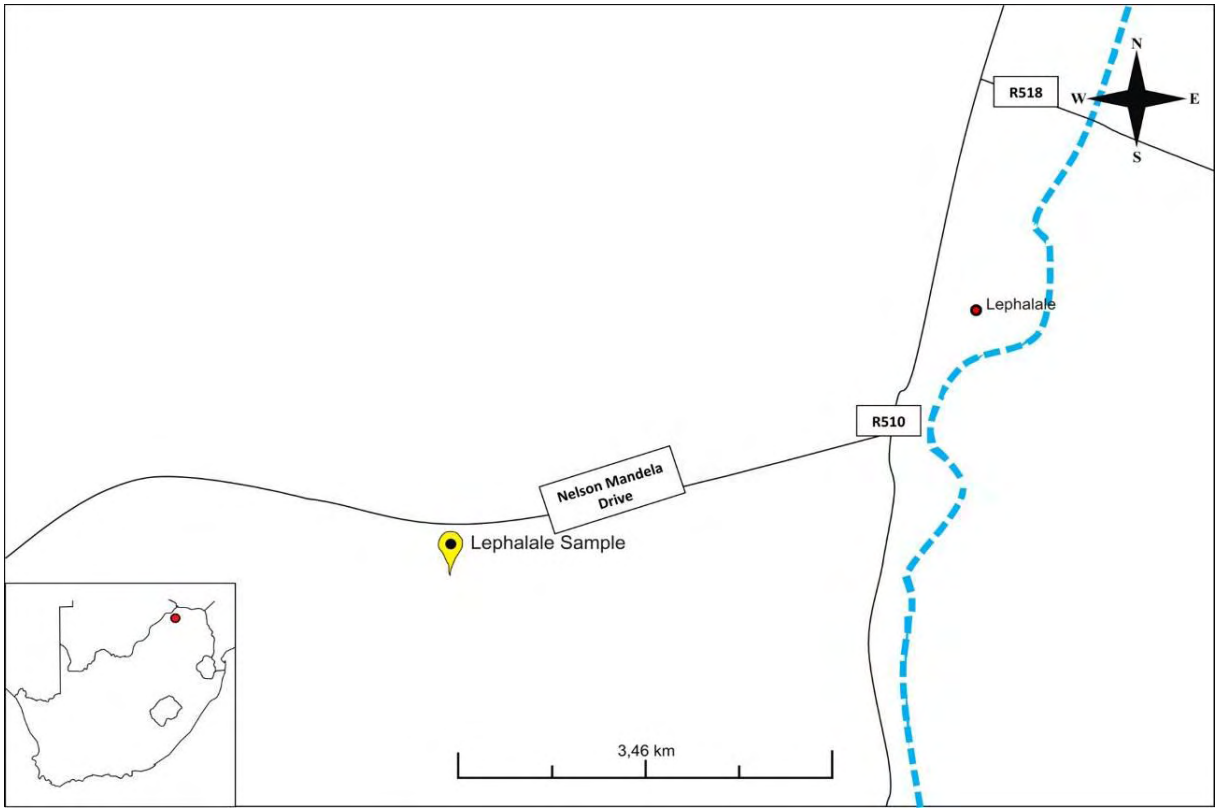

Figure 14: Locality Map – Lephalale aeolian sand

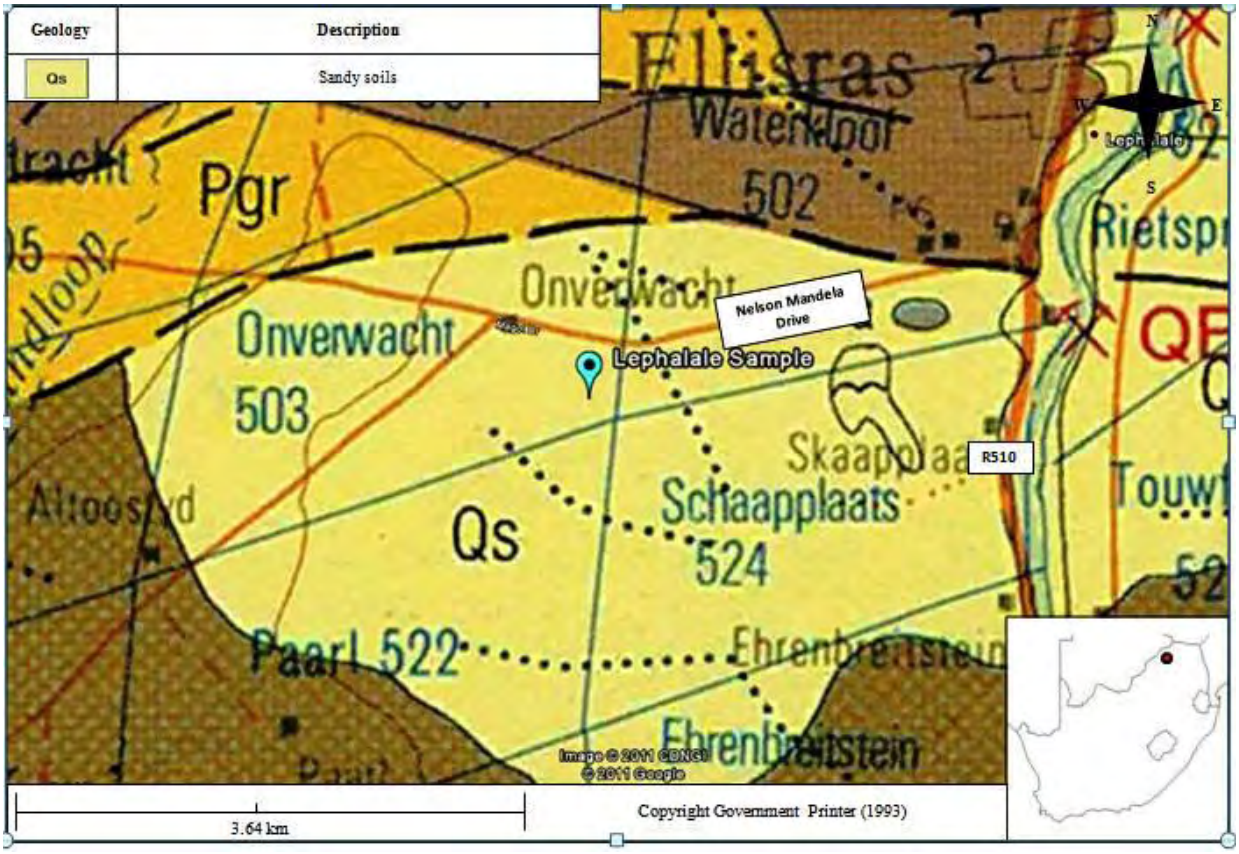

Figure 15: Geology Map – Lephalale aeolian sand (DME, 1993)

During sampling the material was described as being slightly moist, orange brown silty sand of medium dense consistency, with a pinholed structure and scattered calcrete nodules.

Figure 16: General nature of the aeolian material

4.1.4 Magaliesberg colluvium

The sample of colluvial material was collected from an embankment at a newly constructed office site towards the east of Pretoria. The material predominantly consists of sand-sized quartz grains, derived from the weathering and transport of quartzite from the Magaliesberg Quartzite Formation.

The locality map and the local geology of the area where the material has been sampled are indicated in Figures 17 and 18 below.

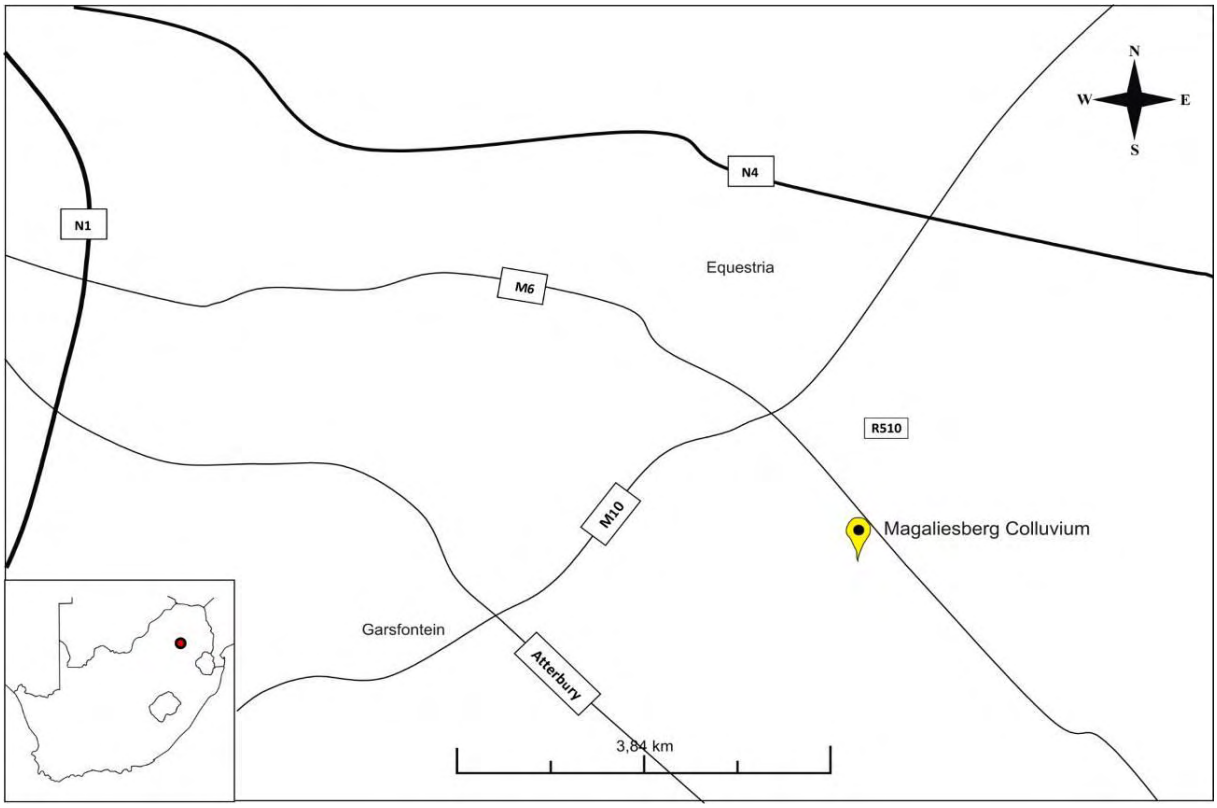

Figure 17: Locality Map – Magaliesberg colluvium

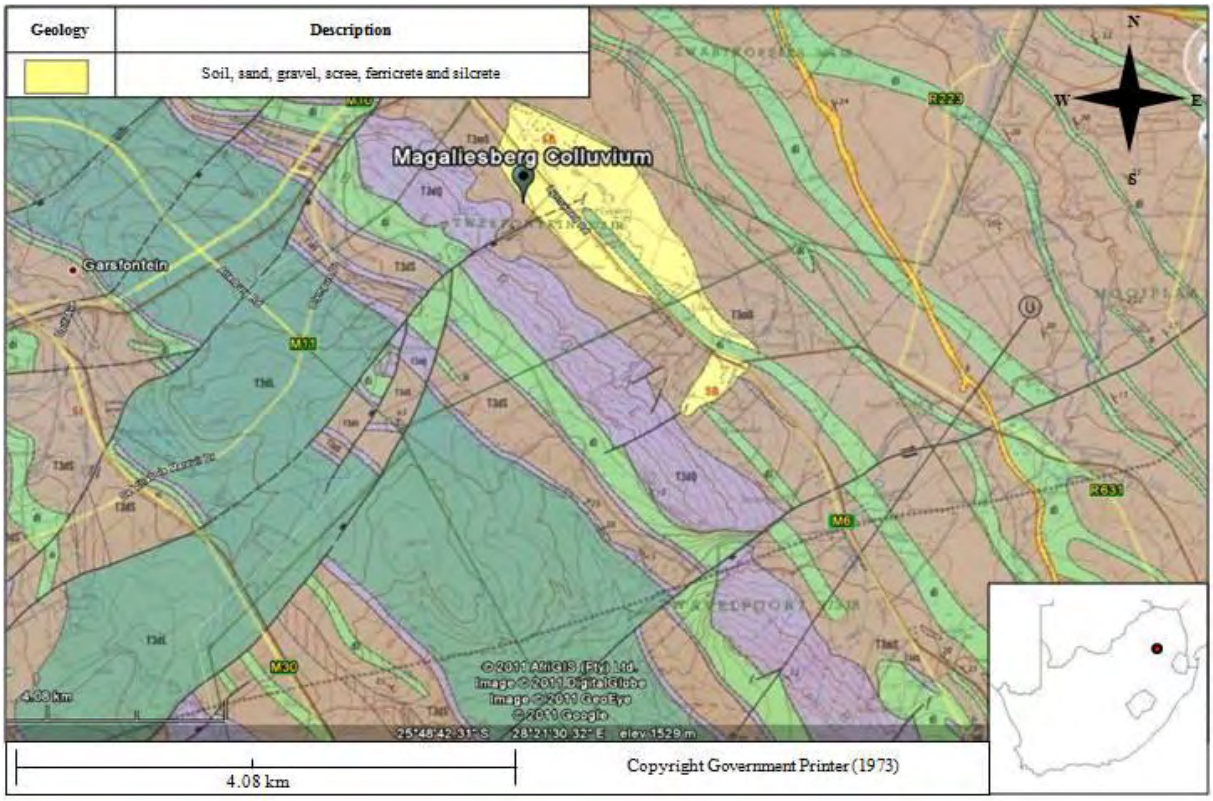

Figure 18: Geology Map – Magaliesberg colluvium (DME, 1973)

During sampling and on site, the material was described as being dry, yellow brown stained orange silty sand of medium dense consistency with a pinholed structure and few open root channels.

Figure 19: Magaliesberg colluvium

Figure 20: Mottled nature of colluvium material

4.2 Laboratory testing

4.2.1 Modified consolidometer testing

Sample preparation and testing of the undisturbed samples in the modified consolidometer represent the bulk of the laboratory testing. The methodology and apparatus is discussed below, and the findings discussed and evaluated in Section 5.

4.2.1.1 Sample preparation and consolidation

Once the undisturbed samples were transported to the laboratory, the blocks of undisturbed material are cut into smaller, more manageable sizes using a toothed hand-saw and metal spatulas. One of these smaller blocks is set aside for consolidometer testing while the rest of the material is carefully wrapped in cling film once again to use at a later stage for suction measurements.

The modified consolidometer is similar to a basic front-loading consolidometer apparatus but allows for the incremental addition of water to the sample through a small hole at the bottom of the loading cell during any stage of the test. The consolidometer apparatus consists of a rigid metal frame to avoid distortion under load. The apparatus is housed in a custom-built box cabinet with closable doors and a flat top.

On the inside of the cabinet a sturdy metal lever arm is connected to the consolidometer framework. The lever arm assembly is self-aligned and can be arranged in two different hanger positions: 1:10 and 1:11. All of the collected samples were tested using the 1:11 hanger position. The sample is loaded using an assembly of slotted plate weights, which are added incrementally onto a metal rod to the apparatus until the desired load is achieved.

Using the 1:11 hanger position and based on the surface (loading) area of the sample in the consolidometer ring, the weight added to sample load ratio equals 1kg = 24.416 kPa. The lever arm is supported during the loading process by a metal supporting beam controlled by a plastic fly-wheel. A second plastic wheel is used to keep the lever arm assembly in a horizontal position and to lower the loading pin into position at the start of the test.

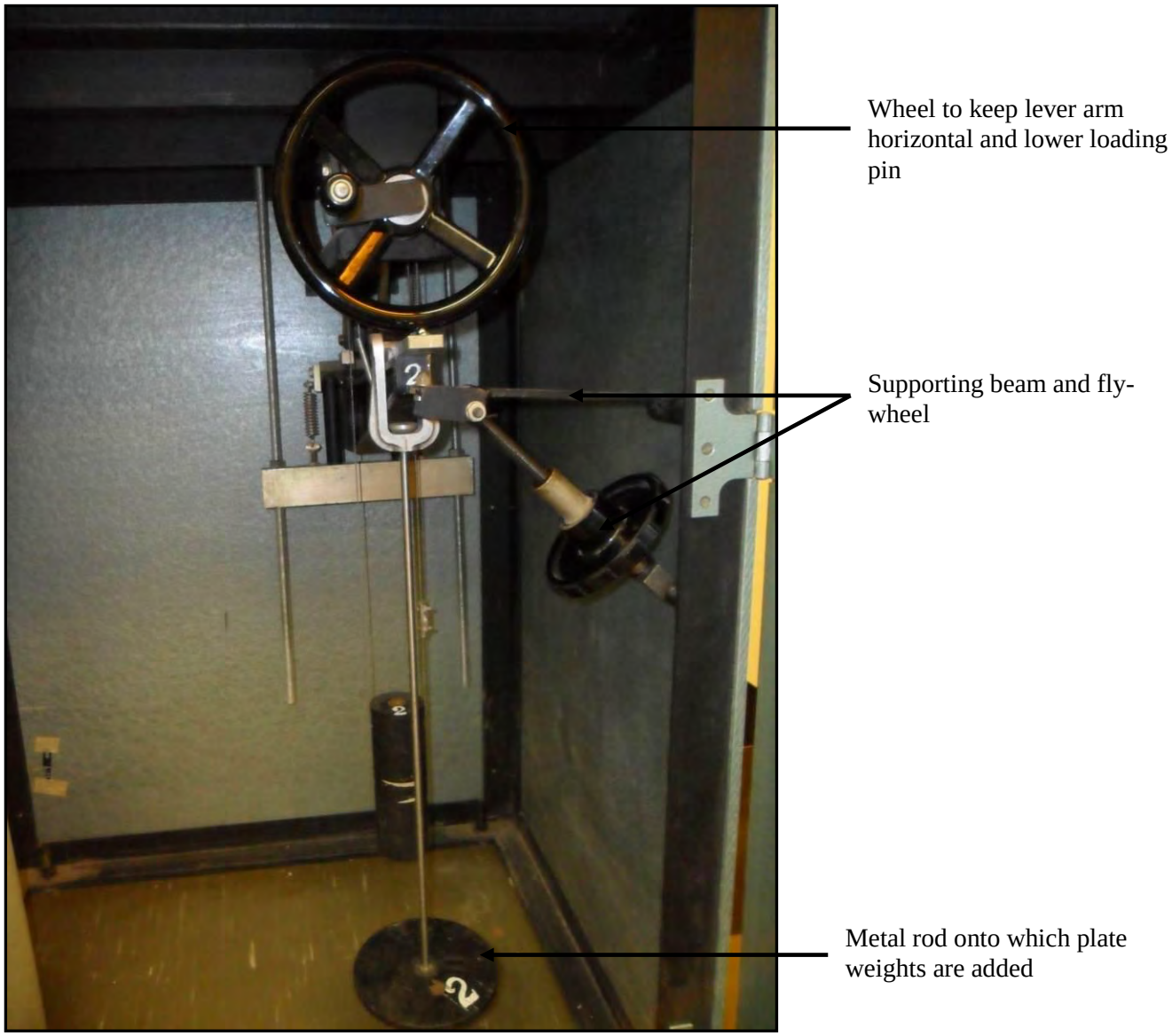

Figure 21: Lever arm assembly (inside cabinet)

The modified loading cell is placed on the loading area on the flat top of the cabinet and consists of a metal tube with a small opening at the bottom which allows for the addition of water during the testing process. The addition of water is controlled using a small turn screw on the side of the cell which opens/closes the hole at the bottom of the cell (Figure 22).

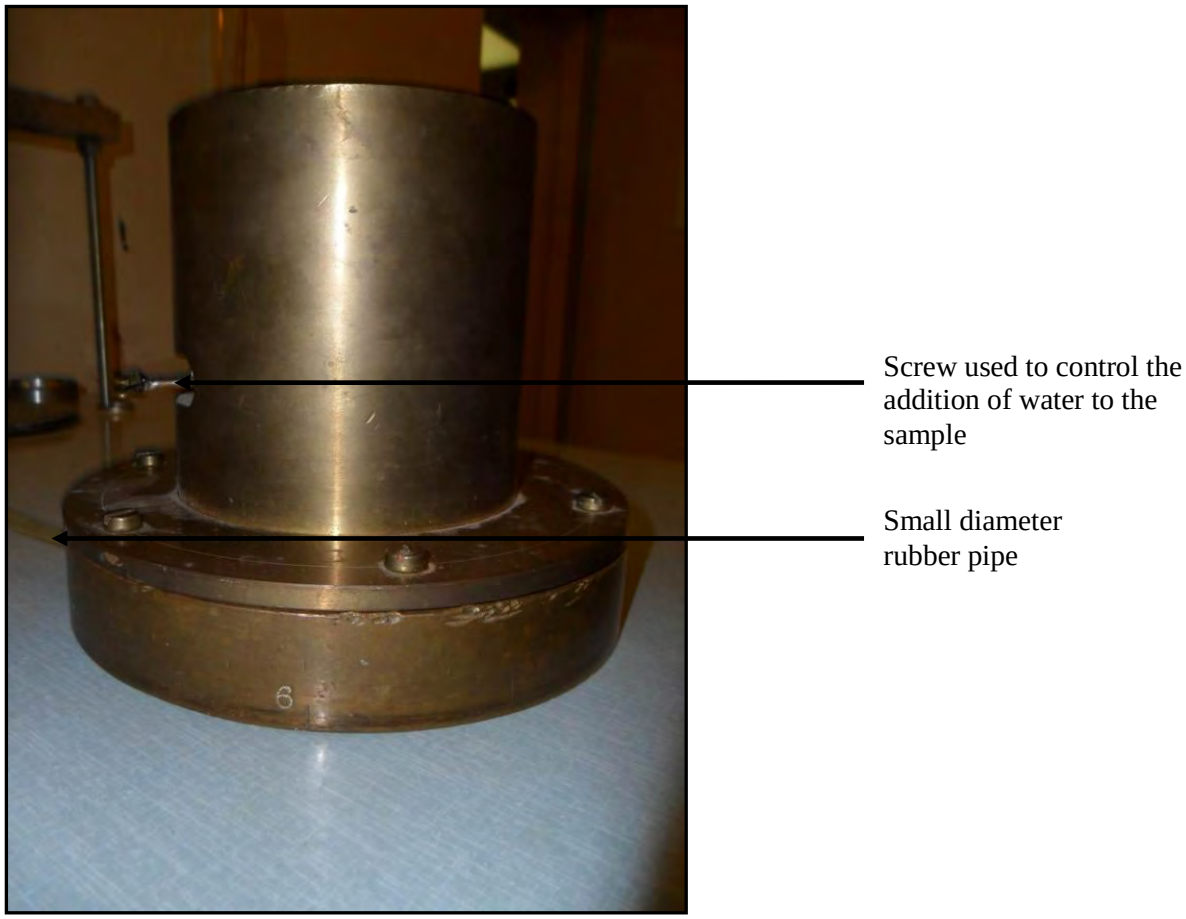

Figure 22: Modified loading cell

The undisturbed block sample is cut and moulded to fit into the consolidometer ring. The ring has an inside diameter of 75 millimetres, height of 20 millimetres and weight of 104.58 grams when empty. Once the sample is fitted in the ring, the sample surfaces at the top and bottom are carefully flattened and filled so as to reduce the effect of bedding errors during the testing process.

The ring is then carefully inserted into the metal loading cell. A metal sleeve and collar of the same diameter is inserted on top of the consolidometer ring, after which the impervious loading cap is lowered on top of the sample. Once the loading cap is in position the entire cell is sealed using petroleum jelly in an effort to minimize the change in moisture during the loading of the sample.

Due to the unique nature of the apparatus a schematic diagram of the complete modified loading cell and accessories were constructed to aid the reader in understanding how the apparatus works. This is illustrated in Figure 23.

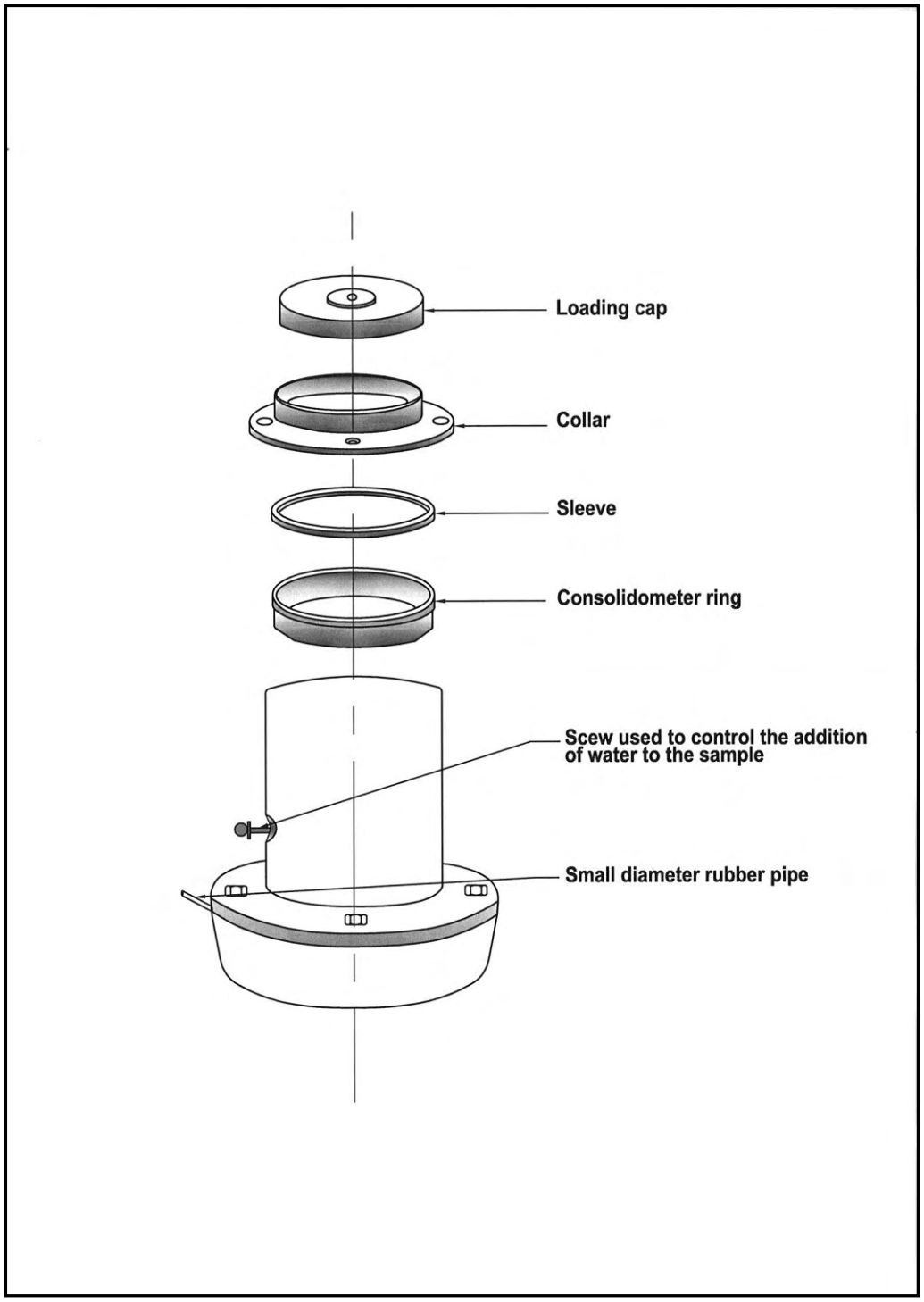

Figure 23: Schematic diagram of the complete modified metal loading cell apparatus

The loading cell is then connected to a marked burette, which is clamped to a metal stand, using a small-diameter rubber tube which allows for the passing of water from the burette to the loading cell once the hole at the bottom of the cell is opened. A dial gauge, used to monitor the amount of consolidation under load, is also attached to the metal stand (Figure 24).

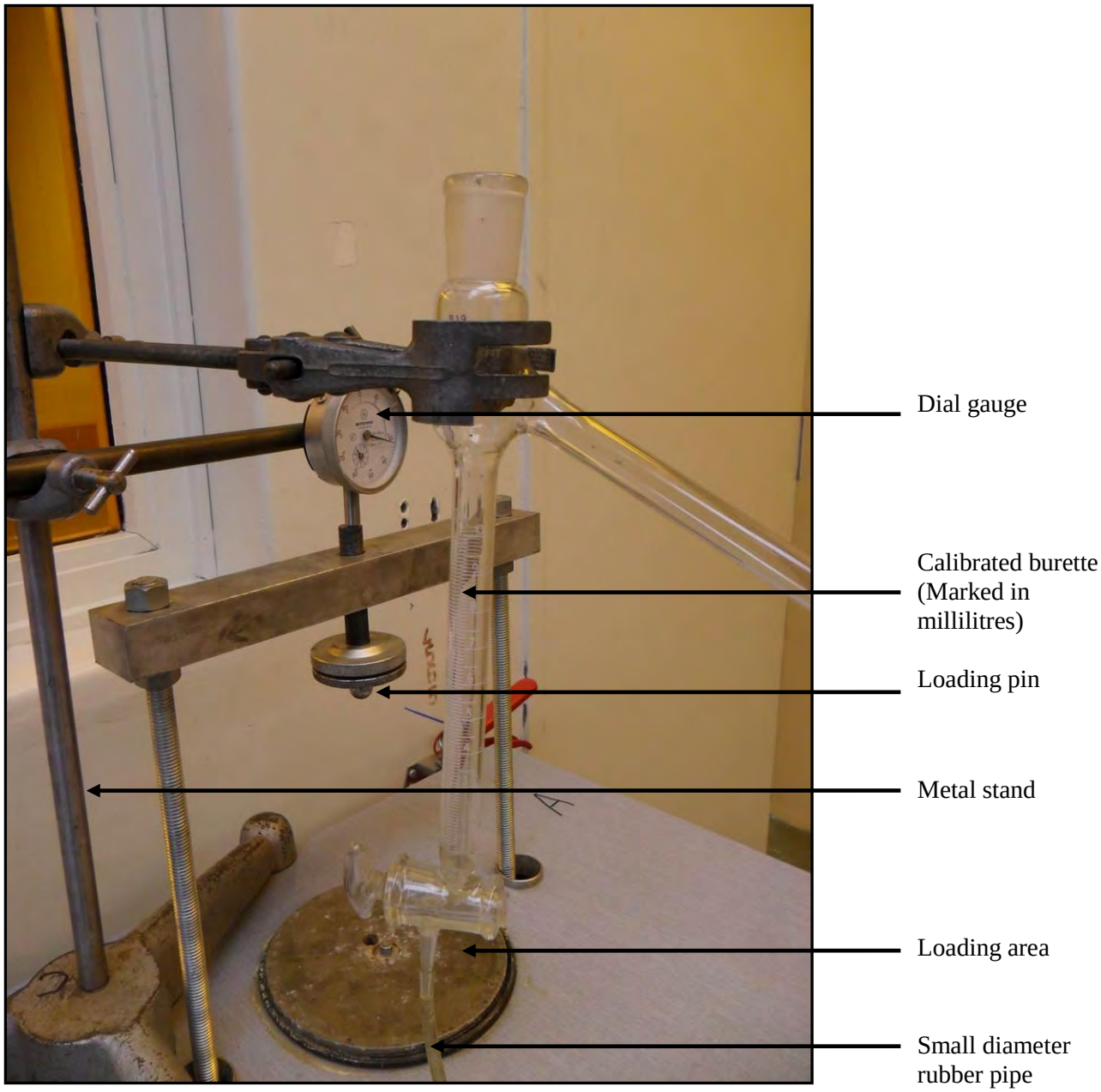

Figure 24: Set-up of apparatus (top of cabinet)

The loading pin is then carefully lowered using the plastic wheel until fitting snugly in the depression in the top of the loading cap. The dial gauge is lowered so as to rest on top of the loading pin and an initial reading is taken. This represents the starting point of the test.

Once the above mentioned setup has been reached, the sample in the cell is loaded incrementally up to 200 kPa. Before a next load is added, the support beam is raised so as to support the lever arm and to prevent a sudden increase in load on the sample. Once the desired weights have been added (Table 5) the support beam is lowered slowly and the sample introduced to the new load. Consolidation readings (millimetre settlement) are taken immediately once the sample is loaded, and then at hour intervals. The load is only increased to the following interval once the rate of creep of the sample is equal to or less than 0.25% of the original height of the sample (Rust *et.al*, 2005). Thus,

if the original sample height equals 20 millimetres, the load is increased once the rate of creep is equal to or less than 0.05 millimetres per hour. Up to this point the testing procedure is similar to that of the commonly used Collapse Potential Test.

Once the sample has been successfully loaded up to 200 kPa it is left overnight to ensure that the sample is completely consolidated before additional moisture is added.

It should be emphasised that up to a load of 200 kPa no change has been made to the natural moisture content of the sample through the addition of water.

Table 5: Corresponding load/weight relationship at 1:11 hanger position

LOAD (kPa)	**TOTAL WEIGHT (Kilogram)**
25	1.126
50	2.252
100	4.504
200	9.008
400	18.016
800	36.032

4.2.1.2 Increase of moisture content and final consolidation

Once the sample is effectively consolidated at 200 kPa, additional moisture is introduced for the first time. Moisture is added from the marked burette and the amount added is regulated by the turn screw on the side of the loading cell. Water flows from the burette to the loading cell through a small diameter rubber pipe. The initial incremental change in moisture is kept at less than 0.5 millilitres for all the samples, with an initial reading taken after half an hour. From this point the amount of moisture added and time intervals at which readings are taken are unique to each sample, and are based on the consolidation reaction of the material to the increase in moisture and the rate at which water is absorbed by the sample. The rate at which water is absorbed is a function of the suction forces of the material. The higher the suction of the material, the faster water is absorbed or taken up in the system and the faster the water level drops in the burette through which water is added to the system. As the moisture content of the material increases, the suction forces decrease and the longer it takes for moisture to be taken up in the system.

The moisture contents are incrementally increased until either total consolidation has taken place (e.g. no further settlement takes place at the current load regardless of the increase in moisture) or the suction has decreased to such an extent that water can no longer be freely added in a reasonable amount of time. In the case of the last mentioned event be the case it is assumed that collapse settlement has already occurred as collapse settlement is typically expected to occur during a decrease in the suction forces of the material (Rust *et.al*, 2005). The burette is then filled with water and left in

the open position overnight. This ensures that the sample is effectively saturated and full collapse settlement at 200 kPa has taken place before the final loads are added.

The sample is then loaded and consolidated up to a final load of 800 kPa using the same procedure as prior to changes in the moisture content.

4.2.1.3 Difficulties encountered during testing

A number of minor challenges had to be overcome during the consolidometer testing procedure. The most noteworthy of these is probably the preparation of the samples for the consolidometer ring. Some of the soils, in particular the aeolian sands from Lephalale and residual granite from Bushbuck Ridge, are extremely difficult to prepare due to the nature of the material. These samples contain abundant coarse sand- / fine gravel-sized quartz particles, which during the sample cutting catch on the spatula or saw blade and in the process rips small chunks of material out of the sample. This leads to voids between the consolidometer ring and the material, which at the very least affects the consolidation readings and more than once caused the sample to slip from the ring and break as it was inserted into the loading cell. These grains also make it very hard to effectively smooth the top and bottom surfaces of the sample, and consequently one must assume that some bedding errors will occur during the initial stages of consolidation.

Figure 25: Quartz grains in aeolian sands affecting sample preparation (20.5 X magnification)

Some difficulty was also experienced in the sample preparation of the slightly cemented Magaliesberg colluvium material. Due to the slightly cemented nature the material consistency is very dense and subsequently extremely hard to mould and shape into the consolidometer ring. The fact that some of the grains are cemented together also lead to the same problem, but to a lesser extent, as was experienced during the preparation of the aeolian samples. Cemented aggregates of material catch on the blade of the spatula or saw, leaving voids and depressions in the material and make it very hard to effectively smooth the top and bottom surfaces of the undisturbed ring sample, subsequently leading to bedding errors and difficult seating of the sample.

A further frustration during the consolidometer testing process is the fact that the opening at the bottom of the loading cell through which water is added tends to get clogged as soon as additional water is introduced to the samples, particularly in those specimens with a higher percentage of fines. At this stage consolidation of the material up to 200 kPa is complete and the testing of the sample has been in progress for approximately a day. However, if the opening is clogged no additional water can accurately be added. Subsequently the sample is removed, the hole unblocked and the entire consolidation process started over. To avoid this frustration it is recommended that the small hole is thoroughly cleaned after the testing of each sample, using a toothpick or needle to effectively remove any material that might have accumulated prior to inserting the next sample and consolidation is started.

4.2.2 Testing of remoulded specimens

Using the calculated dry densities, void ratios and natural moisture contents of the material, remoulded and compacted specimens of each of the materials were prepared for conventional consolidometer testing in an effort to determine the intrinsic consolidation curves of the different materials.

Initially the materials were dried out in the oven for 24 hours at 105 ºC to remove the moisture. Based on the calculated natural moisture contents of the materials water was then added to the dry materials and mixed thoroughly to attain the original natural moisture contents.

The materials were then “moulded” and compacted into the consolidometer ring in two layers of pre-determined thicknesses based on the calculated material properties and the height of the consolidometer ring. The ring was then placed in an ordinary front-loading consolidometer between two porous plates and fully saturated. The sample was loaded in the same increments as that used during the modified consolidometer testing of the materials, and readings taken at pre-determined regular intervals.

From there, the change in void ratio with an increase in load can be plotted. The results for each of the materials, together with the results of the modified consolidometer test, are shown as the change in void ratio with a change in the effective stress state of the material. This is done in an effort to correlate the shape of the intrinsic consolidation curves with the shape of the consolidation curves of the undisturbed materials *after* collapse has occurred.

4.2.3 Matrix suction measurements

Matrix suction measurements of the sampled materials were conducted using the filter paper method proposed by Hamblin (1981), providing an accurate relationship between the moisture content of the filter paper and suction pressures down to 1 kPa.

The filter paper method involves cutting a suitably sized soil sample, usually in an consolidometer ring of known dimensions. Two pieces of untreated Whatman's No. 42 filter paper, marked A and B, are then weighed individually and placed on top of each other against the surface of the prepared soil sample. The sample and filter paper are then sealed by wrapping it in tinfoil and multiple layers of cling wrap to prevent a change in the moisture content of the material.

This process is repeated for a number of prepared samples of the collapsible material at different moisture contents to determine the matrix suctions at the various moisture contents as well as to determine the critical moisture content where matrix suctions suddenly decrease. Testing is started at natural moisture content and moisture is added or removed, depending on the natural moisture content (Table 6) of the material. A number of samples of the same material but at different moisture contents are tested at the same time.

Table 6: Incremental changes in sample moisture condition for matrix suction calculations

Magaliesberg Colluvium	Lephalale Aeolian Sand	Bushbuck Ridge Residual Granite	Tzaneen Residual Granite
Natural moisture content (5.59%)	Natural moisture content (12.82%)	Natural moisture content (7.15%)	Natural moisture content (18.04%)
3ml added	1ml removed	11ml removed	7ml removed
6.5ml added	1ml added	1ml added	1ml added
10ml added	3ml added	3ml added	3ml added
15ml added	5ml added	5ml removed	3ml removed
18ml added	8ml added	5ml added	5ml added
23ml added	12ml added	10ml added	10ml added

The filter paper then wets up to a moisture content in equilibrium with the magnitude of the soil suction, and careful measurement of the moisture content of the filter paper enables the soil suction to be obtained using a previously established relationship.

The samples are left for ten days, allowing the filter paper to reach equilibrium with the soil sample with an assumed magnitude of suction, after which they are dismantled and the pieces of filter paper weighed again. The pieces of filter paper are then placed in an oven and left overnight to dry. Once they are dried they are weighed again and the filter paper moisture content determined using the dry and moist unit weights (Chandler and Gutierrez, 1986).

Once the filter paper moisture content is known the matrix potential for the material at that particular moisture content is determined using the relationship established by Hamblin (1981) and expressed in Equation 5.

$$ln\,\Psi_m = -2.397 - 3.683\,ln\,F \quad (5)$$

Where:

F – Gravimetric water content of filter paper (%)

Ψ_m – Matrix potential (kPa)

It is important to ensure that the pieces of filter paper are not compressed while the samples are sealed with cling wrap and tinfoil, as this would inhibit its water uptake. Two pieces of filter paper are used so as to provide two readings which can be correlated. A further advantage of using two pieces of paper is that the weight of the paper placed on top is not influenced by the adhesion of soil particles as it is not in direct contact with the material.

4.2.4 Foundation indicator testing

Disturbed samples of each material type were submitted to Soillab (Pty) Ltd in Pretoria to determine the grain-size distribution, Atterberg Limits and specific gravities (SG) of the different material types.

4.2.4.1 Bushbuck Ridge residual granite

The particle size analysis and foundation indicator results are summarised in Table 7 below.

Table 7: Particle size analysis and foundation indicator results: Bushbuck Ridge residual granite

Sample Name	Description	Soil composition				Atterberg Limits		LS %	GM	Activity	AASHTO / Unified classification
		Clay %	Silt %	Sand %	Gravel %	LL %	PI %				
Bushbuck Ridge residual granite	Light orange red silty sand	11	20	57	12	36	13	6.0	1.25	Low	A-2-6 (1) / SC

The potassic residual granite from Bushbuck Ridge classifies as “SC” and “A-2-6 (1) “ according to the Unified Soil Classification System AASHTO classification system respectively and predominantly consists of sand-sized particles with moderate percentages of silt, gravel and clay. The material generally classifies as being of medium overall plasticity (Burmeister, 1949) and has a low liquid limit, grading modulus and linear shrinkage. The material has a SG value of 2.664.

4.2.4.2 Tzaneen leucocratic biotite granite

The particle size analysis and foundation indicator results are summarised in Table 8 below.

Table 8: Particle size analysis and foundation indicator results: Tzaneen residual granite

Sample Name	Description	Soil composition				Atterberg Limits		LS %	GM	Activity	AASHTO / Unified classification
		Clay %	Silt %	Sand %	Gravel %	LL %	PI %				
Tzaneen residual granite	Light brown silty sand	3	36	60	1	43	6	2.0	0.89	Low	A-5 (0) / SM

The residual granite from Tzaneen classifies as "SM" and "A-5 (0) " according to the Unified Soil Classification System and AASHTO classification system respectively and predominantly consists of sand-sized particles with a high percentage of silt and virtually no gravel and clay. The material generally classifies as having a low overall plasticity (Burmeister, 1949) and has a low liquid limit, grading modulus and linear shrinkage. The residual leucocratic biotite granite material has a SG value of 2.643.

4.2.4.3 Lephalale aeolian sand

The particle size analysis and foundation indicator results are summarised in Table 9 below.

Table 9: Particle size analysis and foundation indicator results: Lephalale aeolian sand

Sample Name	Description	Soil composition				Atterberg Limits		LS %	GM	Activity	AASHTO / Unified classification
		Clay %	Silt %	Sand %	Gravel %	LL %	PI %				
Lephalale Aeolian Sand	Dark red clayey sand	14	11	71	4	20	6	3.0	1.17	Low	A-2-4 (0) / SM & SC

The aeolian sand classifies as "SC & SM" and "A-2-4 (0)" according to the Unified Soil Classification System and AASHTO classification system respectively. The grain-size distribution indicates that the material predominantly consists of sand-sized particles with moderate percentages of silt and clay and very little gravel. The material generally classifies as being of low overall plasticity (Burmeister, 1949) and has a low liquid limit, grading modulus and linear shrinkage. The aeolian material has a SG value of 2.635.

4.2.4.4 Magaliesberg Colluvium

The particle size analysis and foundation indicator results are summarised in Table 10 below.

Table 10: Particle size analysis and foundation indicator results: Magaliesberg colluvium

Sample Name	Description	Soil composition				Atterberg Limits		LS %	GM	Activity	AASHTO / Unified classification
		Clay %	Silt %	Sand %	Gravel %	LL %	PI %				
Magaliesberg Colluvium	Dark brown clayey sand	17	17	66	0	22	8	4.0	0.78	Low	A-4 (0) / SC

The colluvium classifies as "SC" and "A-4 (0)" according to the Unified Soil Classification System and AASHTO classification system respectively. The grain-size distribution indicates that the material predominantly consists of sand-sized particles with moderate percentages of silt and clay and no gravel. The material generally classifies as being of low overall plasticity (Burmeister, 1949) and has a low liquid limit, grading modulus and linear shrinkage. The material has a SG value of 2.653.

4.2.5 Material property calculations

The dry density, initial moisture content and other material properties are determined while the consolidometer testing is in progress.

4.2.5.1 Moisture content:

The initial moisture content or the moisture content of the material as it was in its natural state can be calculated as the ratio of the weight of water to the weight of the solids in a given volume of soil (Das, 2005), and is determined using any piece of material left over from the consolidometer sample preparation process. The piece of material is placed in a tin container of a known weight, weighed, and then placed in the oven at 105 ºC and left overnight. The material is weighed again the next day inside the tin container and the change in weight recorded. Any change in weight of the total sample is assumed to be the result of a change in the moisture content. The moisture content, expressed as a percentage, is then determined using Equation 6 as expressed in Das (2005).

$$Mc = \frac{Ww}{Ws} \times 100 \tag{6}$$

Where:

Mc – Moisture content (%)

Ww – Weight of the water, equal to the difference in weight of the material before and after oven drying (g)

Ws – Weight of the solids, equal to the total weight of the material after oven drying (g)

Once the initial or natural moisture content of the material is known and the dry weight of the material in the consolidometer ring is determined, the increase in moisture content with the addition of water can be determined. This is done by using the dry unit weight of the material in the ring after drying overnight in the oven at 105 ºC and then determining the sample weight as well as the weight of the water in the sample at the start of the test at its natural moisture content using the determined moisture content *Mc*. If it is assumed that 1milliliter of water is equal to 1 gram, it is possible to calculate the different moisture contents as water is added and the weight of the water in the sample increases.

The calculated moisture contents can be related to the degree of saturation using Equation 7.

$$Se = wGs \tag{7}$$

Where:

S = Degree of saturation (%)

e = Void ratio

w = Moisture content (%)

Gs = Specific gravity

4.2.5.2 Dry density:

The dry density can be seen as the weight per unit volume of soil without the water, and is expressed as the ratio of the weight of the solids to the total volume of material (Das, 2005). Brink *et.al* (1982) in Schwartz (1985) argues that the dry densities of collapsible soils typically fall within the 900 to 1600 kg/m^3 range, but that materials of dry densities outside this range cannot be excluded.

$$\Upsilon d = \frac{Ws}{Vt} \tag{8}$$

Where:

Yd – Dry density (g/mm^3)

Ws – Weight of the solids (g)

Vt – Total volume of sample (mm^3)

The dry density is determined using the material from the consolidometer ring after testing is complete. The total volume of the sample is equal to and determined by determining the volume of the consolidometer ring using the known dimensions of the ring. After the consolidometer test is complete, the sample is placed in a tin container of a known weight, weighed, and then placed in the oven at 105 ºC and left overnight. The weight of the material after oven drying is equal to the weight of the solids.

4.2.5.3 Void ratio:

The void ratio is defined as the ratio of the volume of voids to the volume of solids (Das, 2005).

$$e = \frac{Vv}{Vs} \tag{9}$$

Where:

e – Void ratio

Vv – Volume of the voids

Vs – Volume of the solids

The initial void ratio of the material (before testing and consolidation) is calculated using the initial moisture content and determined SG value for the material. Once the sample is inserted into the loading cell and consolidation is in progress, the change in the void ratio is determined by the change in sample height in relation to the original sample height. The change in sample height (millimetres) is read from the dial gauge with each additional loading of the sample.

4.3 Optical microscope analysis

Small samples of the collapsible material selected for consolidometer testing were set aside for analysis under the optical microscope. Samples of the material both before and after consolidometer testing were selected for analysis in an effort to detect a change in soil structure and/or the average dimensions of the voids after collapse settlement has taken place in the consolidometer.

Photographs were taken at both small and large magnifications of each of the samples before and after consolidation. This was done in an effort to represent the structure of the sample as a whole and to focus on the dimensions and characteristics of the individual voids.

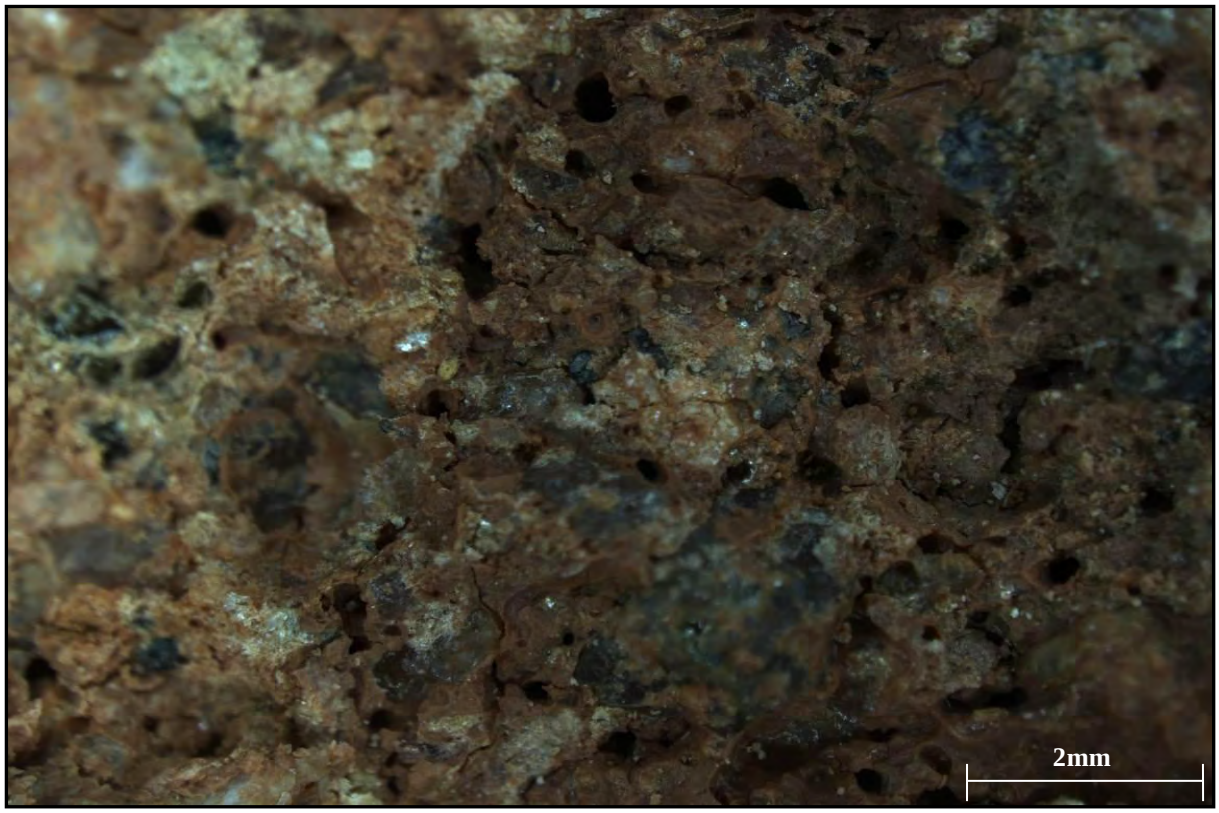

Figure 26: Optical microscope photograph: Unconsolidated Bushbuck Ridge material (11.3x Magnification)

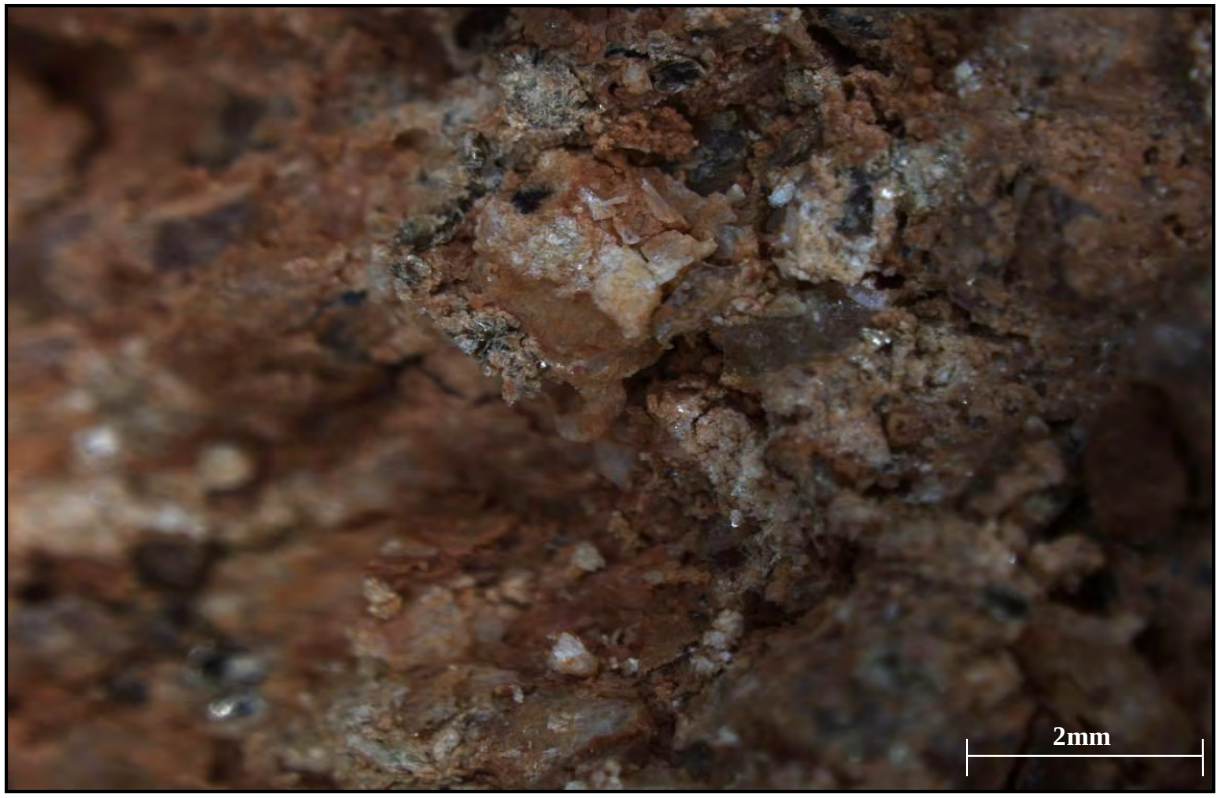

Figure 27: Optical microscope photograph: Consolidated Bushbuck Ridge material (11.3x Magnification)

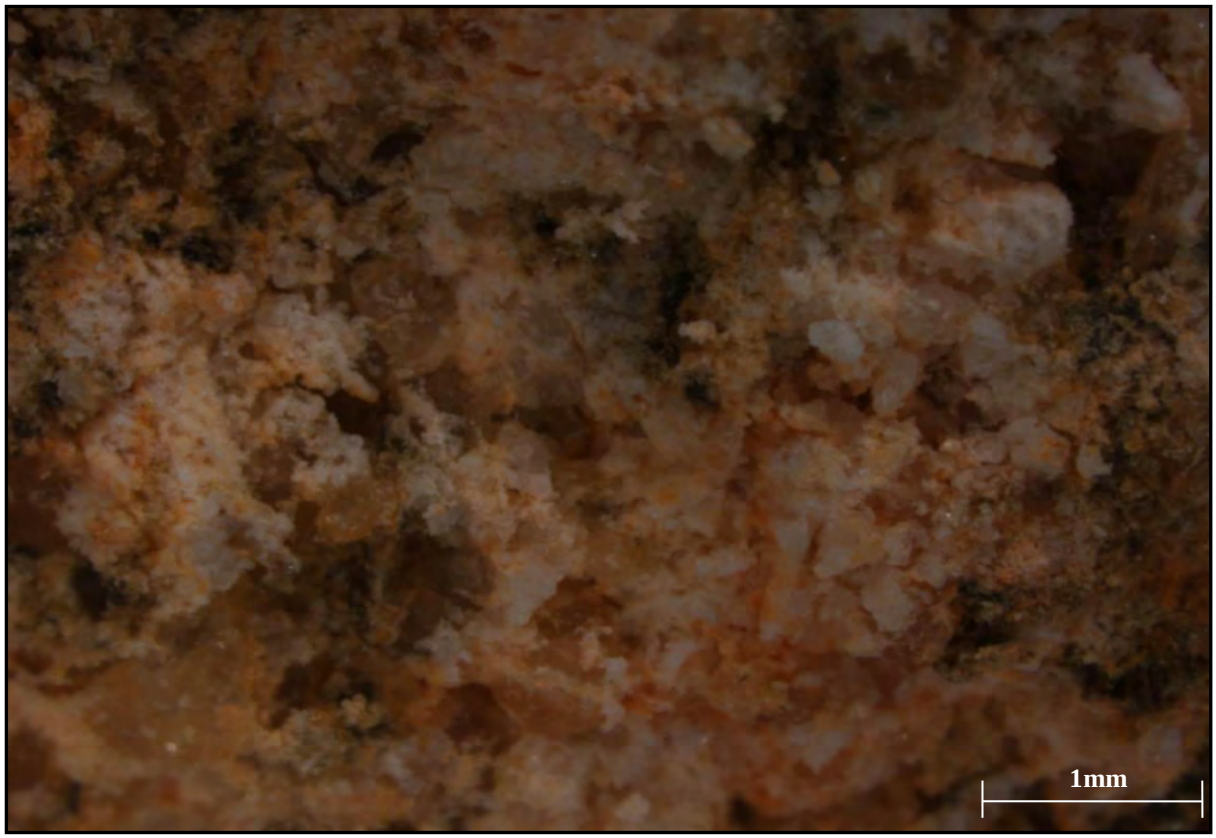

Figure 28: Optical microscope photograph - Unconsolidated Tzaneen material (20x Magnification)

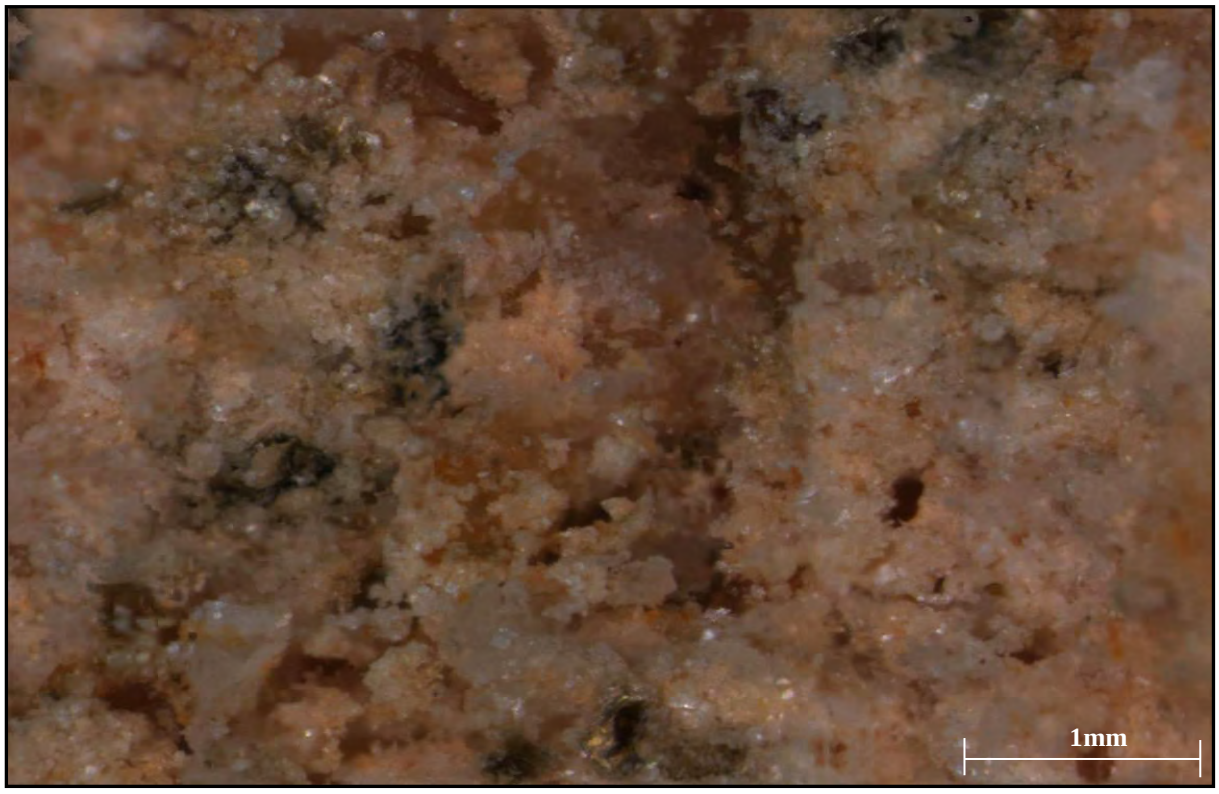

Figure 29: Optical microscope photograph - Consolidated Tzaneen material (20x Magnification)

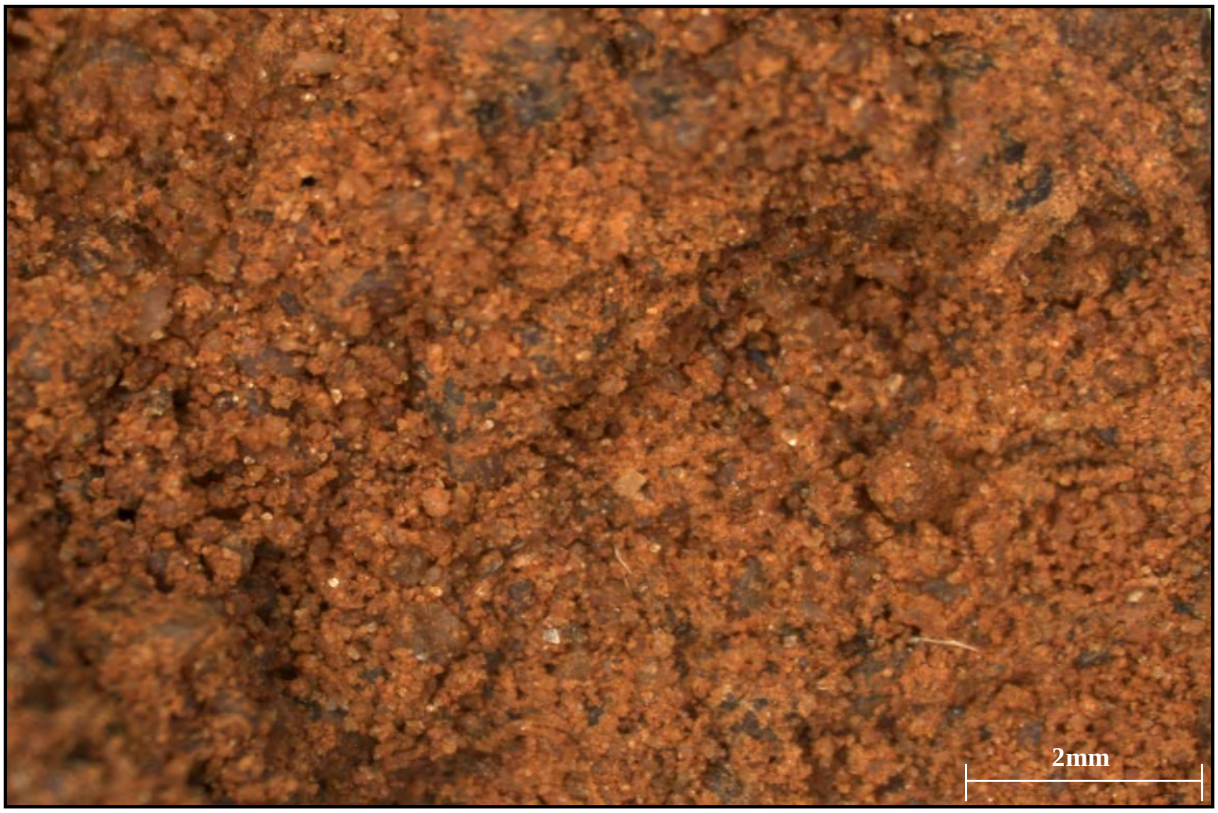

Figure 30: Optical microscope photograph - Unconsolidated Lephalale aeolian sand (11.3x Magnification)

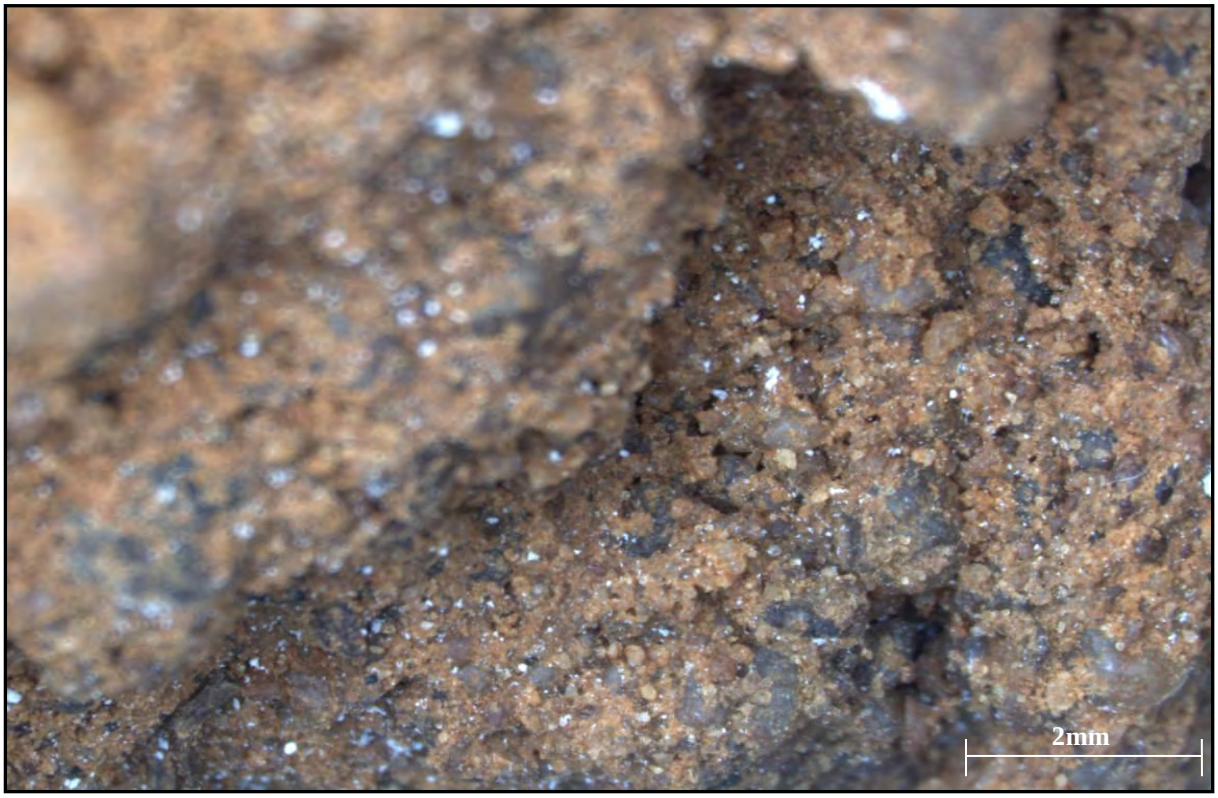

Figure 31: Optical microscope photograph - Consolidated Lephalale aeolian sand (11.3x Magnification)

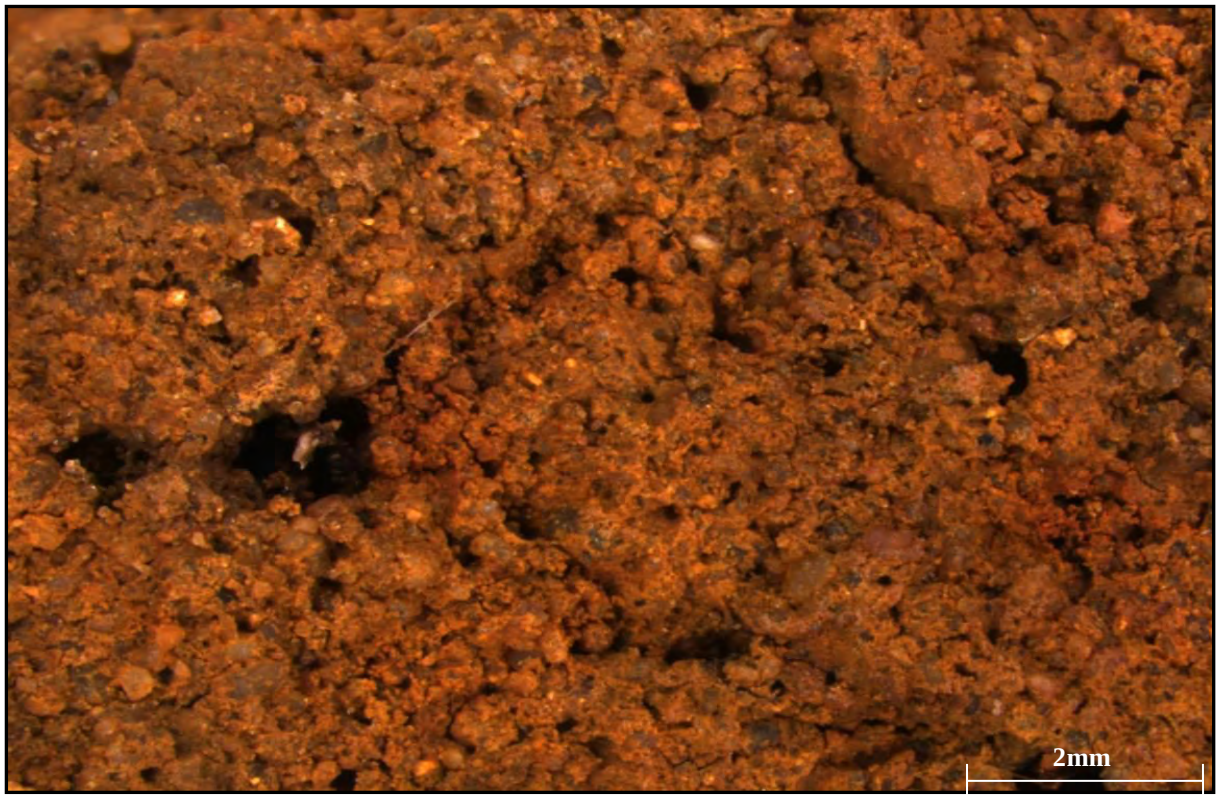

Figure 32: Optical microscope photograph - Unconsolidated Magaliesberg colluvium material (11.3x Magnification)

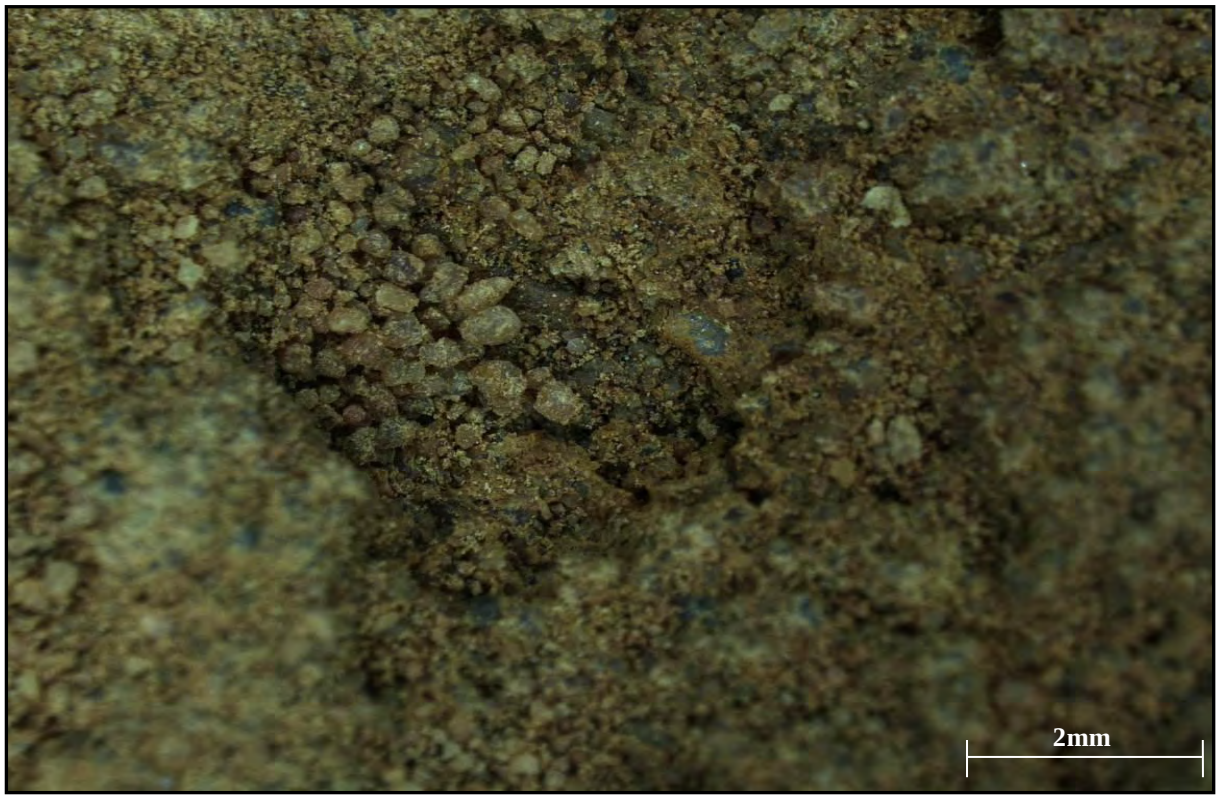

Figure 33: Optical microscope photograph - Consolidated Magaliesberg colluvium material (11.3x Magnification)

4.4 XRD/XRF analysis

Representative samples of the collected material were submitted for Qualitative and Quantitative XRD (X-Ray Diffraction) and XRF (X-Ray Fluorescence) analysis at the University of Pretoria. The sample preparation and analysis was conducted according to the methodology and process stated in Loubser and Verryn (2008),

XRD analysis is performed on the samples to determine the crystalline compounds or mineral phases that comprise the material, whereas XRF analysis is used to determine the major and trace elemental or oxide content of a material (LSM Analytical Services, 2011).

The samples are prepared for XRD analysis using the back loading sample preparation method. They are analyzed using a PANalytical X'Pert Pro powder diffractometer with X'Celerator detector and variable divergence- and receiving slits with Fe filtered Co-Kα radiation. The different mineral phases are identified using X'Pert Highscore plus software.

The relative phase amounts or weight percentages are estimated using the Rietveld method with help of the Autoquan Program. Amorphous phases, if present, are not taken into consideration in the quantification of phases that are present.

For XRF analysis, the samples are roasted at 1000°C to determine Loss On Ignition (LOI). One gram of the roasted sample is then placed together with six grams of Li2 B4 O7 into a Platinum/Gold crucible and fused. The samples are then introduced to the ARL9400XL+ spectrometer where analyses are conducted using Quantas software. The Quantas software analyzes for all elements in the periodic table between Na and U, but only elements found above the detection limits are reported. The results are also monitored and filtered to eliminate the presence of the flux, wetting and oxidising agent elements.

4.4.1 Bushbuck Ridge residual granite

The qualitative XRD results of the Bushbuck Ridge residual granite are presented in Figure 34 below.

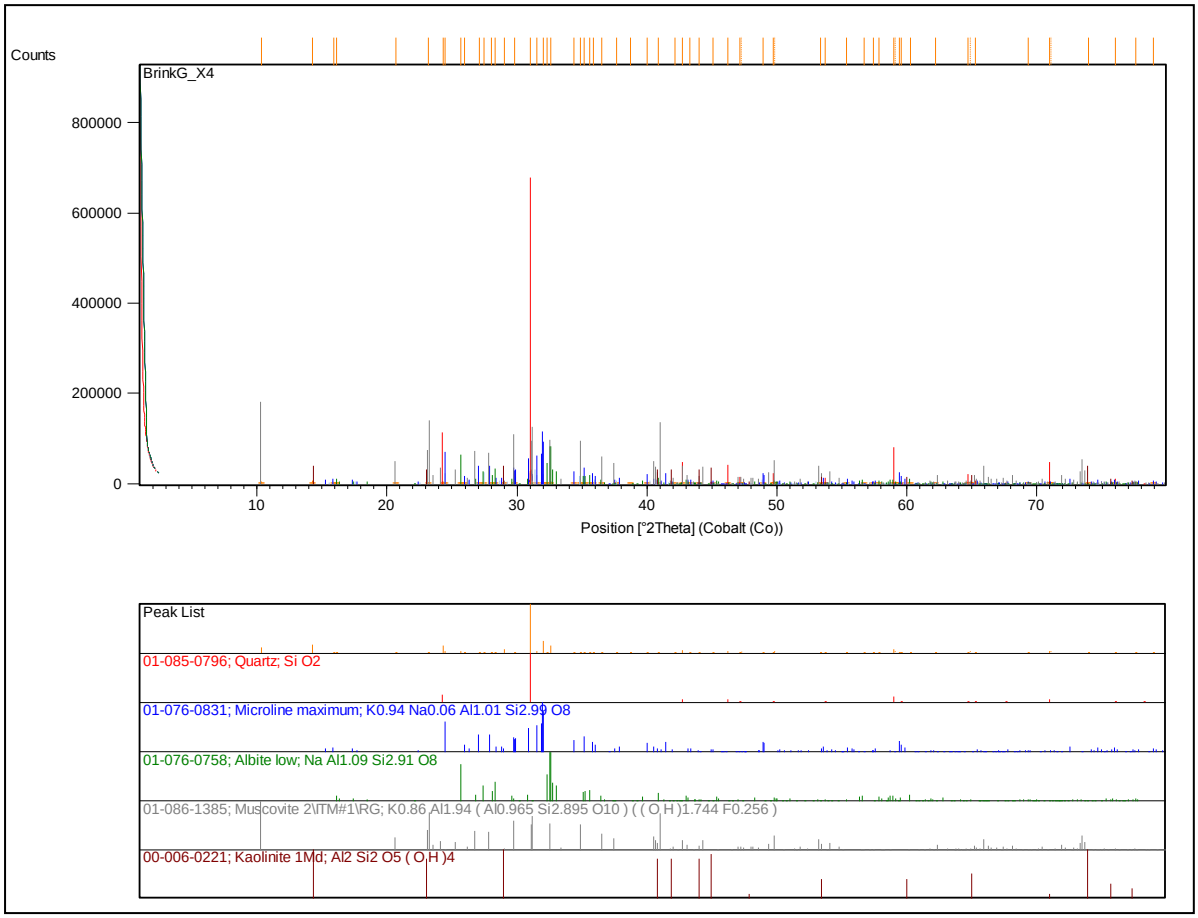

Figure 34: Qualitative XRD results: Bushbuck Ridge residual granite

The quantitative XRD results, indicating the type and abundance of the minerals constituting the material, are summarized in Table 11. Errors are on the Sigma 3 level and can be considered negligible.

Table 11: Quantitative XRD results: Bushbuck Ridge residual granite

Mineral	Abundance (%)	Deviation (%)
Kaolinite	38.95	1.29
Microcline	12.02	0.93
Muscovite	10.66	1.08
Albite	16.41	0.9
Quartz	21.96	0.81

From the results it can be seen that the material largely consists of kaolinite and quartz, with moderate percentages of sodium-rich feldspar (microcline and albite) and muscovite. The high kaolinite content is largely due to the decomposition of muscovite and the feldspar in the original parent rock during the weathering process and will account for the clay fraction present in the material.

The elemental composition of the material is determined from XRF analysis using a spectrometer. The results are summarised in Table 12 below, with only elements existing above the detection limit being reported.

Table 12: XRF results: Bushbuck Ridge residual granite

Element	XRF (%)
SiO_2	68.58
TiO_2	0.33
Al_2O_3	18.09
Fe_2O_3	2.60
MnO	0.01
MgO	0.12
CaO	0.35
Na_2O	1.25
K_2O	3.33
P_2O_5	*<0.01*
Cr_2O_3	*<0.01*
NiO	0.02
V_2O_5	*<0.01*
ZrO_2	0.01
SO_3	0.04
WO_3	0.03
BaO	0.11
Cl	0.11
CuO	*<0.01*
SrO	0.02
LOI	5.00

The major elements present in the material include silicon and aluminium oxides which occur in the majority of the minerals identified and discussed during the XRD analysis.

4.4.2 Tzaneen leocucratic biotite granite

The qualitative XRD results of the Tzaneen leucocratic biotite granite are presented in Figure 35 below.

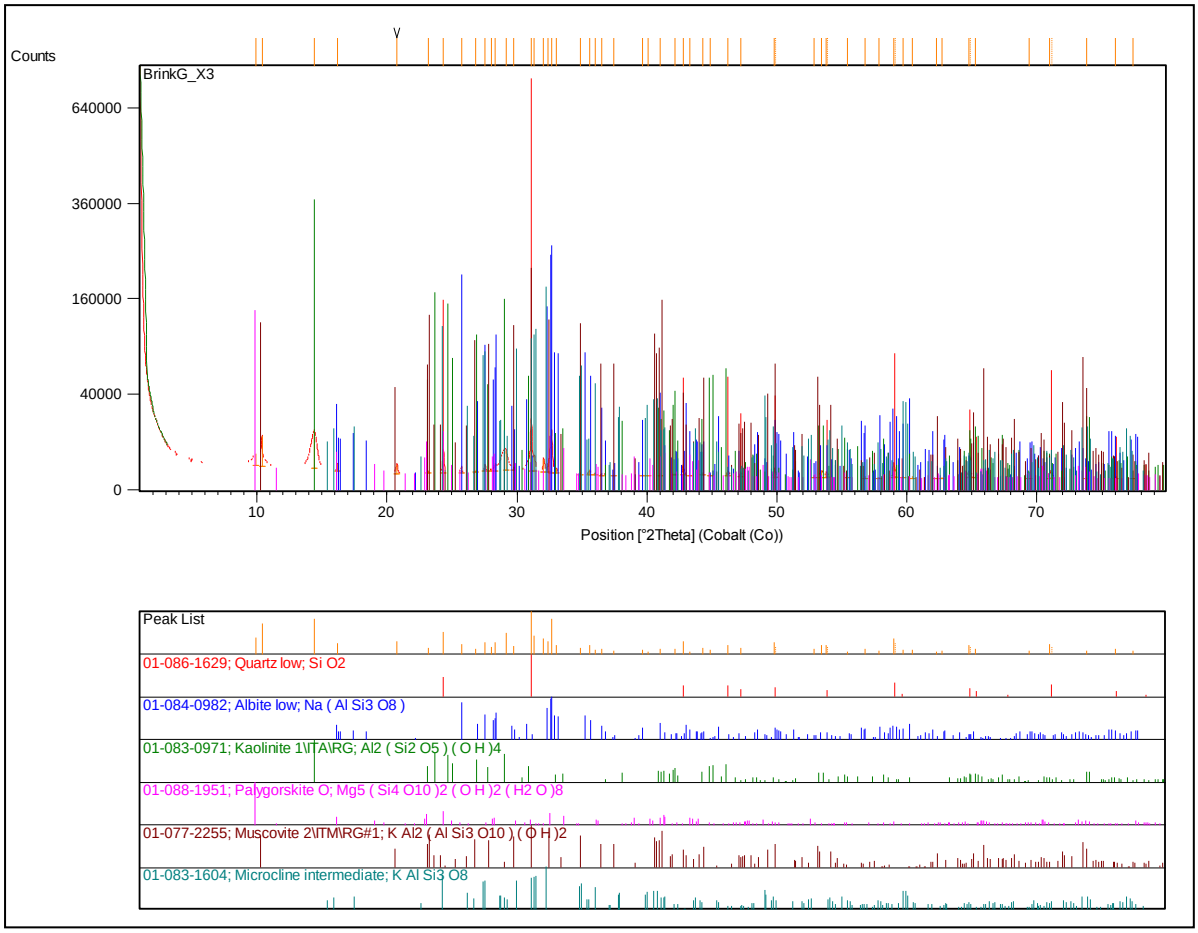

Figure 35: Qualitative XRD results – Tzaneen leucocratic biotite granite

The quantitative XRD results, indicating the type and abundance of the minerals constituting the material, are summarized in Table 13. Errors are on the Sigma 3 level and can be considered negligible.

Table 13: Quantitative XRD results: Tzaneen leucocratic biotite granite

Mineral	Abundance (%)	Deviation (%)
Kaolinite	29.73	1.92
Microcline	6.66	1.14
Muscovite	6.85	0.87
Palygorskite	22.65	2.37
Albite	13.51	1.44
Quartz	20.6	1.14

From the results it can be seen that the material largely consists of kaolinite, palygorskite and quartz, with moderate percentages of sodium-rich feldspar (microcline and albite) and muscovite.

The elemental composition of the material is determined from XRF analysis using a spectrometer. The results are summarised in Table 14 below, with only elements existing above the detection limit being reported.

Table 14: XRF results: Tzaneen leucocratic biotite granite

Element	XRF (%)
SiO_2	72.23
TiO_2	0.25
Al_2O_3	15.90
Fe_2O_3	2.17
MnO	0.03
MgO	0.65
CaO	0.63
Na_2O	1.80
K_2O	1.42
P_2O_5	*<0.01*
Cr_2O_3	*<0.01*
NiO	0.01
V_2O_5	*<0.01*
ZrO_2	*<0.01*
SO_3	*<0.01*
WO_3	0.01
BaO	*<0.01*
Cl	0.03
CuO	*<0.01*
SrO	*<0.01*
LOI	4.84

The major elements present in the material include silicon and aluminium oxides which occur in the majority of the minerals identified and discussed during the XRD analysis.

4.4.3 Lephalale aeolian sand

The qualitative XRD results of the Lephalale aeolian sand are presented in Figure 36 below.

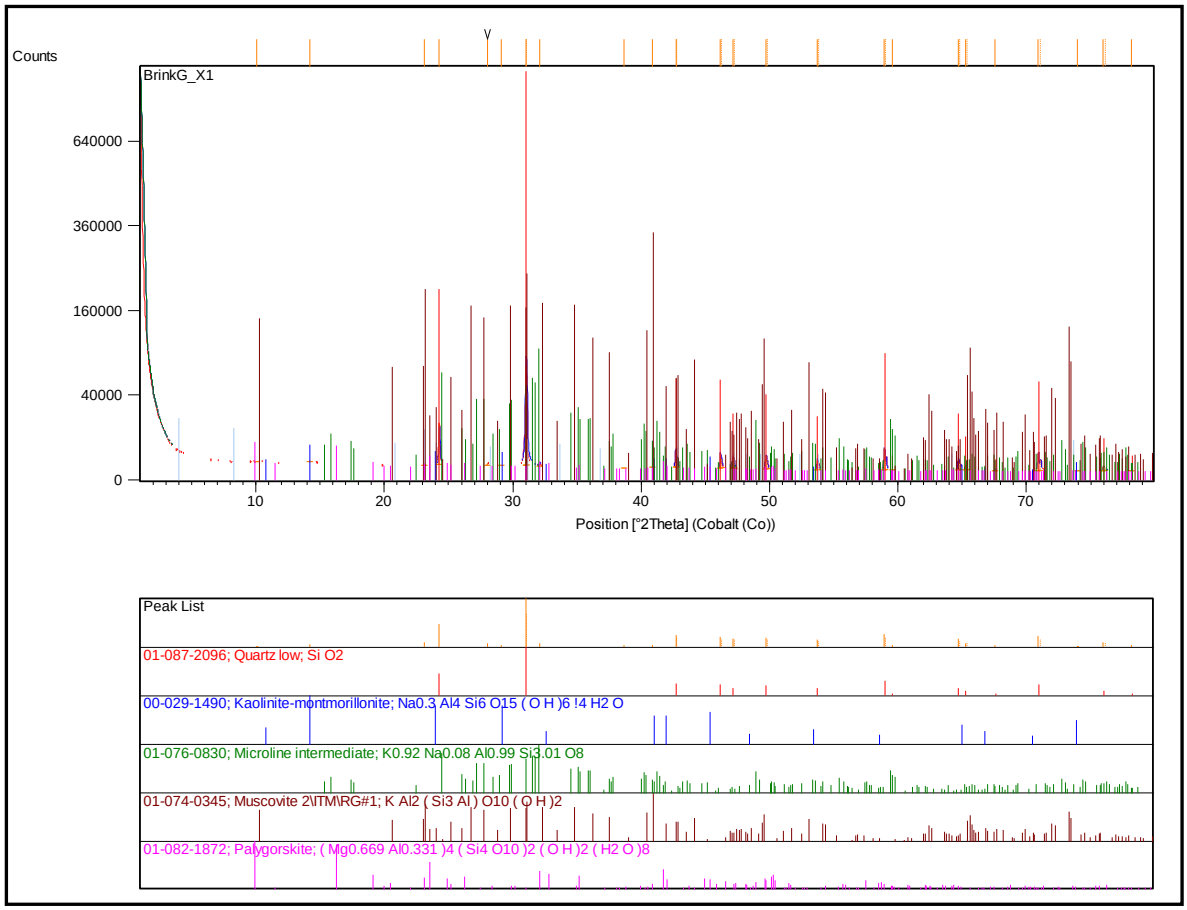

Figure 36: Qualitative XRD results - Lephalale aeolian sand

The quantitative XRD results, indicating the type and abundance of the minerals constituting the material, are summarized in Table 15. Errors are on the Sigma 3 level and can be considered negligible.

Table 15: Quantitative XRD results: Lephalale aeolian sand

Mineral	Abundance (%)	Deviation (%)
Kaolinite	18.56	1.14
Muscovite	3.87	0.78
Orthoclase	2.96	0.81
Palygorskite	1.94	1.44
Quartz	72.67	1.71

From the results it can be seen that the material largely consists of kaolinite and quartz, with low percentages of orthoclase, palygorskite and muscovite. The high quartz content is reflected in the grain size distribution results by the high percentage sand in the material.

The elemental composition of the material is determined from XRF analysis using a spectrometer. The results are summarised in Table 16 below, with only elements existing above the detection limit being reported.

Table 16: XRF results: Lephalale aeolian sand

Element	XRF (%)
SiO_2	86.32
TiO_2	0.36
Al_2O_3	7.02
Fe_2O_3	1.91
MnO	0.01
MgO	0.08
CaO	0.08
Na_2O	0.24
K_2O	0.47
P_2O_5	0.01
Cr_2O_3	0.01
NiO	0.02
V_2O_5	*<0.01*
ZrO_2	0.02
SO_3	*<0.01*
WO_3	0.03
BaO	*<0.01*
Cl	0.07
CuO	*<0.01*
SrO	*<0.01*
LOI	3.35

The major elements present in the material include silicon and aluminium oxides which occur in the majority of the minerals identified and discussed during the XRD analysis.

4.4.4 Magaliesberg colluvium

The qualitative XRD results of the Magaliesberg colluvium are presented in Figure 37 below.

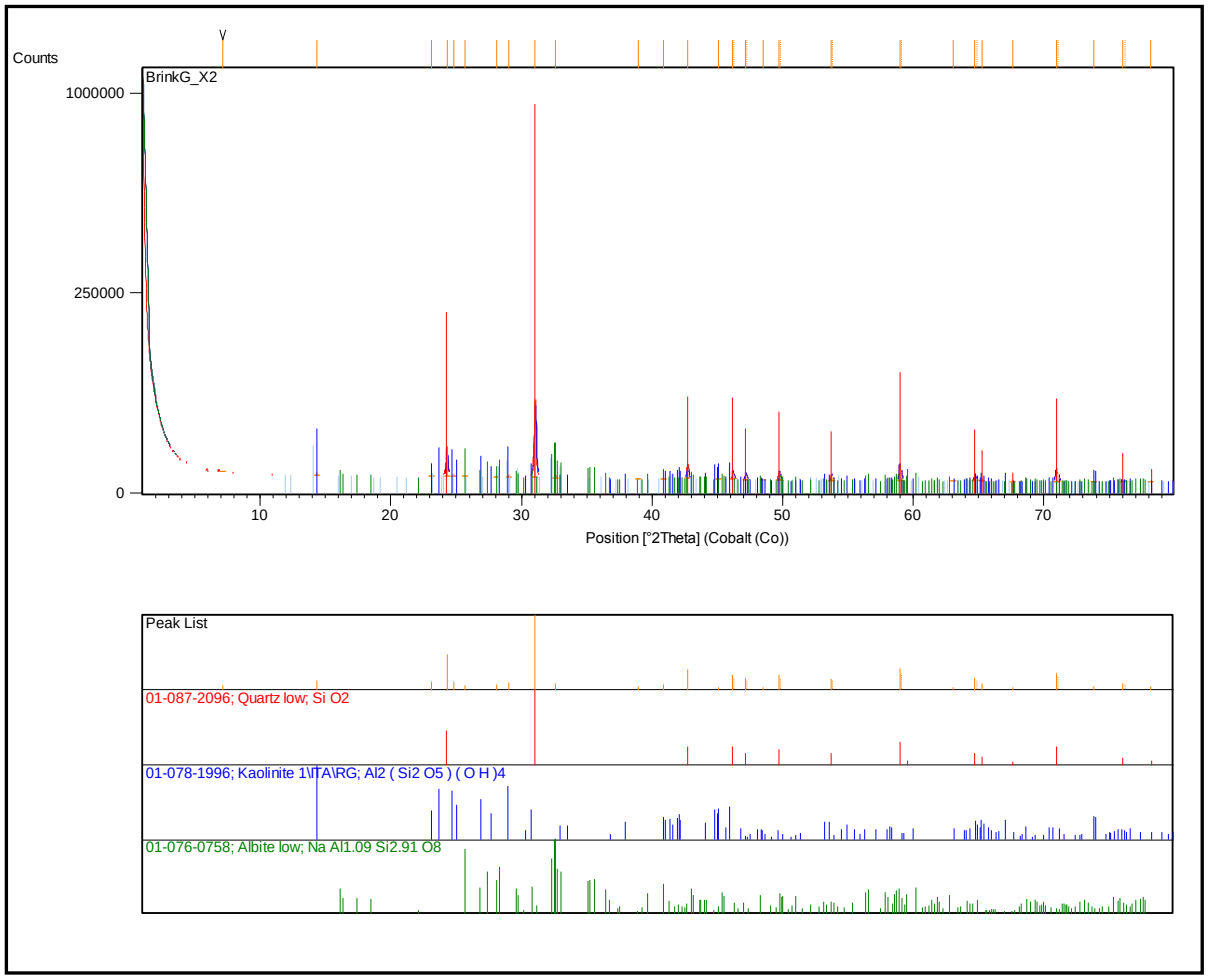

Figure 37: Qualitative XRD results - Magaliesberg colluvium

The quantitative XRD results, indicating the type and abundance of the minerals constituting the material, are summarized in Table 17. Errors are on the Sigma 3 level and can be considered negligible.

Table 17: Quantitative XRD results: Magaliesberg colluvium

Mineral	Abundance (%)	Deviation (%)
Kaolinite	35.87	1.26
Plagioclase	2.9	0.66
Quartz	61.23	1.32

From the results it can be seen that the material largely consists of kaolinite and quartz, with a low percentage of plagioclase feldspar. The high quartz content is reflected in the grain-size distribution results by the high percentage sand in the material.

The elemental composition of the material is determined from XRF analysis using a spectrometer. The results are summarised in Table 18 below, with only elements existing above the detection limit being reported.

Table 18: XRF results: Magaliesberg colluvium

Element	XRF (%)
SiO_2	78.31
TiO_2	0.57
Al_2O_3	8.27
Fe_2O_3	6.06
MnO	0.02
MgO	0.17
CaO	0.17
Na_2O	0.29
K_2O	0.30
P_2O_5	*<0.01*
Cr_2O_3	0.01
NiO	0.02
V_2O_5	0.05
ZrO_2	0.02
SO_3	*<0.01*
WO_3	0.02
BaO	*<0.01*
Cl	0.06
CuO	0.01
SrO	*<0.01*
LOI	5.66

The major elements present in the material include silicon and aluminium oxides which occur in the majority of the minerals identified and discussed during the XRD analysis.

5. DATA EVALUATION AND DISCUSSION

The discussion and evaluation of data is based on all of the available results and observations made during the testing procedure of the collapsible materials. The results are evaluated and discussed individually for each of the samples in the sections below.

5.1 Residual Material: Bushbuck Ridge residual granite

5.1.1 Material property description

Using the calculations as summarised and discussed in Section 4.2.5, the *in-situ* void ratio (before consolidation), dry density, degree of saturation and natural moisture content of the material can be determined. These properties were determined whilst consolidation testing was in progress and is vital in characterizing the consolidation behaviour of the material during increased applied stress and moisture content. The results are summarised in Table 19 below.

Table 19: Calculated material properties: Bushbuck Ridge residual granite

Material Property	Value
Dry density (kg/m^3)	1392
Initial void ratio	0.864
Natural moisture content (%)	7.15
Degree of saturation (%)	22

5.1.2 Optical microscope analysis

From the microscope analysis and photographs a visible change in structure was noticed after consolidation of the material, with the most noticeable change being that there is a significant decrease in the **number** of voids in the material after consolidation has taken place, with the average **size** of the voids remaining constant. This implies that volume change through collapse settlement in the material is governed by the total loss in volume of some voids whilst the rest remained unchanged during an increase in moisture content or applied stress.

5.1.3 Consolidation characteristics

The results and behaviour of the Bushbuck Ridge residual granite material during consolidometer testing are summarised in Figures 38 and 39 below. Figure 38 illustrates the change in void ratio of the material from its natural *in-situ* void ratio (e_0) throughout an increase in applied stress and moisture content up to a final stress of 800 kPa. Figure 39 highlights that part of consolidation testing where the moisture content is incrementally increased at a constant applied stress (200 kPa), subsequently indicating the change in void ratio (e) as the natural moisture content of the material is incrementally increased.

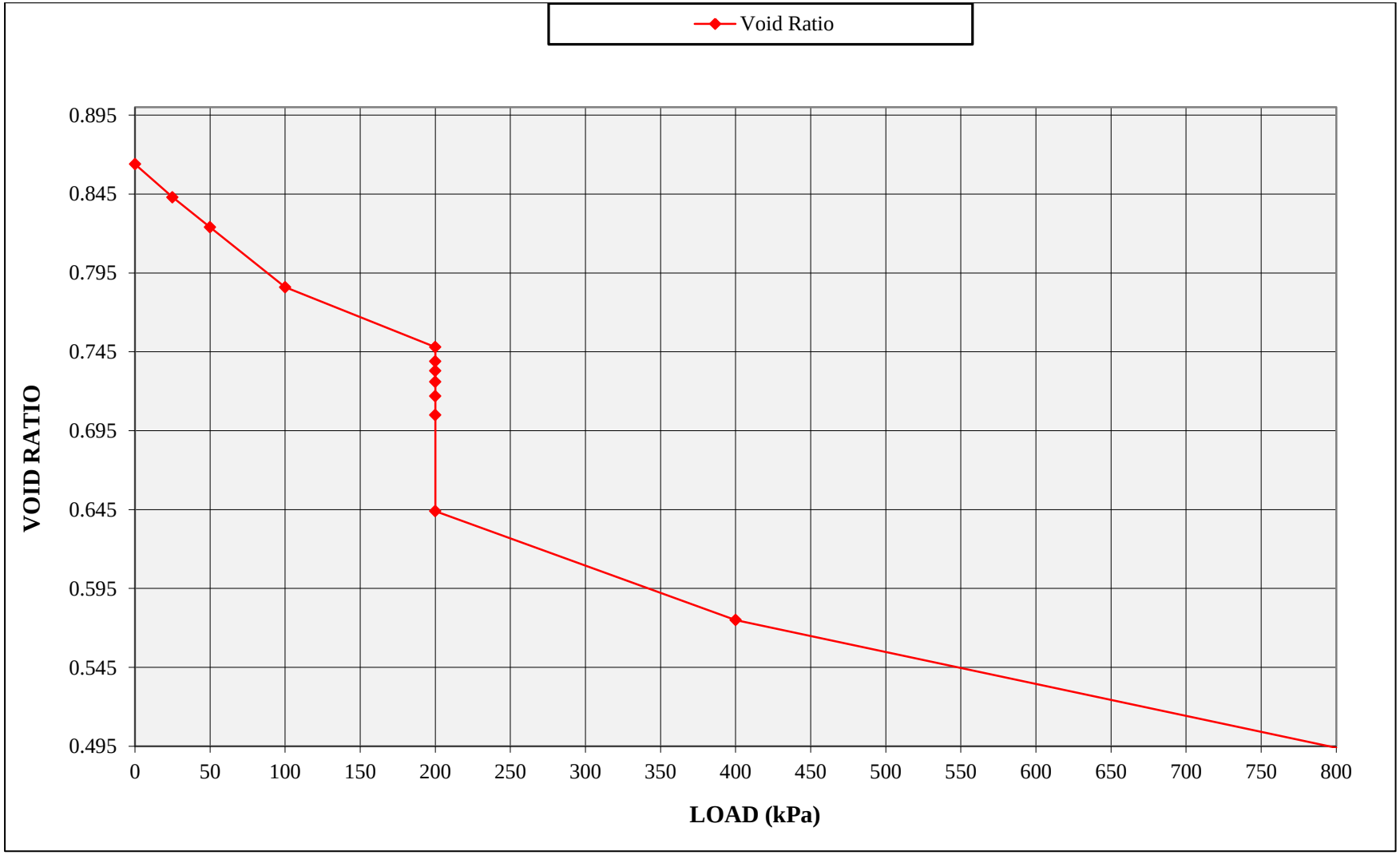

Figure 38: Consolidation and collapse settlement - Bushbuck Ridge residual granite

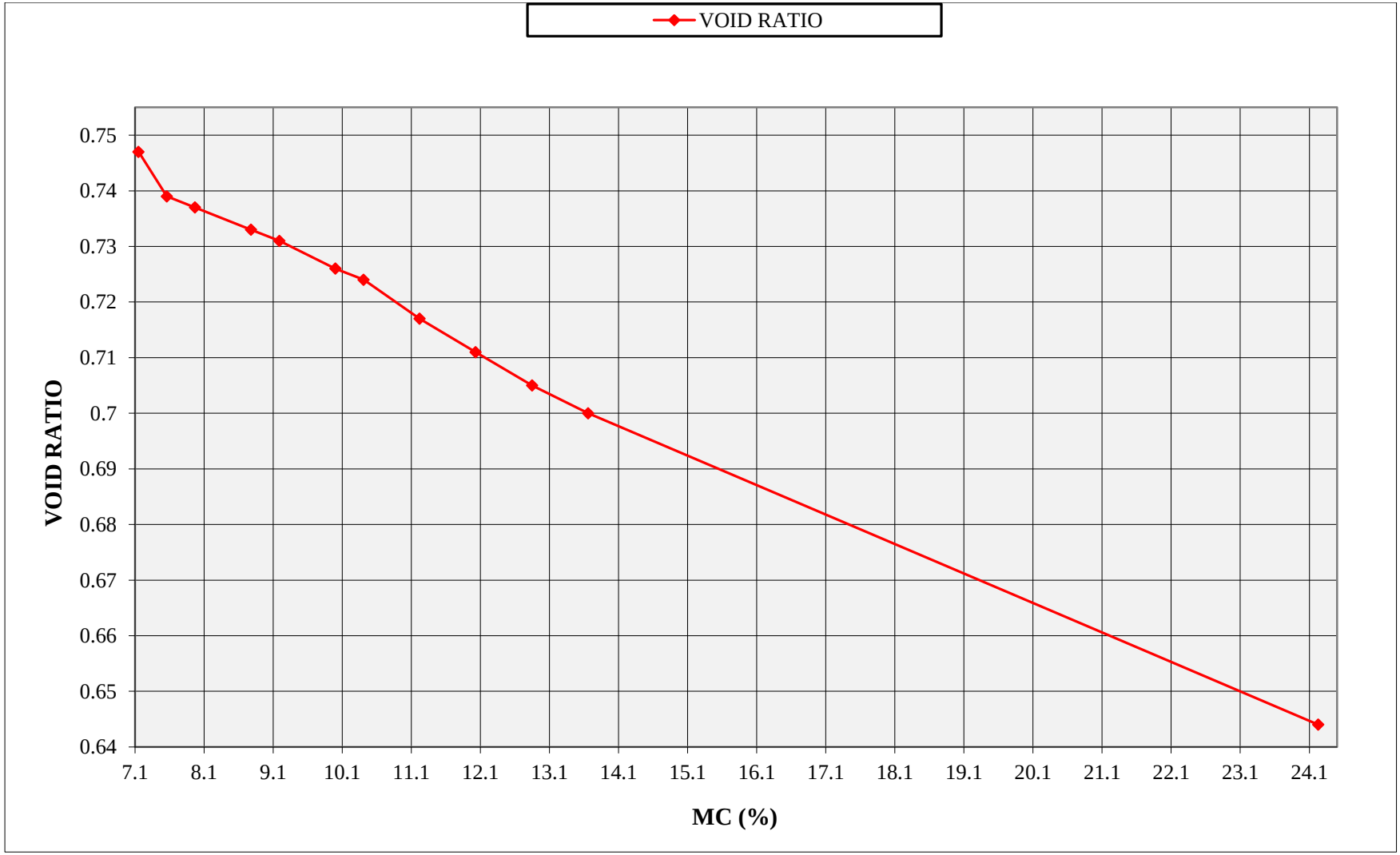

Figure 19: Change in void ratio with change in moisture content at a constant load of 200 kPa - Bushbuck Ridge residual granite

From Figure 38 it can be seen that with an increase in the applied stress the void ratio of the material decreases due to the reduction in the total volume of voids in the material. Once the applied stress has reached 200 kPa and the rate of creep has subsided sufficiently, additional moisture is added to the system for the first time and collapse of the soil structure occurs.

Figure 39 shows that for the Bushbuck Ridge residual material an almost linear relationship exists between the increase in moisture content and the decrease in void ratio. This means that as the moisture content of the material is increased a decrease in the overall void ratio of the material takes place. The moisture content is increased incrementally from the natural moisture content of 7.15 % up to a final moisture content of 24.2 %, with sufficient time permitted between increments to allow the creep rate to subside to less than 0.25% per hour (as in Rust *et al.*, 2005).

Once creep associated with the collapse event decreased sufficiently, loading was continued up to the final applied stress of 800 kPa.

The collapse potential for the Bushbuck Ridge residual granite is calculated at 5.5 %, which can be classified according to Jennings and Knight (1975) as indicating “trouble”.

5.1.4 Pore fluid suction pressure measurements

Matrix suction measurements were conducted using the filter paper method as described in Section 4.2.3. Suction pressure was taken as the average value of the two measurements derived from using two pieces of Whatman no 42 filter paper, Paper A and Paper B and plotted on a log-scale. The results of the suction measurements for the Bushbuck Ridge residual granite material are indicated in Figure 40.

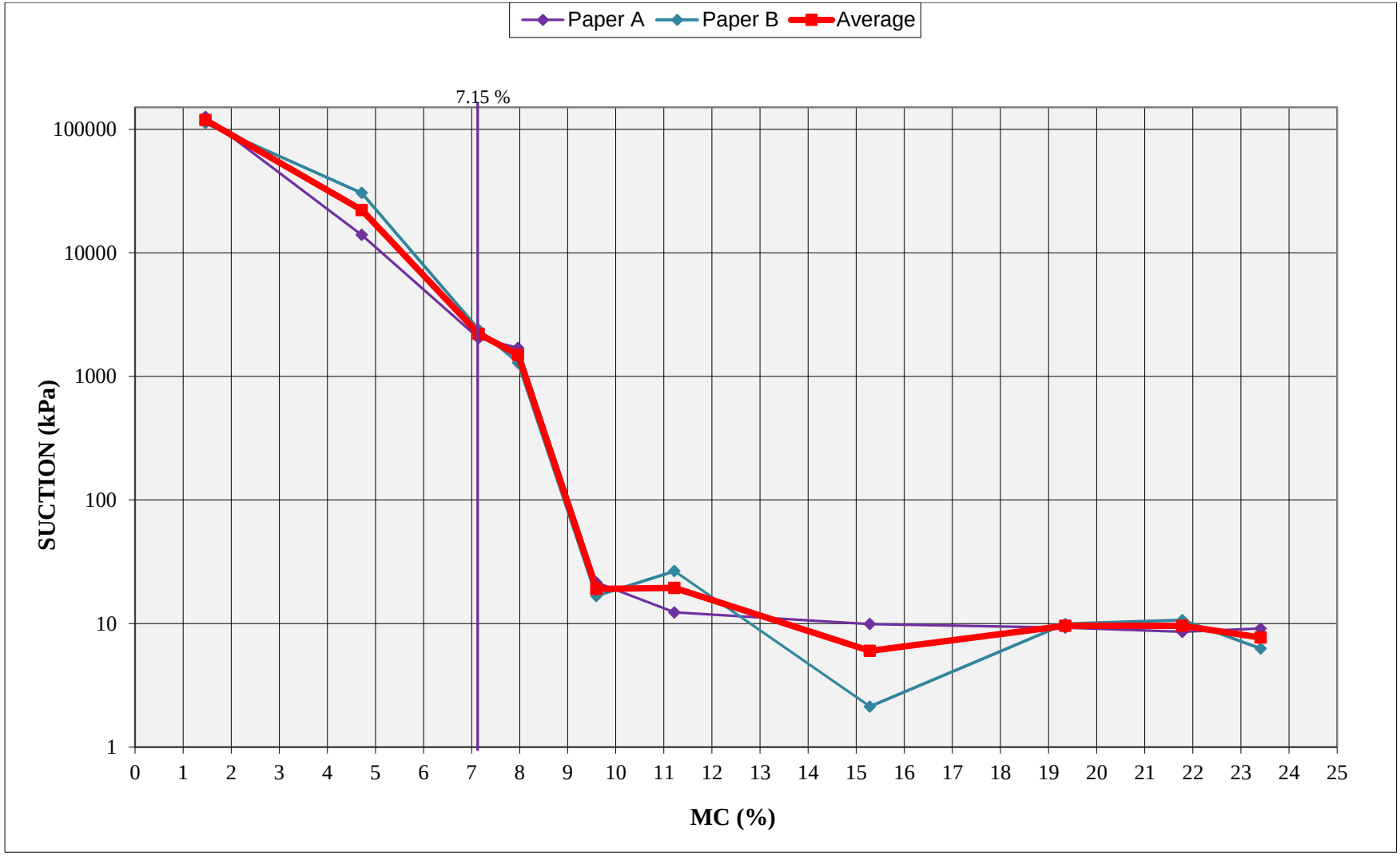

Figure 40: Matrix suction measurements - Bushbuck Ridge residual granite

The figure indicates that suction pressures are high in the residual granite material at the *in-situ* moisture content of 7.15 %, roughly equalling 2210 kPa. As the moisture content of the material increases the suctions decrease steadily, until a threshold or "critical" moisture content is reached (approximately 8 %). Once this moisture content is reached there is a sudden and dramatic decrease in the suction pressures. The suctions continue to decrease up to moisture content of between 9 % and 10 %, from where further increase in the moisture content no longer appears to have a significant effect on the suction pressures of the material and the magnitude of the suction forces can be considered negligible.

5.1.5 Relationship between pore fluid suction pressures and consolidation

Using the data represented in Figures 38 to 40, it is possible to relate the decrease in void ratio during wetting with the reduction in suction pressures as the moisture content is increased at a constant applied stress of 200 kPa. By interpolating the suction pressure values for the different moisture contents of the material during consolidometer testing, the change in void ratio can be plotted against the change in suction pressures, with suction pressures plotted on a log-scale in a decreasing order (Figure 41). The void ratio and suction pressure values for the different moisture contents are summarized in Table 20.

Table 20: Void ratio and suction values at different moisture contents: Bushbuck Ridge residual granite

MC (%):	7.15	7.56	7.97	8.78	9.19	10	10.41	11.22	12.03	12.85	13.66	23.41
VOID RATIO	0.747	0.739	0.737	0.733	0.731	0.726	0.724	0.717	0.711	0.705	0.7	0.65
SUCTION (kPa)	2208	1866	1495	1126	934	580	388	19.44	18.66	17.94	17.06	7.7

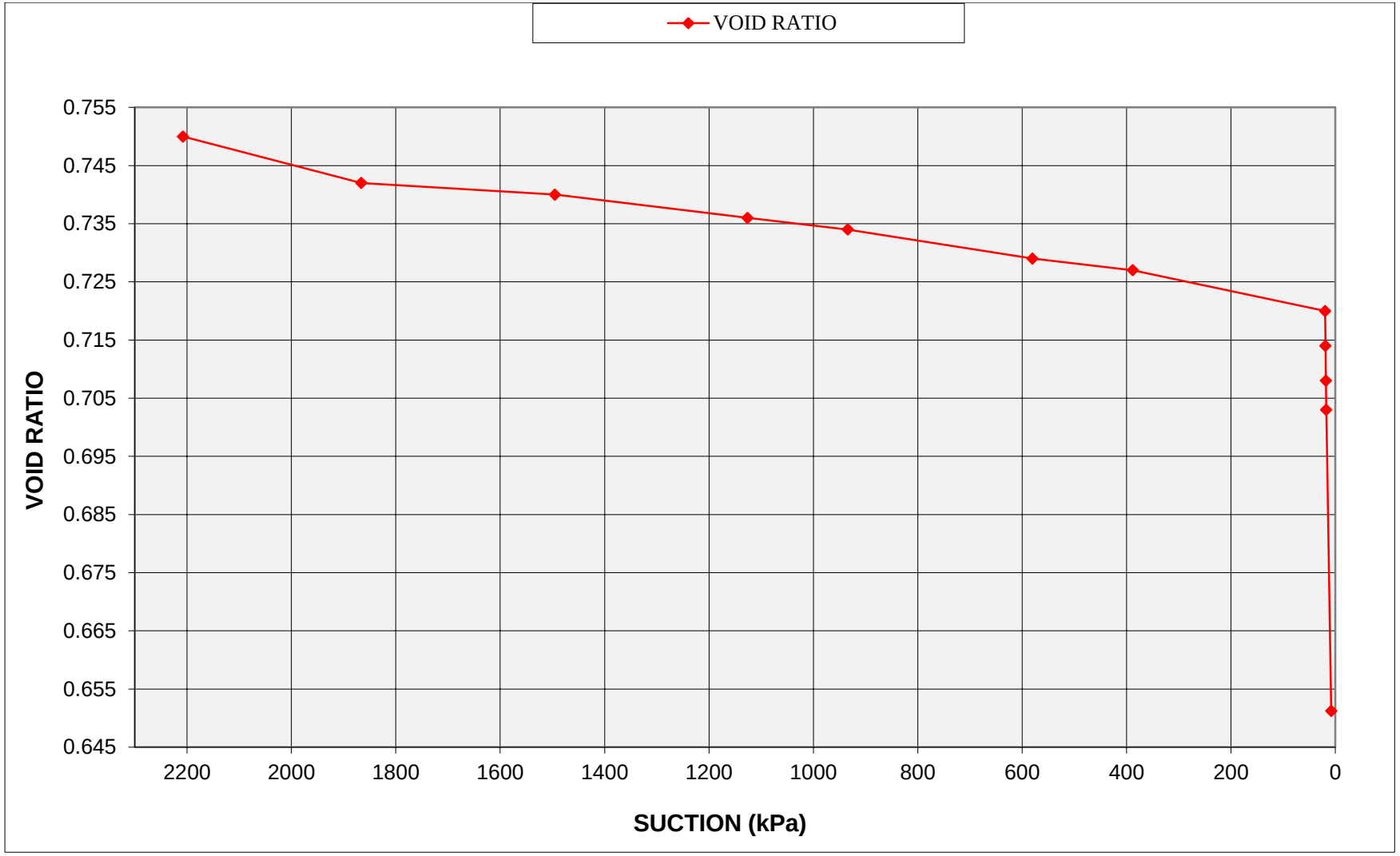

Figure 41: Relationship between consolidation and soil suction pressures with increasing moisture content - Bushbuck Ridge residual granite

It is evident from Table 20 and Figure 41 that the overall void ratio of the residual material decreases as the suction pressures in the material decrease during the increase in moisture content of the material. This relationship between void ratio and suction pressures can be expressed in terms of two phases (Figure 42).

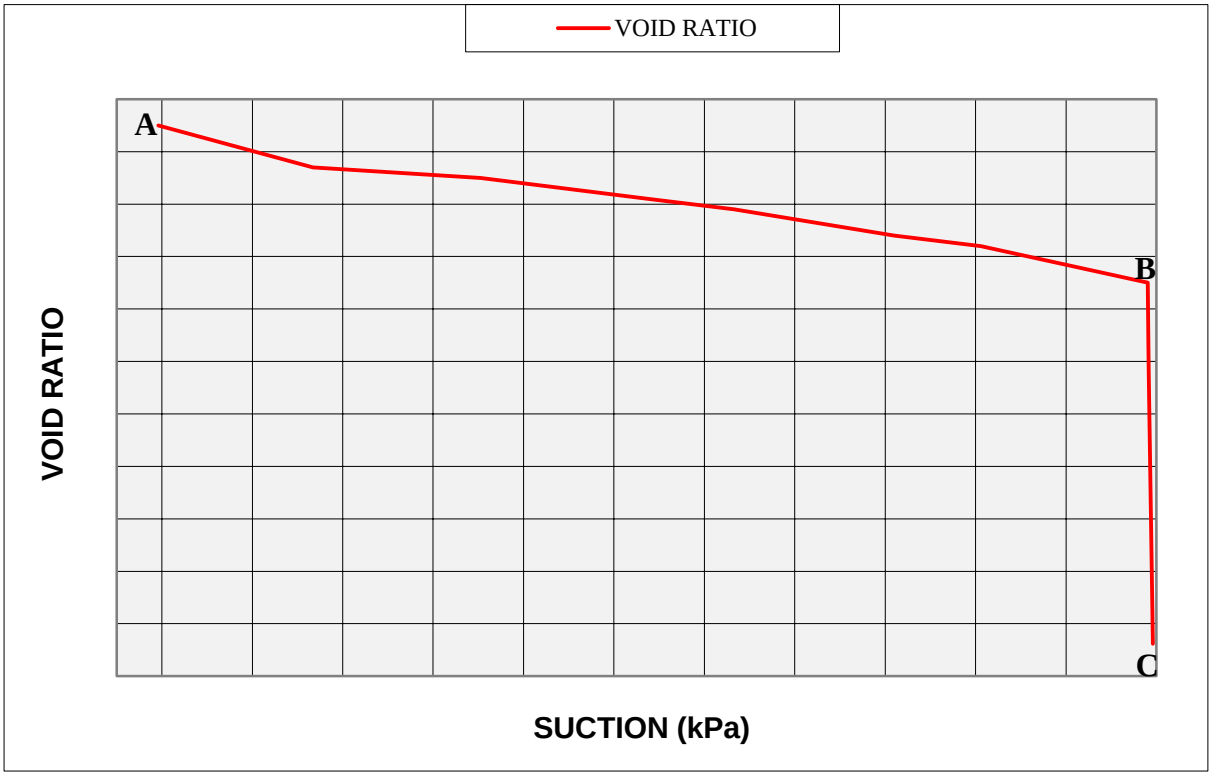

Figure 42: Two-phase behaviour between suction pressures and void ratio at a constant load of 200 kPa - Bushbuck Ridge residual granite

During the first phase (A-B) both the void ratio and the suction pressures of the material decrease steadily with an increase in moisture content. The void ratio decreases from its initial value (consolidated at 200 kPa) of 0.747 to 0.717 and suction pressures from 2208 kPa to 19 kPa with an increase in the natural moisture content of the material from 7.15 % to 11.22 %.

The second phase (B-C) is characterized by a sudden, very significant drop in the void ratio of the material, dropping from 0.717 to 0.650. Suction pressures continue to decrease, but the decrease is much less significant when compared to the decrease in suction pressures during the first phase.

It can therefore be argued that the void ratio and suction pressures will decrease steadily as the moisture content is increased (A-B) up to a **critical point** (Point B) where suction pressures have decreased sufficiently to trigger collapse (B-C) and a subsequent sudden decrease in void ratio.

5.1.6 Relationship between effective stress and soil collapse

The effective stress is assumed to be the sum of the applied stress (total stress) and the pore water suction pressures. The change in the void ratio of the material with a change in the effective stress of the residual granitic material is plotted on a log-scale and illustrated in Figure 43.

The intrinsic consolidation curve, representing the consolidation properties of the material independent of the natural state of the material is also indicated in Figure 43.

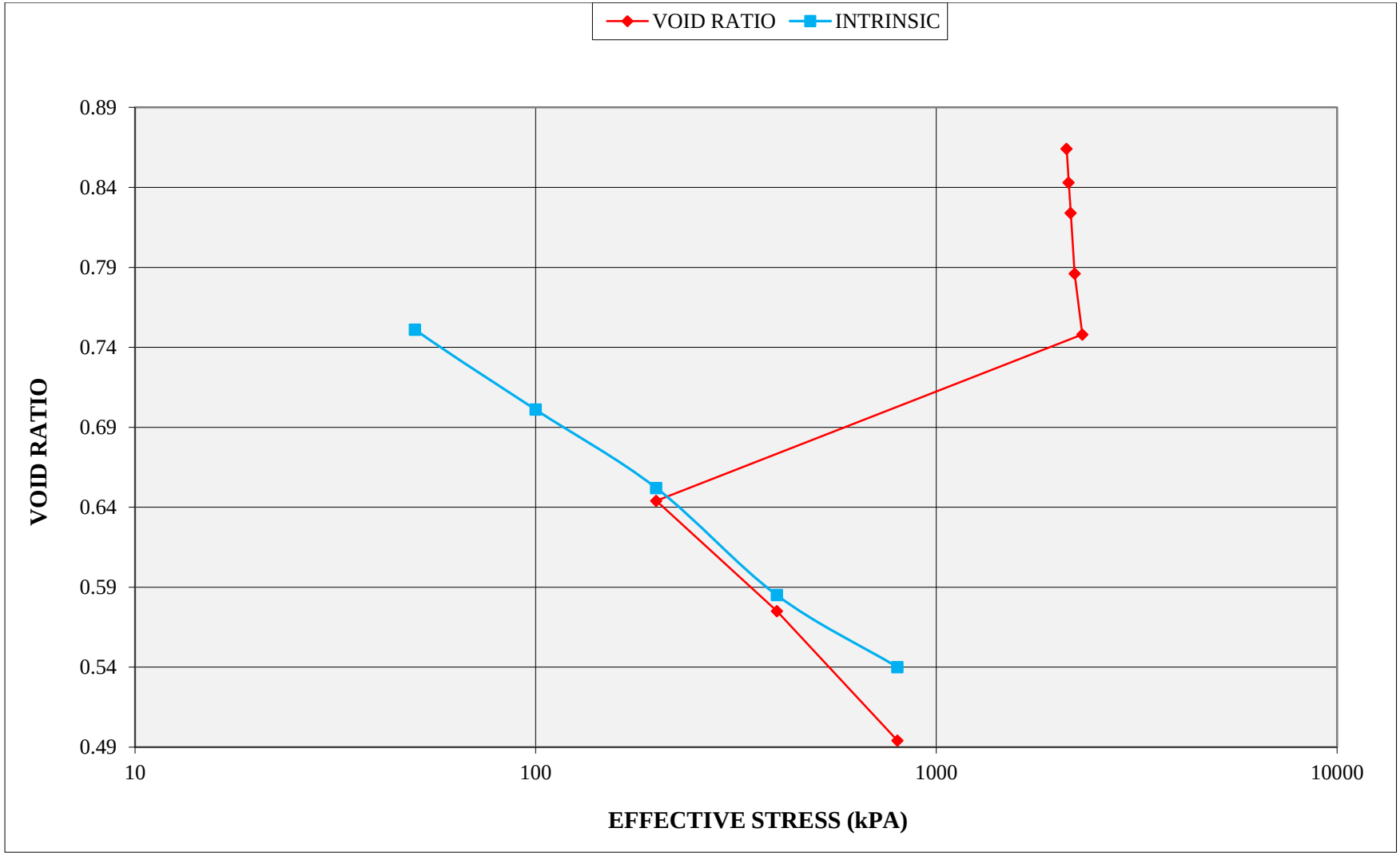

Figure 43: Effect of change in effective stress state on consolidation - Bushbuck Ridge residual granite

It is clear that the effective stress state of the material is controlled by the magnitude of the pore water suction pressures at lower moisture contents. Initially the void ratio decreases as the effective stress increases with an increase in the applied stress up to 200 kPa. At this stage the influence of the applied stress on the overall effective stress and consolidation behaviour is minimal due to the magnitude of the suction pressures influencing the effective stress state. However, as soon as additional moisture is introduced to the material at 200 kPa and the "critical" moisture content is reached, the pore water suction pressures and subsequently the effective stress decreases dramatically. It should be appreciated that this is an immediate change in the effective stress state that occurs as soon as the material has reached the particular "critical" moisture content and suction pressures decrease. Once this point is reached, the influence of the applied stress becomes the predominant influence on the consolidation behaviour of the material.

The void ratio of the Bushbuck Ridge material decreases up to its final value of 0.494 as the effective stress state of the material increases, almost exclusively now due to the influence of the increase in applied stress and the effect of suction pressures being considered negligible.

When comparing the consolidation of the material after the drop in effective stress (and thus after collapse) with the intrinsic compressibility of the material, it is evident that the void ratios at the particular effective stresses correlate very closely for the two samples. As the reconstituted sample represents the compressibility of the material without being affected by the soil structure, this close correlation of the void ratios of the two samples implies that after collapse has occurred the remaining soil structure, if any, has very little influence on the consolidation behaviour of the material.

5.2 Residual Material: Tzaneen residual leucocratic biotite granite

5.2.1 Material property description

Using the calculations as summarised and discussed in Section 4.2.5, the *in-situ* void ratio (before consolidation), dry density, degree of saturation and natural moisture content of the material can be determined. These properties were determined whilst consolidation testing was in progress and is vital in characterizing the consolidation behaviour of the material during increased applied stress and moisture content. The results are summarised in Table 21 below.

Table 21: Calculated material properties: Tzaneen residual granite

Material Property	Value
Dry density (kg/m^3)	1400
Initial void ratio	0.852
Natural moisture content (%)	18
Degree of saturation (%)	55.9

5.2.2 Optical microscope analysis

From the microscope analysis and photographs a definitive change in the structure of the material was noticed after consolidation of the material, with the most noticeable change being that there is a significant decrease in the **number** of voids in the material after consolidation has taken place, with the average **size** of the voids remaining constant. This implies that volume change through collapse settlement in the material is governed by the total loss in volume of some voids whilst the rest remain unchanged with an increase in moisture content or applied stress.

5.2.3 Consolidation characteristics

The results and behaviour of the Tzaneen residual granite material during consolidometer testing are summarised in Figures 44 and 45 below. Figure 44 illustrates the change in void ratio of the material from its natural *in-situ* void ratio (e_0) throughout an increase in applied stress and moisture content up to a final stress of 800 kPa. Figure 45 highlights that part of consolidation testing where the moisture content is incrementally increased at a constant applied stress (200 kPa), subsequently indicating the change in void ratio (e) as the natural moisture content of the material is incrementally increased.

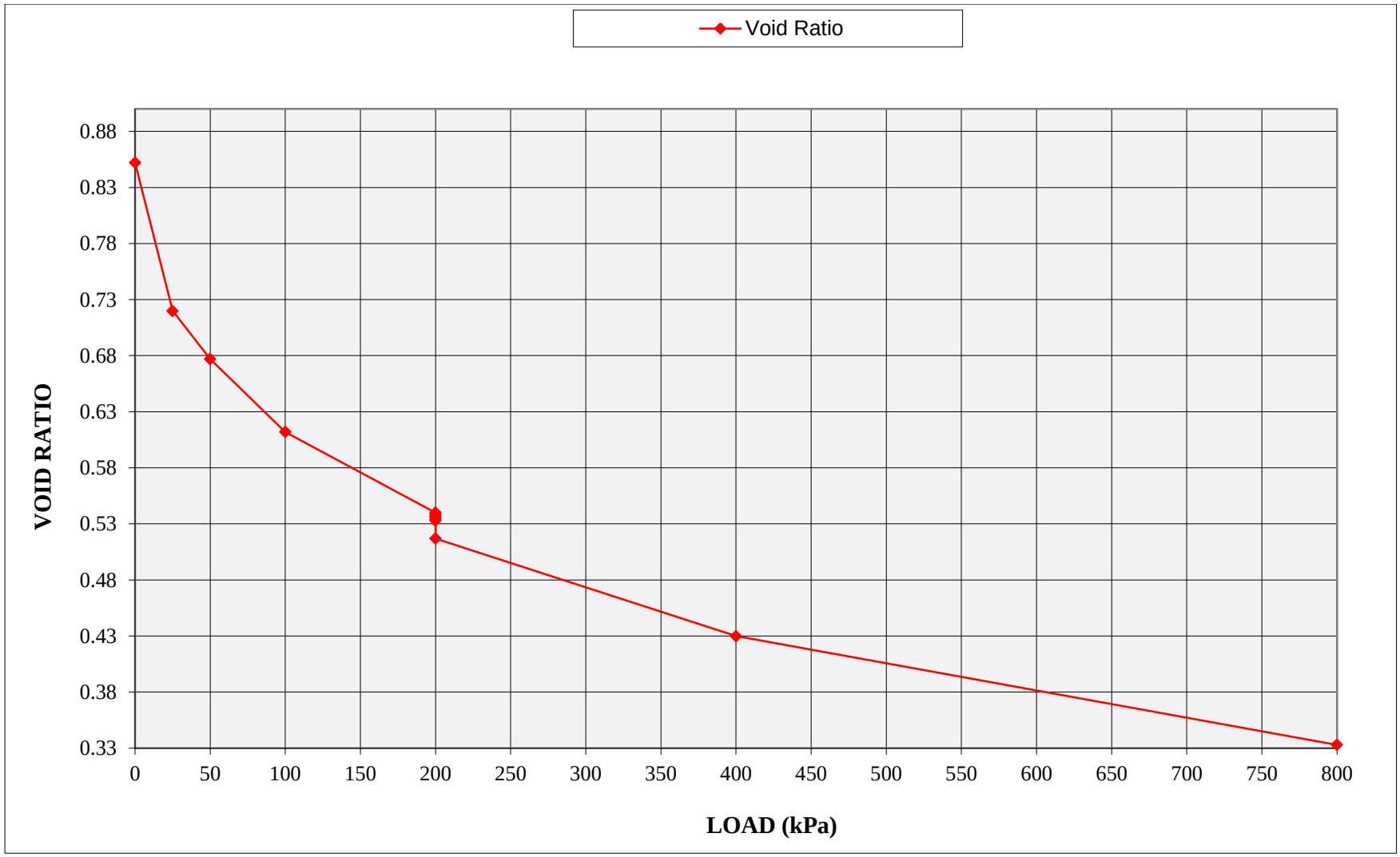

Figure 44: Consolidation and collapse settlement - Tzaneen residual granite

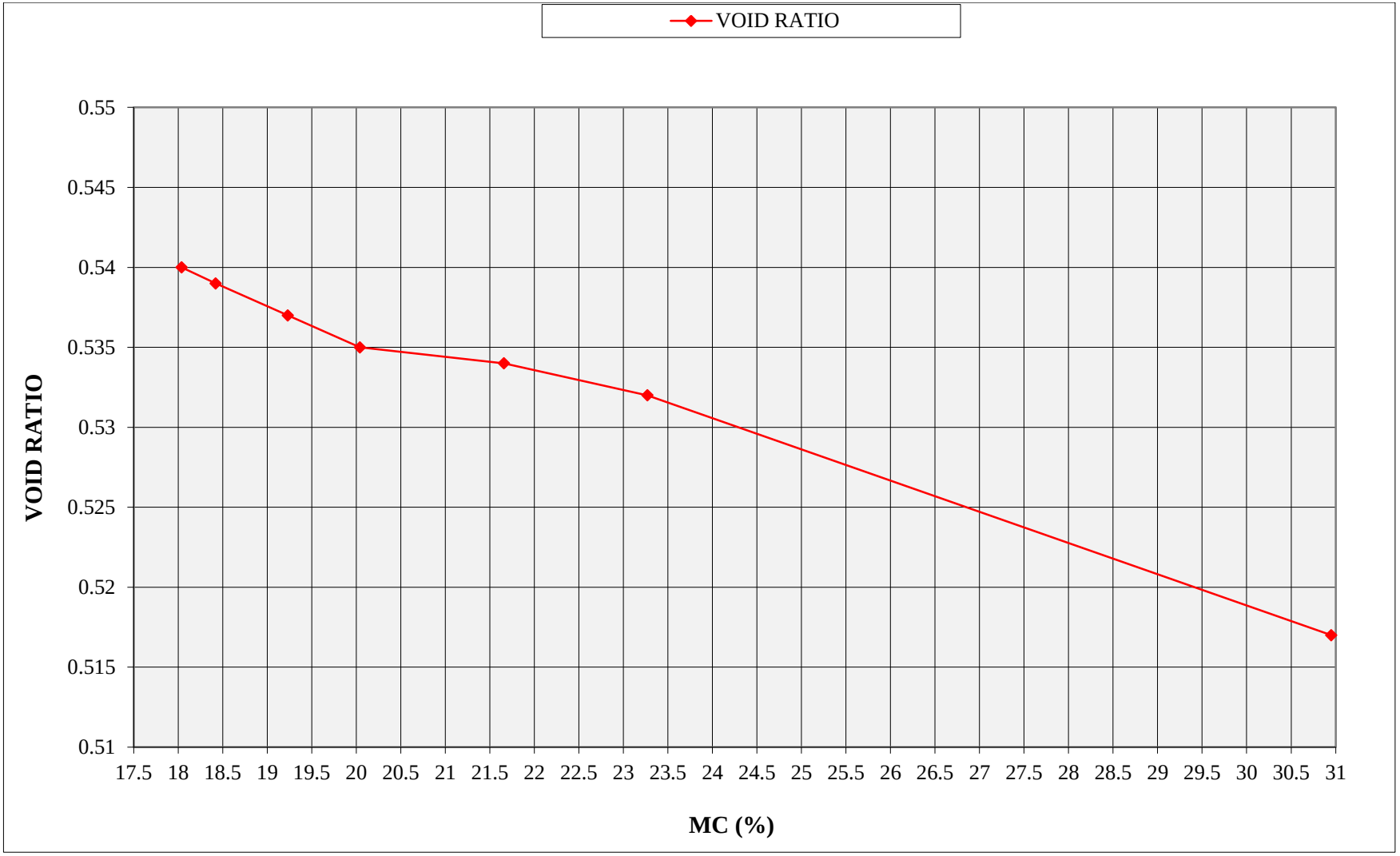

Figure 45: Change in void ratio with change in moisture content at a constant load of 200 kPa - Tzaneen residual granite

From Figure 44 it can be seen that there is a significant decrease in void ratio at low applied stress. Once the applied stress has reached 200 kPa and the rate of creep has subsided sufficiently, additional moisture is added to the system for the first time and collapse of the soil structure occurs. The initial consolidation of the Tzaneen residual material (from 0 to 200 kPa) is much more pronounced than for the previously discussed residual granite material from the Bushbuck Ridge area, largely due to the higher initial moisture content. As a result, the amount of collapse settlement occurring once additional moisture is introduced at 200 kPa is comparatively little, decreasing from 0.540 to 0.517, due to a large percentage of the voids already being consolidated.

Figure 45 shows that for the Tzaneen residual material an almost linear relationship exists between the increase in moisture content and the decrease in void ratio. This means that as the moisture content of the material is increased a decrease in the overall void ratio of the material takes place. The moisture content is increased incrementally from the natural moisture content of 18%, with sufficient time permitted between increments to allow the creep rate to subside to less than 0.25% per hour (as in Rust *et al.*, 2005).

Once creep associated with the collapse event decreased sufficiently, loading was continued up to the final applied stress of 800 kPa.

The collapse potential is calculated at 1.24 %, which can be classified by Jennings and Knight (1975) as indicating “moderate trouble”.

5.2.4 Pore fluid suction pressure measurements

Matrix suction measurements were conducted using the filter paper method as described in Section 4.2.3. Suction pressure was taken as the average value of the two measurements derived from using two pieces of Whatman no 42 filter paper, Paper A and Paper B and plotted on a log scale. The results of the suction measurements for the Tzaneen residual granite material are indicated in Figure 46.

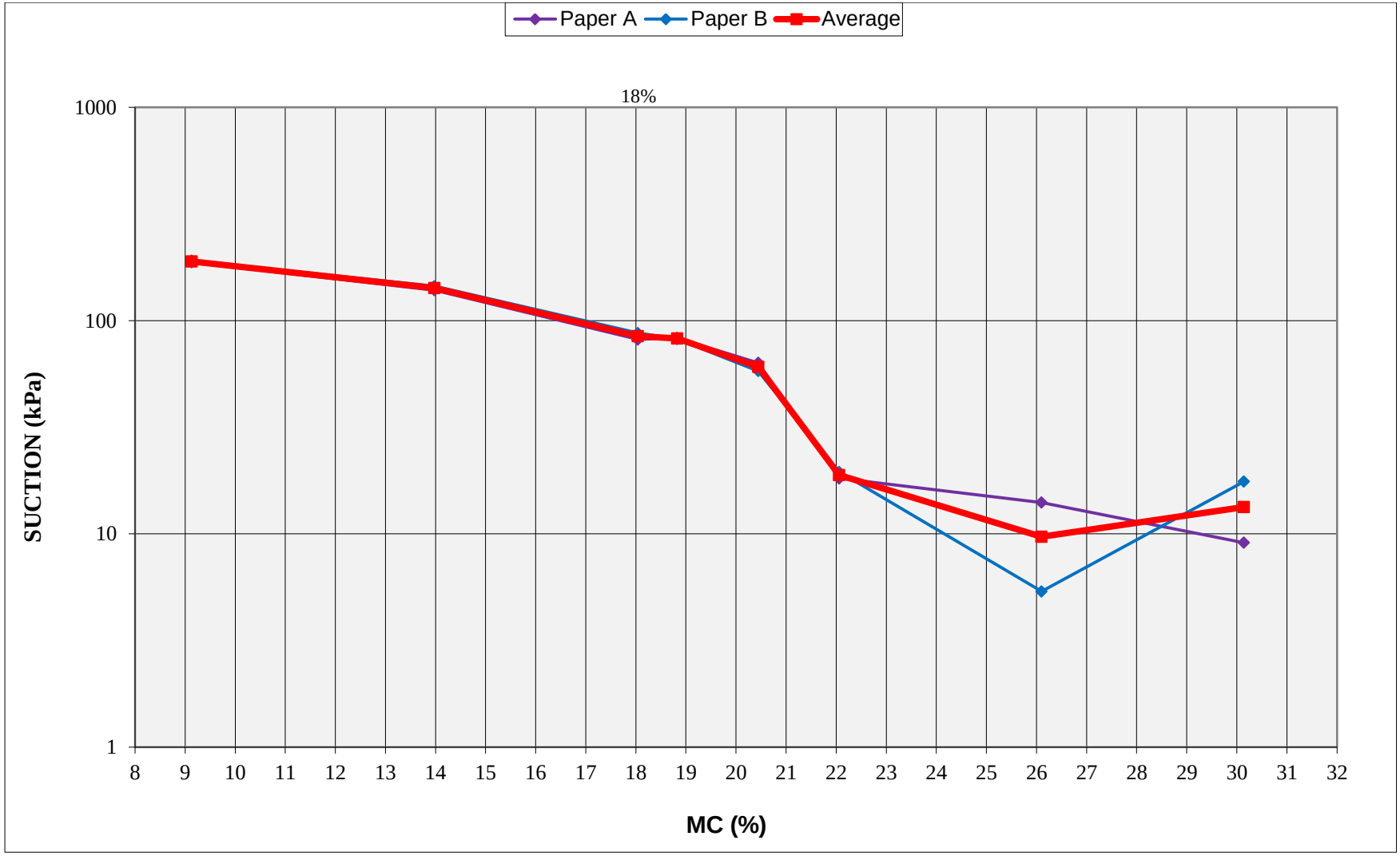

Figure 46: Matrix suction measurements - Tzaneen residual granite

Due to the comparatively high natural moisture content and degree of saturation of the material (18 % and 55.9 % respectively), the matrix suction pressure at the natural moisture content is small (85 kPa) compared to the suction pressures of the same material at lower moisture contents. The high natural moisture content is also the reason why the incremental increase in moisture content has a less pronounced effect on the matrix suction pressures than that which was experienced with the other tested samples that had lower natural moisture contents.

5.2.5 Relationship between pore fluid suction pressures and consolidation

From the data represented in Figures 44 to 46, it is possible to relate the decrease in void ratio during wetting with the reduction in suction pressures as the moisture content is increased at a constant applied stress of 200 kPa. By interpolating the suction pressure values for the different moisture contents of the material during consolidometer testing, the change in void ratio can be plotted against the change in suction pressures, with suction pressures plotted in a decreasing order (Figure 47). The void ratio and suction pressure values for the different moisture contents are summarized in Table 22.

Table 22: Void ratio and suction values at different moisture contents: Tzaneen residual granite

MC (%):	18.04	18.42	19.23	20.04	21.66	23.27	30.95
VOID RATIO	0.54	0.539	0.537	0.535	0.534	0.532	0.517
SUCTION (kPa)	85	83	72	60.7	53	46	13

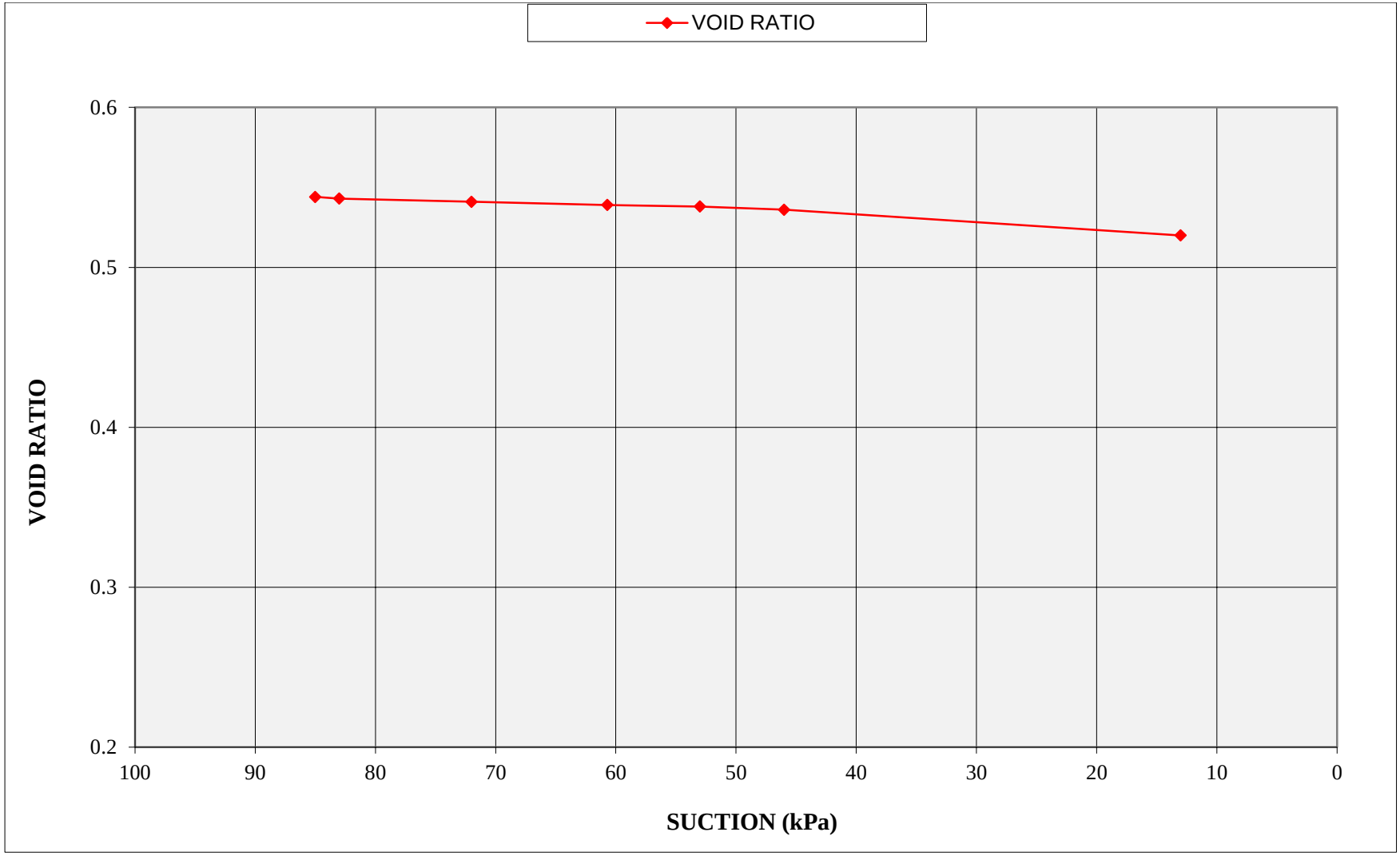

Figure 47: Relationship between consolidation and soil suction pressures with increasing moisture content - Tzaneen residual granite

From Table 22 and Figure 47 it is evident that the overall void ratio of the residual material decreases as the suction pressures in the material decrease during the increase in moisture content of the material. However, this change in void ratio, as well as the decrease in suction pressures, is much less pronounced than the changes experienced in the other samples. This relationship between void ratio and suction pressures for the Tzaneen residual granite can is expressed in Figure 48.

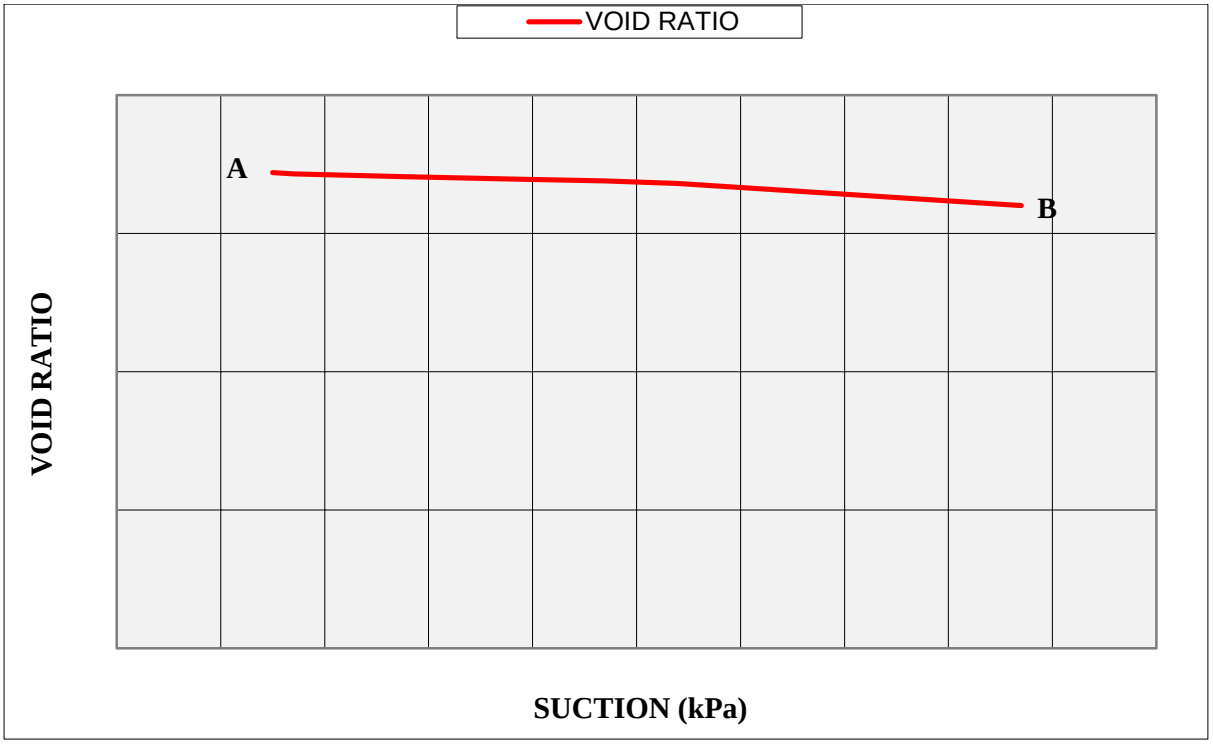

Figure 48: Relationship between suction pressures and void ratio at a constant load of 200 kPa - Tzaneen residual granite

It can be seen from Figure 48 that suction pressures and void ratios continue to decrease as the moisture content is incrementally increased at a constant load of 200 kPa. This decrease is much less pronounced compared to the changes experienced in the other tested materials, with the void ratio decreasing from 0.540 to 0.517 and suction pressures from 85 kPa to 13 kPa (A-B).

It is argued that the main reason for this is the high initial or natural moisture content of the material (18%). The material at its natural moisture content already exceeds the “critical” moisture content (Point B for other tested materials) where suction pressures are sufficiently low enough to trigger collapse. As a result collapse occurs immediately once the sample is loaded at the start of the test and the additional increase in moisture content/decrease in suction pressures at 200 kPa have little effect on the overall void ratio of the material.

5.2.6 Relationship between effective stress and soil collapse

The total effective stress is assumed to be the sum of the applied stress (total stress) and the pore water suction pressures. The change in the void ratio of the material with a change in the effective stress state of the residual granitic material is plotted on a log-scale and illustrated in Figure 49.

The intrinsic consolidation curve, representing the consolidation properties of the material independent of the natural state of the material is also indicated in Figure 49.

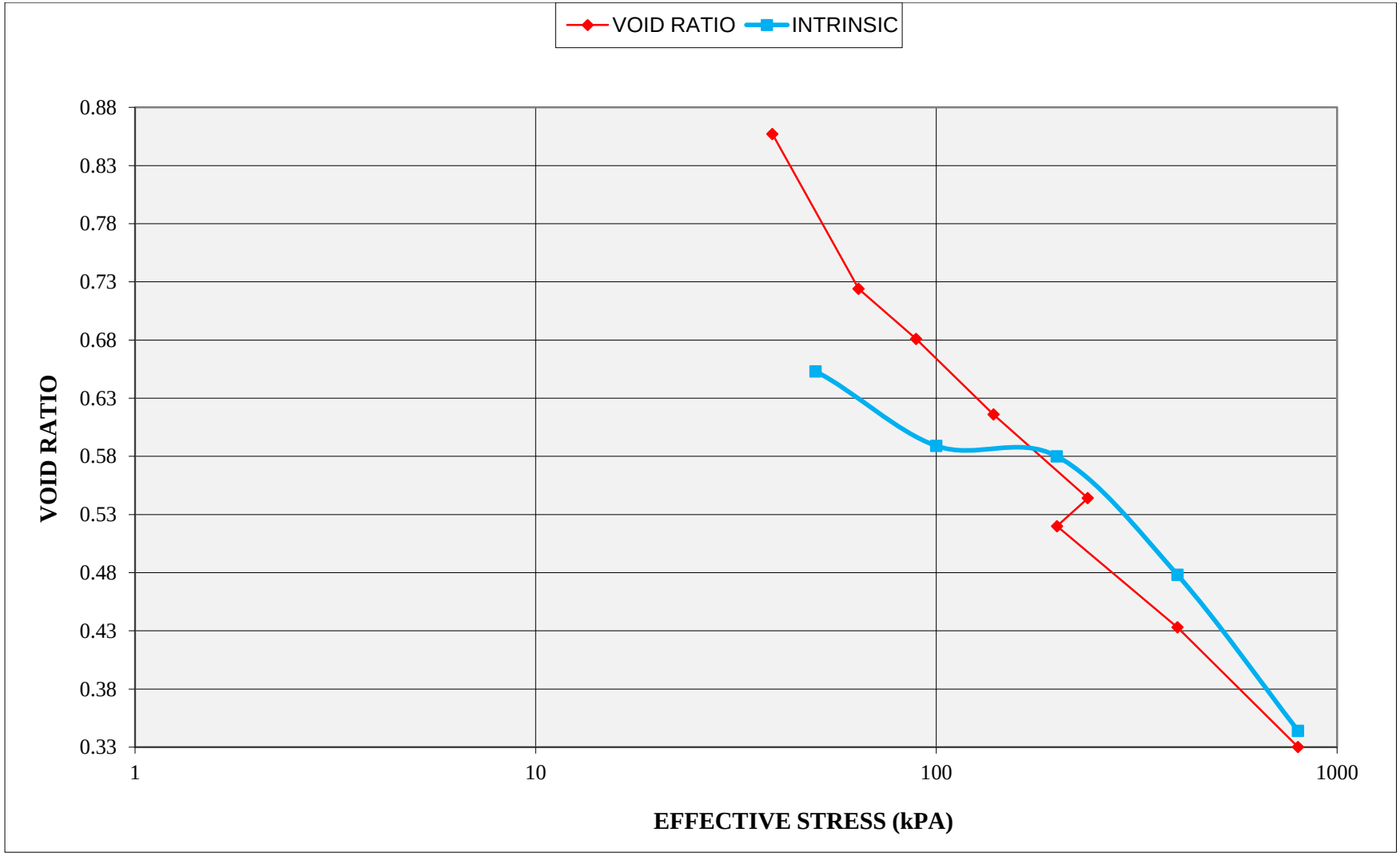

Figure 49: Effect of change in effective stress state on consolidation - Tzaneen residual granite

Due to the high natural moisture content of the material and subsequent low matrix suction pressures, the effective stress state of the Tzaneen residual material is governed by the magnitude of the applied stress from the start. The applied stress can be considered to be the single driving force behind consolidation of the material. The void ratio decreases as the effective stress increases with an increase in the applied stress up to 200 kPa.

Once the material is loaded up to 200 kPa additional moisture is added to the material. This leads to a decrease in the pore water suction pressures and in the effective stress. As mentioned, the decrease in effective stress due to the decrease in pore water suction pressures and the subsequent decrease in void ratio is less pronounced than that of the other tested samples due to the high initial moisture content of the Tzaneen material. The void ratio of the material decreases up to its final value of 0.33 as the effective stress state of the material is increased with increased loading of the sample.

When comparing the consolidation of the Tzaneen material with the intrinsic compressibility of the material, it is evident that the void ratios for all the effective stresses correlate very closely for the two samples. As the reconstituted sample represents the compressibility of the material without being affected by the soil structure, this close correlation of the void ratios of the two samples implies that for the Tzaneen residual granite, the soil structure has very little influence on the consolidation behaviour of the material in its natural state.

5.3 Transported Material: Lephalale aeolian sand

5.3.1 Material property description

Based on the calculations as summarised and discussed in Section 4.2.5, the *in-situ* void ratio (before consolidation), dry density, degree of saturation and natural moisture content of the material can be determined. These properties were determined whilst consolidation testing was in progress and is vital in characterizing the consolidation behaviour of the material during increased applied stress and moisture content. The results are summarised in Table 23 below.

Table 23: Calculated material properties: Lephalale aeolian sand

Material Property	Value
Dry density (kg/m^3)	1620
Initial void ratio	0.595
Natural moisture content (%)	12.8
Degree of saturation (%)	56.7

5.3.2 Optical microscope analysis

From the microscope analysis and photographs a definitive change in structure was noticed after consolidation of the material, and as in the previously discussed samples there is a significant decrease in the **number** of voids in the material after consolidation has taken place, with the average void **size** remaining constant. This implies that volume change through collapse settlement in the

material is governed by the total loss in volume of some voids whilst the rest remain unchanged with an increase in moisture content or applied stress.

During microscope analysis a white precipitate was noticed on the aeolian material that has been subjected to consolidation (Figure 31). This is due to calcium and nitrates that were deposited together with the aeolian material and precipitate when the moisture content of the material is increased during consolidometer testing.

5.3.3 Consolidation characteristics

The results and behaviour of the Lephalale aeolian sand during consolidometer testing are summarised in Figures 50 and 51 below. Figure 50 illustrates the change in void ratio of the material from its natural *in-situ* void ratio (e_0) throughout an increase in applied stress and moisture content up to a final stress of 800 kPa. Figure 51 highlights that part of consolidation testing where the moisture content is incrementally increased at a constant applied stress (200 kPa), subsequently indicating the change in void ratio (e) as the natural moisture content of the material is incrementally increased.

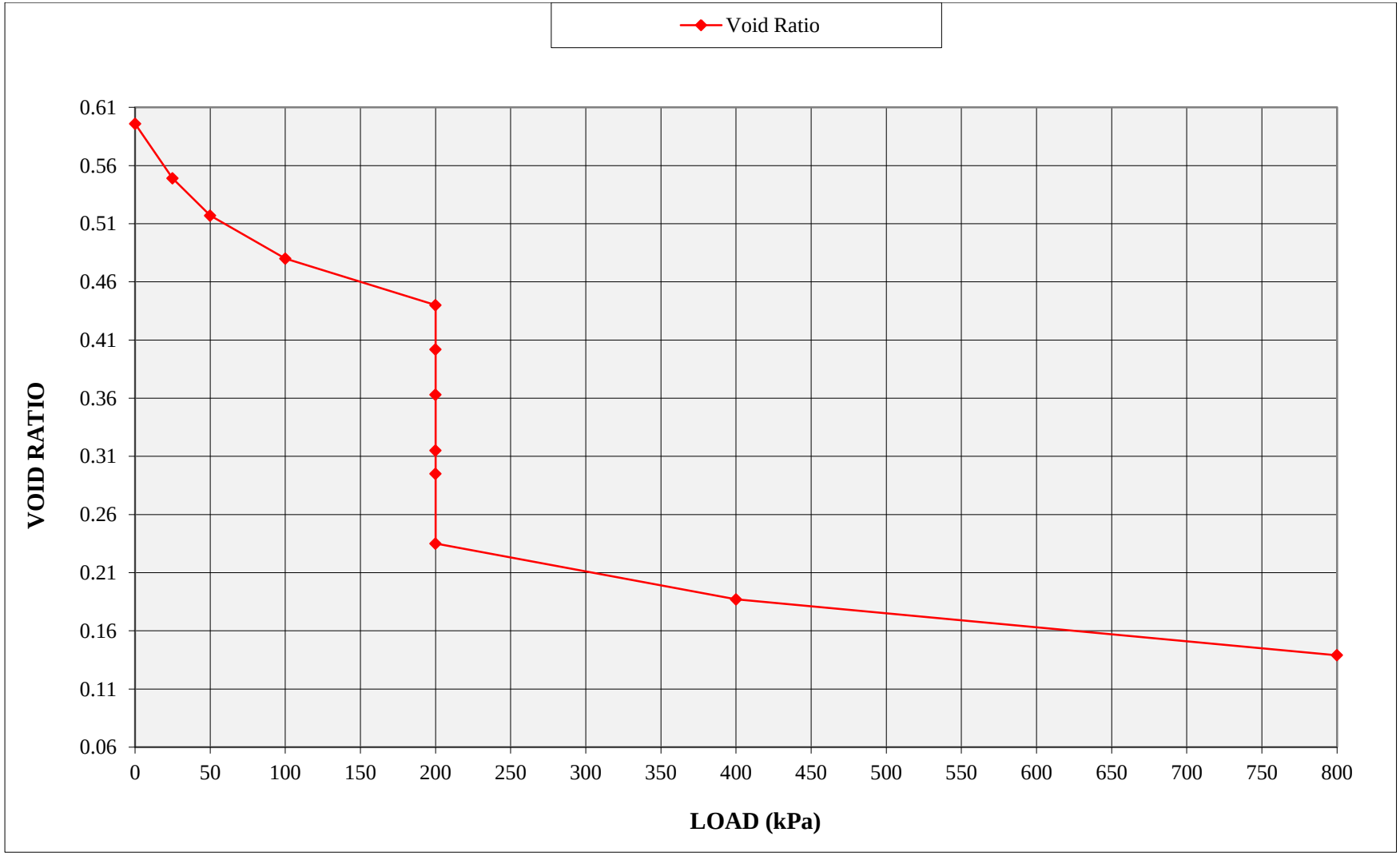

Figure 50: Consolidation and collapse settlement - Lephalale aeolian sand

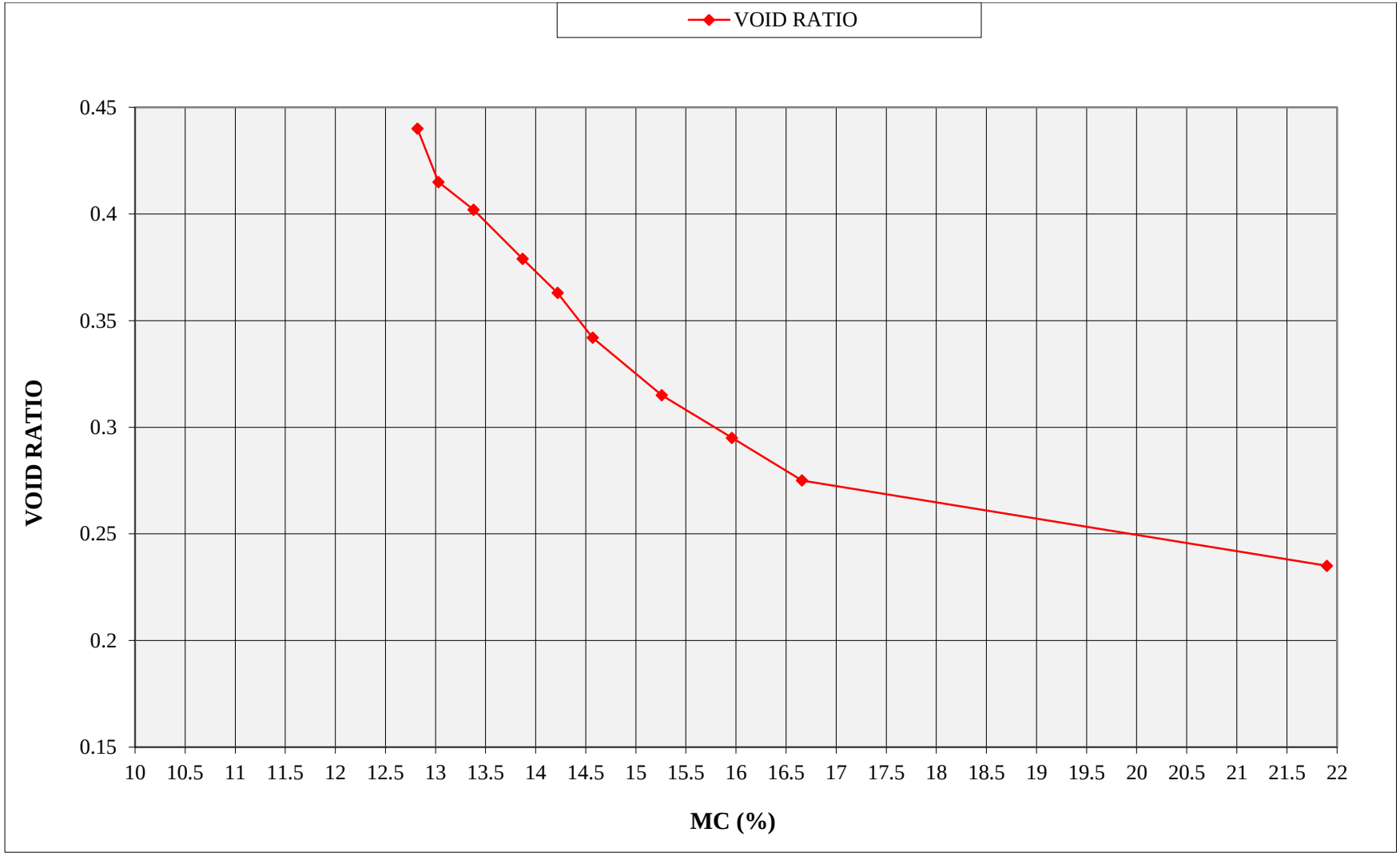

Figure 51: Change in void ratio with change in moisture content at a constant load of 200 kPa - Lephalale aeolian sand

From Figure 50 it can be seen that with an increase in the applied stress the void ratio of the material decreases due to the reduction in the total volume of voids in the material. Once the applied stress has reached 200 kPa and the rate of creep has subsided sufficiently, additional moisture is added to the system for the first time and collapse of the soil structure occurs.

Figure 51 shows that for the aeolian material a linear relationship exists between the increase in moisture content and the decrease in void ratio up to a moisture content of 16.66%. Once this moisture content has been passed the reduction in the void ratio with increase in moisture content appears to decrease, causing the graph to "flatten out" towards the final moisture content of 21.9 %. This means that once the aeolian material has reached a certain moisture content a further increase in the moisture content of the material will not have as significant effect on the consolidation behaviour of the material.

The moisture content is increased incrementally from the natural moisture content of 12.8 %, with sufficient time permitted between increments to allow the creep rate to subside to less than 0.25% per hour (as in Rust *et al.*, 2005).

Once creep associated with the collapse event decreased sufficiently, loading was continued up to the final applied stress of 800 kPa.

It is acknowledged that the final void ratio of 0.136 at 800 kPa is uncharacteristically low and when back-calculated gives dry-density values that are not typically associated with aeolian sand. These low final void ratios can either be attributed to testing error or disturbance to the equipment during periods where the testing apparatus was left unsupervised. However, for the purpose of this dissertation the final void ratios are not considered critical as emphasis is placed on the behaviour of the material during the increase in moisture content at a constant load.

The collapse potential for the aeolian material is calculated at 12.8 %, which can be classified by Jennings and Knight (1975) as indicating "severe trouble".

5.3.4 Pore fluid suction pressure measurements

Matrix suction measurements were conducted using the filter paper method as described in Section 4.2.3. Suction pressure was taken as the average value of the two measurements derived from using two pieces of Whatman no 42 filter paper, Paper A and Paper B and plotted on a log -scale. The results of the suction measurements for the Lephalale aeolian material are indicated in Figure 52.

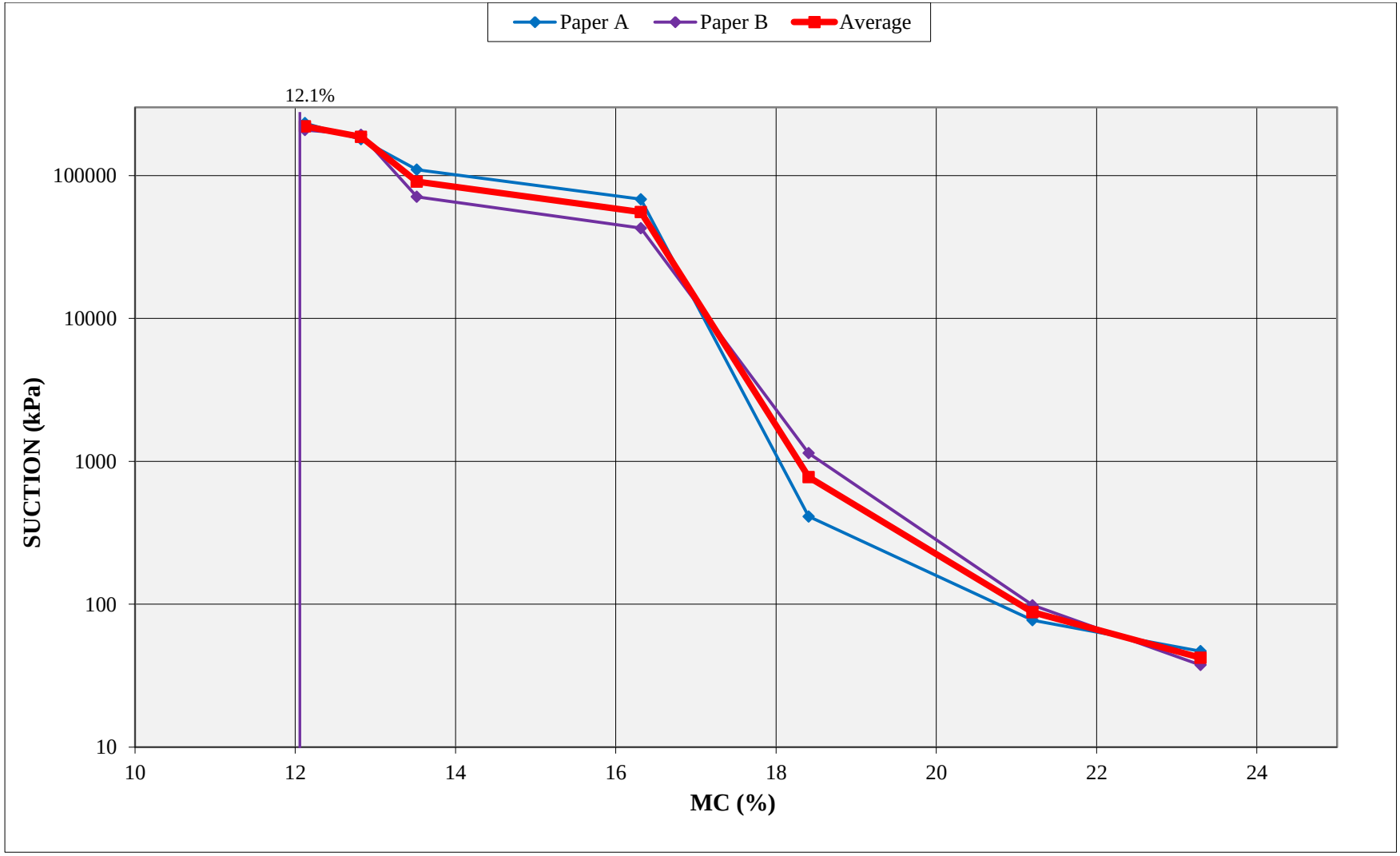

Figure 52: Matrix suction measurements - Lephalale aeolian sand

From Figure 52 it can be seen that the matrix suction pressures are very high at the natural moisture content of 12.1 % in the aeolian material, roughly equalling 186000 kPa. As the moisture content of the material increases the suctions decrease steadily, until a threshold or "critical" moisture content is reached (approximately 16.6 %). Once the "critical" moisture content is reached there is a sudden and dramatic decrease in the suction pressures. This "critical" moisture content closely correlates with the moisture content above which the rate of reduction in void ratio with increasing moisture content decreases.

The suctions continue to decrease steadily up to moisture content of 23.3 %, with a final value of 42 kPa.

5.3.5 Relationship between pore fluid suction pressures and consolidation

From the data represented in Figures 50 to 52, it is possible to relate the decrease in void ratio during wetting with the reduction in suction pressures as the moisture content is increased at a constant applied stress of 200 kPa. By interpolating the suction pressure values for the different moisture contents of the material during consolidometer testing, the change in void ratio can be plotted against the change in suction pressures (Figure 53). The void ratio and suction pressure values for the different moisture contents are summarized in Table 24.

Table 24: Void ratio and suction values at different moisture contents: Lephalale aeolian sand

MC (%):	12.12	13.03	13.38	13.87	14.22	14.57	15.26	15.96	16.66	21.9
VOID RATIO	0.44	0.415	0.402	0.379	0.363	0.342	0.315	0.295	0.275	0.235
SUCTION (kPa)	186470	157711	109780	100569	94066	90815	75101	62097	44314	8897

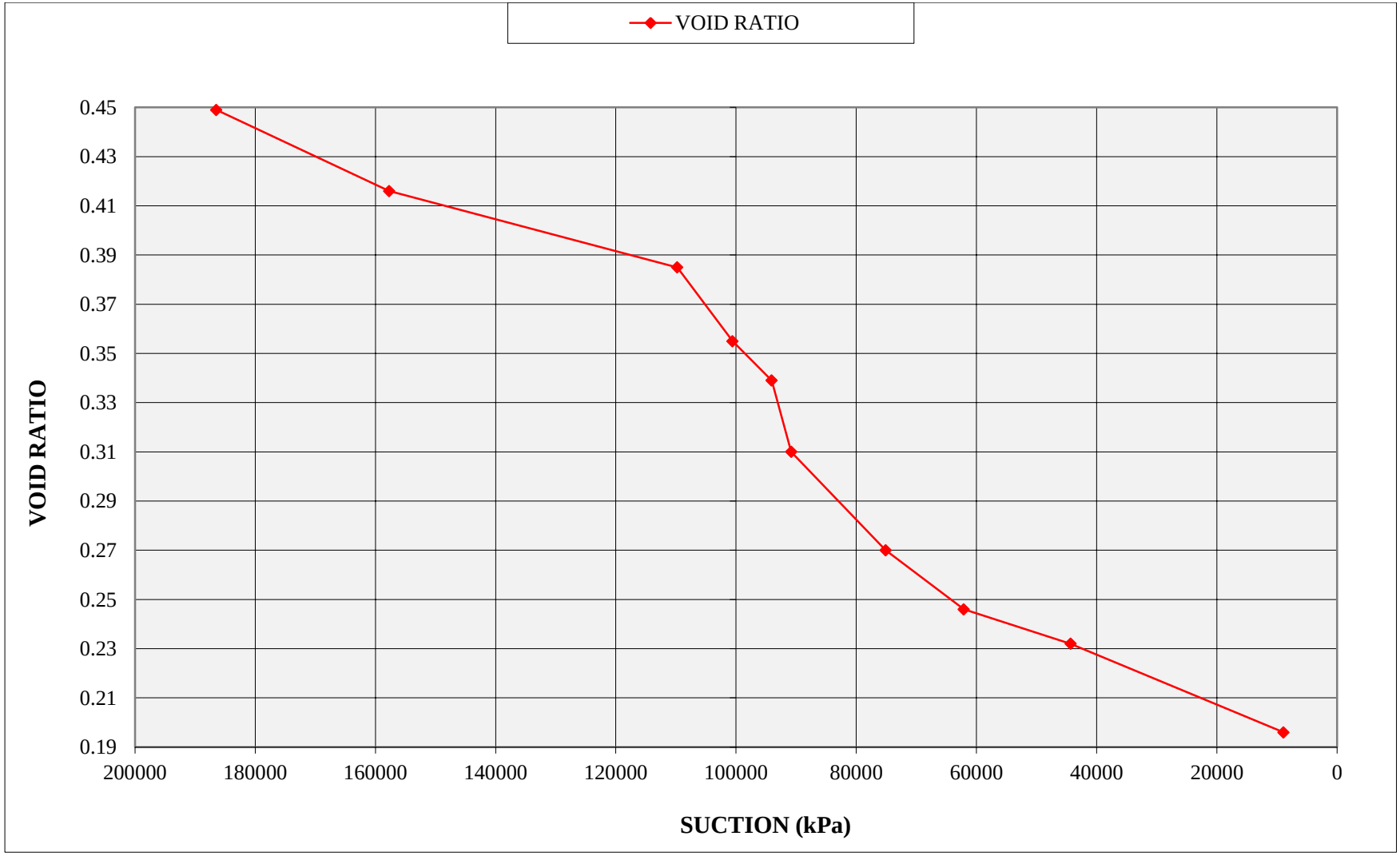

Figure 53: Relationship between consolidation and soil suction pressures with increasing moisture content - Lephalale aeolian sand

From Table 24 and Figure 53 it is evident that the overall void ratio of the residual material decreases as the suction pressures in the material decrease during the increase in moisture content of the material. This relationship between void ratio and suction pressures can be expressed in terms of two phases (Figure 54).

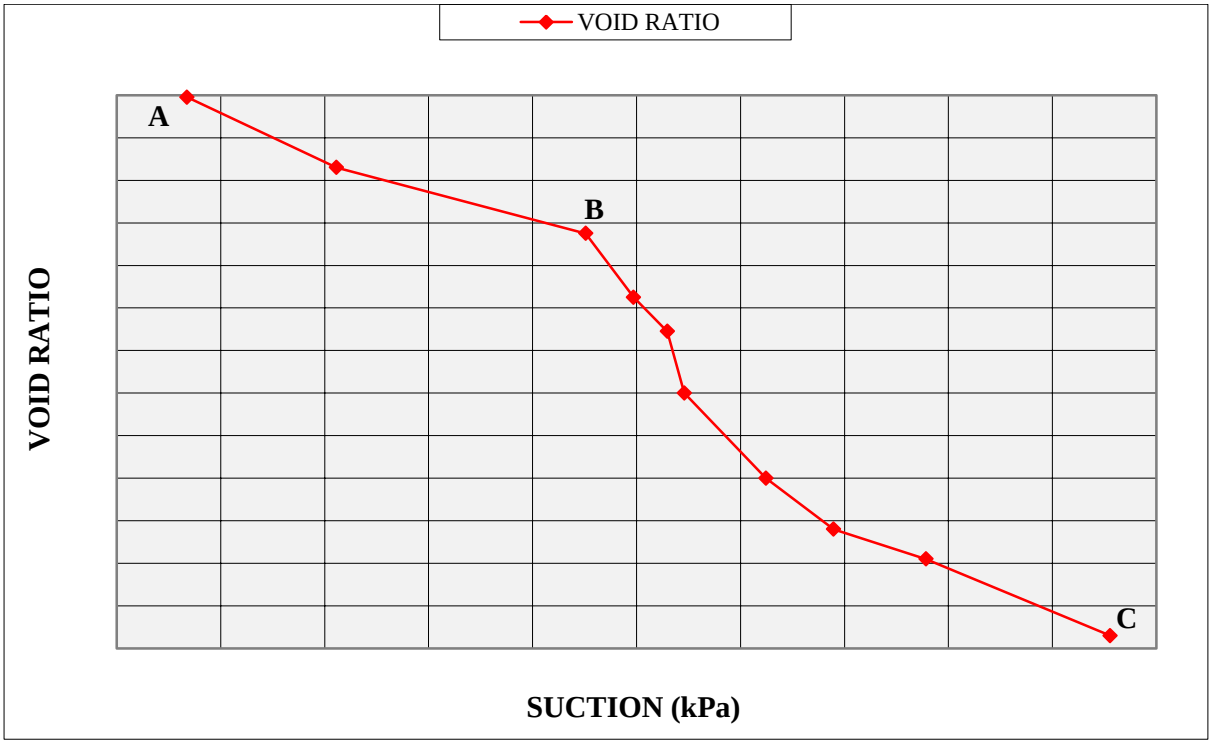

Figure 54: Two-phase behaviour between suction pressures and void ratio at a constant load of 200 kPa - Lephalale aeolian sand

During the first phase (A-B) both the void ratio and the suction pressures of the material decrease steadily with change in moisture content. The void ratio decreases from its initial value (consolidated at 200 kPa) of 0.449 to 0.402 and suction pressures from 186470 kPa to 109780 kPa with an increase in the natural moisture content of the material from 12.12 % to 13.38 %.

The second phase (B-C) is characterized by a steady, significant drop in the void ratio of the material, dropping from 0.402 to 0.235. Matrix suction pressures continue to decrease steadily as additional moisture is added to the material.

It can therefore be argued that the void ratio and suction pressures will decrease steadily as the moisture content is increased (A-B) up to a **critical point** (Point B) where suction pressures have decreased sufficiently to trigger collapse (B-C) and a subsequent sudden decrease in void ratio.

5.3.6 Relationship between effective stress and soil collapse

The total effective stress is assumed to be the sum of the applied stress and the pore water suction pressures. The change in the void ratio of the material with a change in the effective stress state of the residual granitic material is plotted on a log-scale and illustrated in Figure 55.

The intrinsic consolidation curve, representing the consolidation properties of the material independent of the natural state of the material is also indicated in Figure 55.

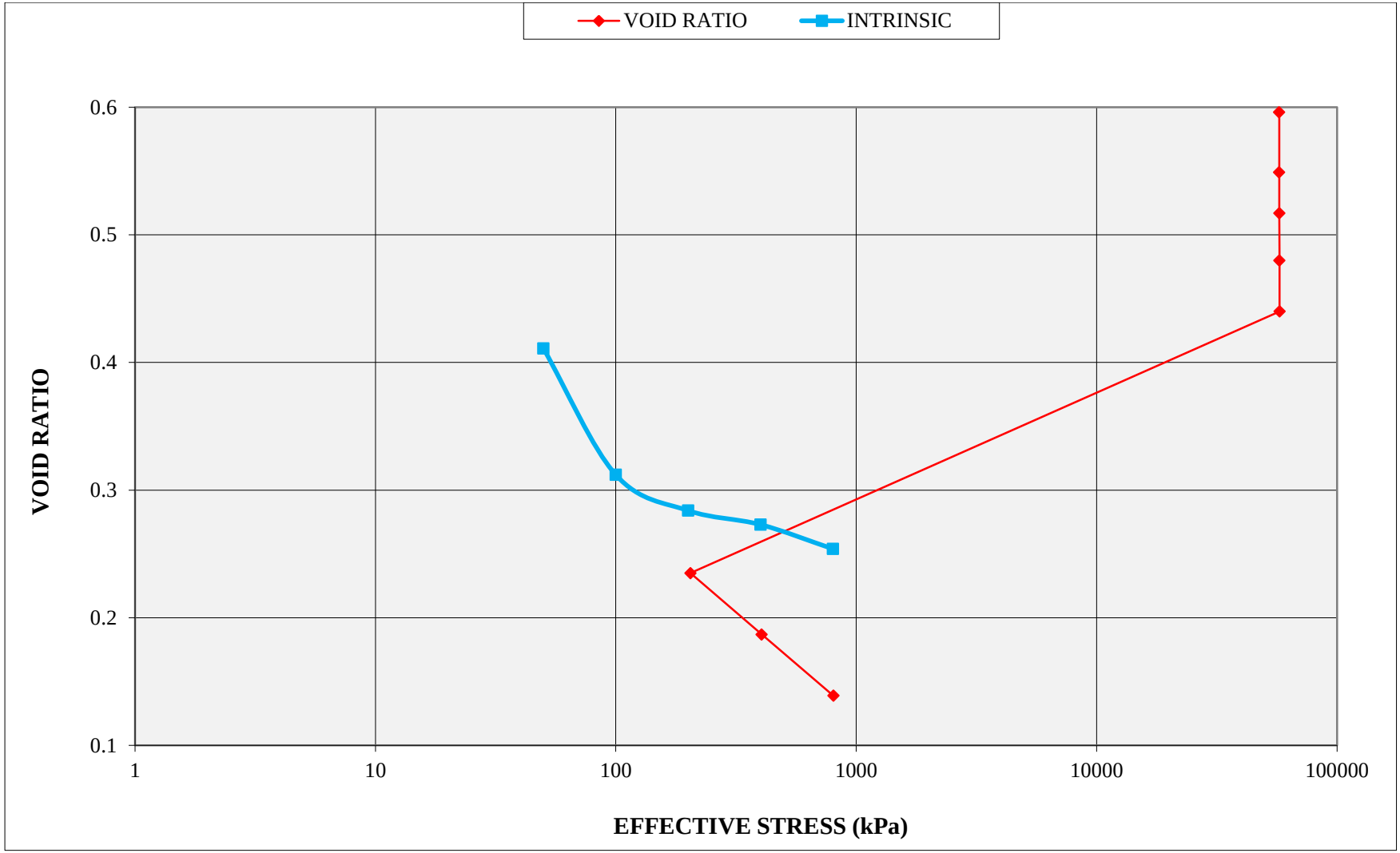

Figure 55: Effect of change in effective stress state on consolidation - Lephalale aeolian sand

It is clear that the effective stress state of the material is controlled by the magnitude of the pore water suction pressures at lower moisture contents. Initially the void ratio decreases as the effective stress increases with an increase in the applied stress up to 200 kPa. At this stage the influence of the applied stress on the overall effective stress and consolidation behaviour is minimal due to the magnitude of the suction pressures influencing the effective stress state. However, as soon as additional moisture is introduced to the material at 200 kPa and the "critical" moisture content is reached, the pore water suction pressures and subsequently the effective stress decreases dramatically. It should be appreciated that this is an immediate change in the effective stress state that occurs as soon as the material has reached the particular "critical" moisture content and suction pressures decrease. Once this point is reached, the influence of the applied stress becomes the predominant influence on the consolidation behaviour of the material.

The void ratio of the aeolian material decreases up to its final value of 0.136 as the effective stress state of the material increases, almost exclusively now due to the influence of the increase in applied stress and the effect of suction pressures being considered negligible.

When comparing the consolidation of the material after the drop in effective stress (and thus after collapse) with the intrinsic compressibility of the material, it can be seen that there is some variation between the samples. As mentioned in Section 5.3.3 the final void ratio of the tested sample is uncharacteristically low and can be blamed on testing error or disturbance of the test apparatus. It is expected that the decrease in void ratio once the incremental increase in moisture is completed and the sample load increased will rather be the same or very similar to the intrinsic compressibility of the reconstituted sample, as was the case for the two residual granite samples.

5.4 Transported Material: Magaliesberg colluvium

5.4.1 Material property description

Based on the calculations as summarised and discussed in Section 4.2.5, the *in-situ* void ratio (before consolidation), dry density, degree of saturation and natural moisture content of the material can be determined. These properties were determined whilst consolidation testing was in progress and is vital in characterizing the consolidation behaviour of the material during increased applied stress and moisture content. The results are summarised in Table 25 below.

Table 25: Calculated material properties: Magaliesberg colluvium material

Material Property	Value
Dry density (kg/m^3)	1650
Initial void ratio	0.576
Natural moisture content (%)	5.6
Degree of saturation (%)	25.7

5.4.2 Optical microscope analysis

From the microscope analysis and photographs a definitive change in structure was noticed after consolidation of the material, and as in the previously discussed samples there is a significant decrease in the **number** of voids in the material after consolidation has taken place, with the average void **size** remaining constant. This implies that volume change through collapse settlement in the material is governed by the total loss in volume of some voids whilst other remain unchanged with an increase in moisture content or applied stress.

5.4.3 Consolidation characteristics

The results and behaviour of the Magaliesberg colluvium material during consolidometer testing are summarised in Figures 56 and 57 below. Figure 56 illustrates the change in void ratio of the material from its natural *in-situ* void ratio (e_0) throughout an increase in applied stress and moisture content up to a final stress of 400 kPa. Figure 57 highlights that part of consolidation testing where the moisture content is incrementally increased at a constant applied stress (200 kPa), subsequently indicating the change in void ratio (e) as the natural moisture content of the material is incrementally increased.

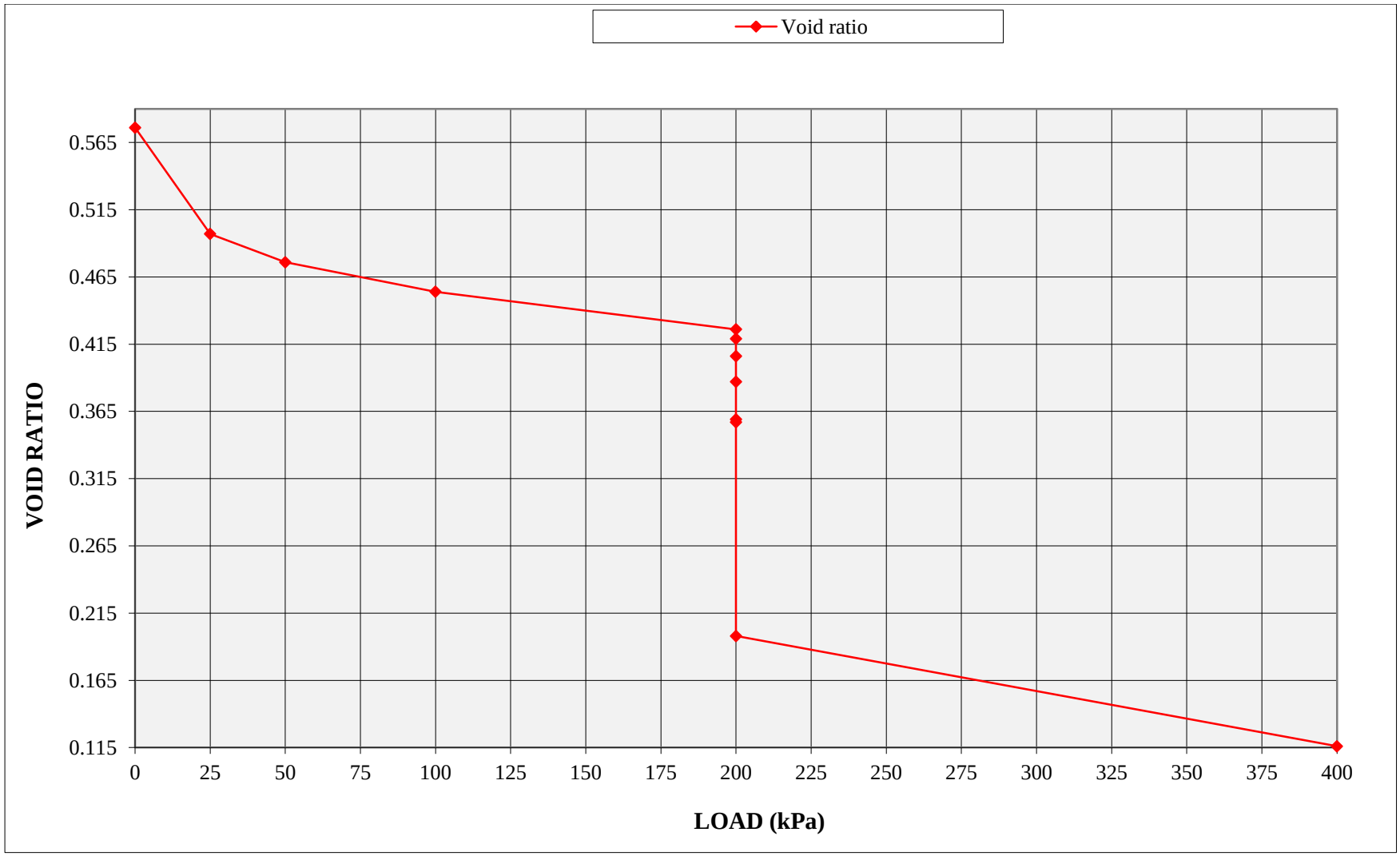

Figure 56: Consolidation and collapse settlement - Magaliesberg colluvium

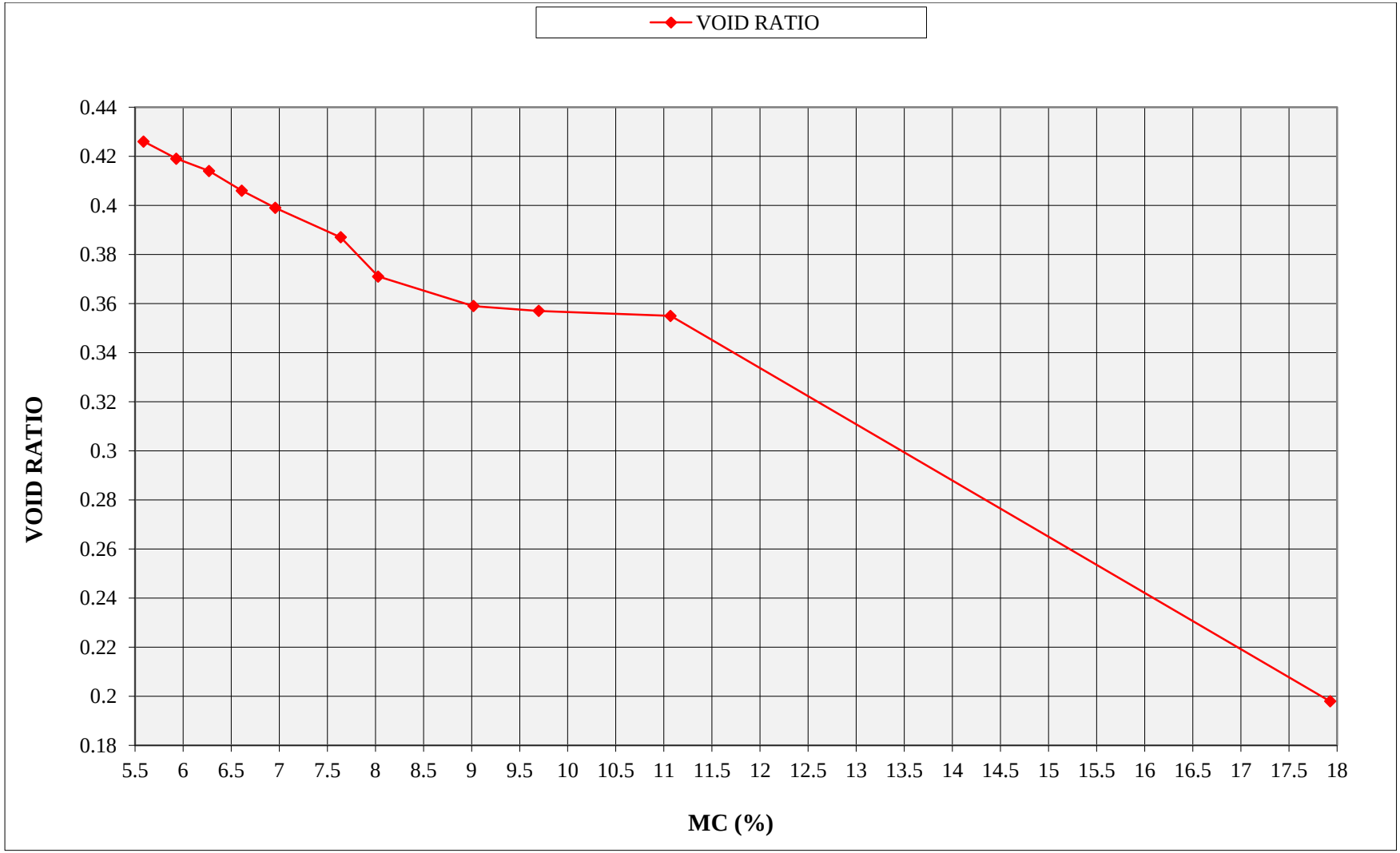

Figure 57: Change in void ratio with change in moisture content at a constant load of 200 kPa - Magaliesberg colluvium

From Figure 56 it can be seen that with an increase in the applied stress the void ratio of the material decreases steadily due to the reduction in the total volume of voids in the material. Once the applied stress has reached 200 kPa and the rate of creep has subsided sufficiently, additional moisture is added to the system for the first time and collapse of the soil structure occurs.

Figure 57 shows that for the aeolian material an almost linear relationship exists between the increase in moisture content and the decrease in void ratio. The moisture content is increased incrementally from the natural moisture content of 5.6 % up to a final moisture content of 18 %, with sufficient time permitted between increments to allow the creep rate to subside to less than 0.25% per hour (as in Rust *et al.*, 2005).

Once creep associated with the collapse event decreased sufficiently, loading was continued up to the final applied stress of 400 kPa and the material assumed to be completely consolidated.

It is acknowledged that the final void ratio of 0.116 at 800 kPa is uncharacteristically low and when back-calculated gives dry-density values that are not typically associated with aeolian sand. These low final void ratios can be attributed to testing error or disturbance to the equipment during periods where the testing apparatus was left unsupervised. However, for the purpose of this dissertation the final void ratios are not considered critical as emphasis is placed on the behaviour of the material during the increase in moisture content at a constant load.

The collapse potential is calculated at 14.48 %, which can be classified by Jennings and Knight (1975) as indicating “severe trouble”.

5.4.4 Pore fluid suction pressure measurements

Matrix suction measurements were conducted using the filter paper method as described in Section 4.2.3. Suction pressure was taken as the average value of the two measurements derived from using two pieces of Whatman no 42 filter paper, Paper A and Paper B and plotted on a log -scale. The results of the suction measurements for the Magaliesberg colluvium material are indicated in Figure 58.

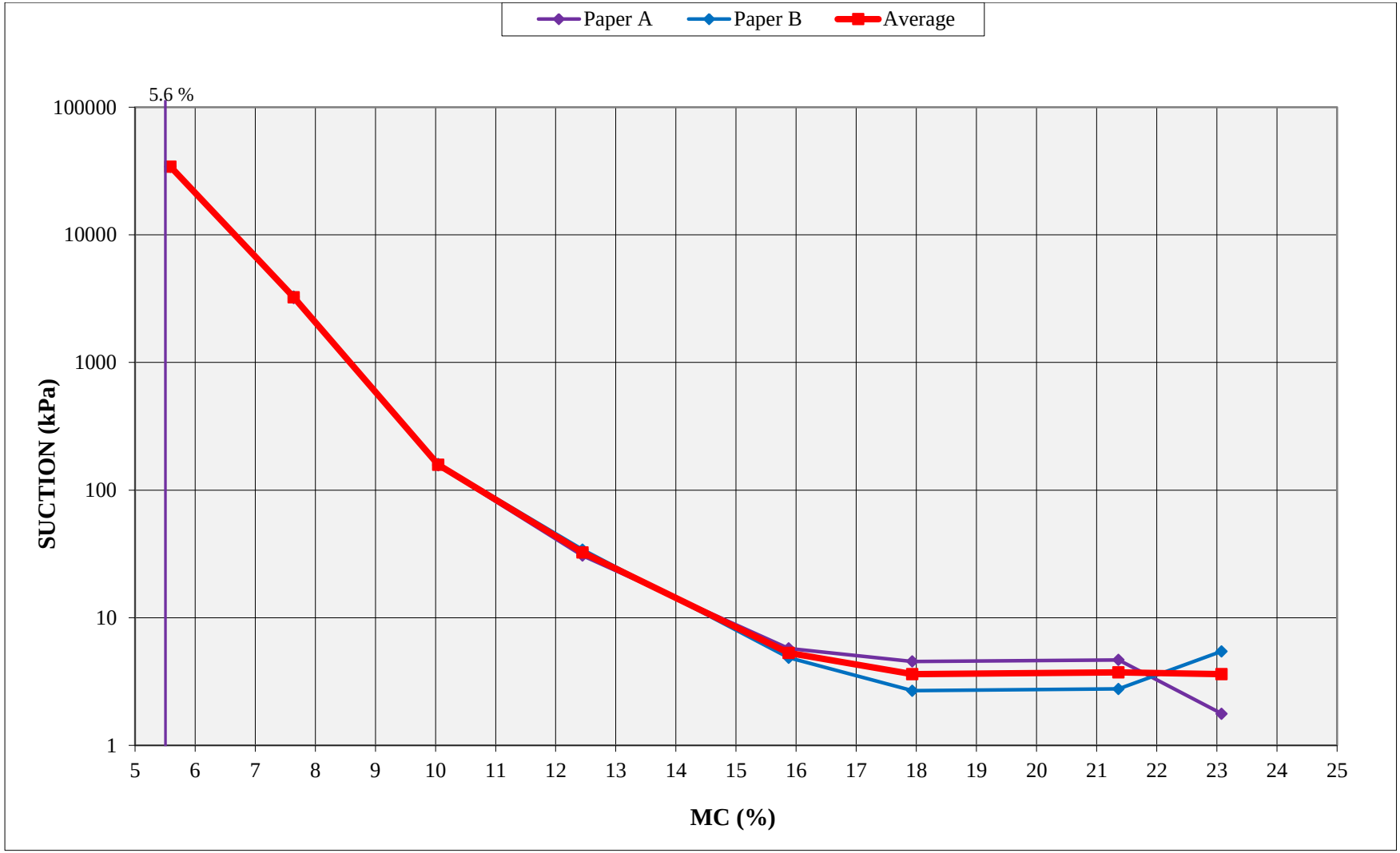

Figure 58: Matrix suction measurements - Magaliesberg colluvium

From Figure 58 it is evident that the matrix suction pressures at the natural moisture content of 5.6 % are high, roughly equalling 32000 kPa. As the moisture content of the material increases the matrix suction pressuresd decrease dramatically, down to 5 kPa at a moisture content of 15.8 %. Once this moisture content is exceeded the decrease in suction pressure with a further increase in moisture content becomes less significant, with the additional moisture above 15.8 % having very little effect on the remaining pore water suction pressures.

5.4.5 Relationship between pore fluid suction pressures and consolidation

From the data represented in Figures 56 to 58, it is possible to relate the decrease in void ratio during wetting with the reduction in suction pressures as the moisture content is increased at a constant applied stress of 200 kPa. By interpolating the suction pressure values for the different moisture contents of the material during consolidometer testing, the change in void ratio can be plotted against the change in suction pressures (Figure 59). The void ratio and suction pressure values for the different moisture contents are summarized in Table 26.

Table 26: Void ratio and suction values at different moisture contents: Magaliesberg colluvium

MC (%):	5.59	5.93	6.27	6.61	6.96	7.64	8.03	9.02	9.7	11.07	18
VOID RATIO	0.426	0.419	0.414	0.406	0.399	0.387	0.371	0.359	0.357	0.355	0.198
SUCTION (kPa)	34240	29094	24010	18741	13471	3242	2733	1453	559	264	3.61

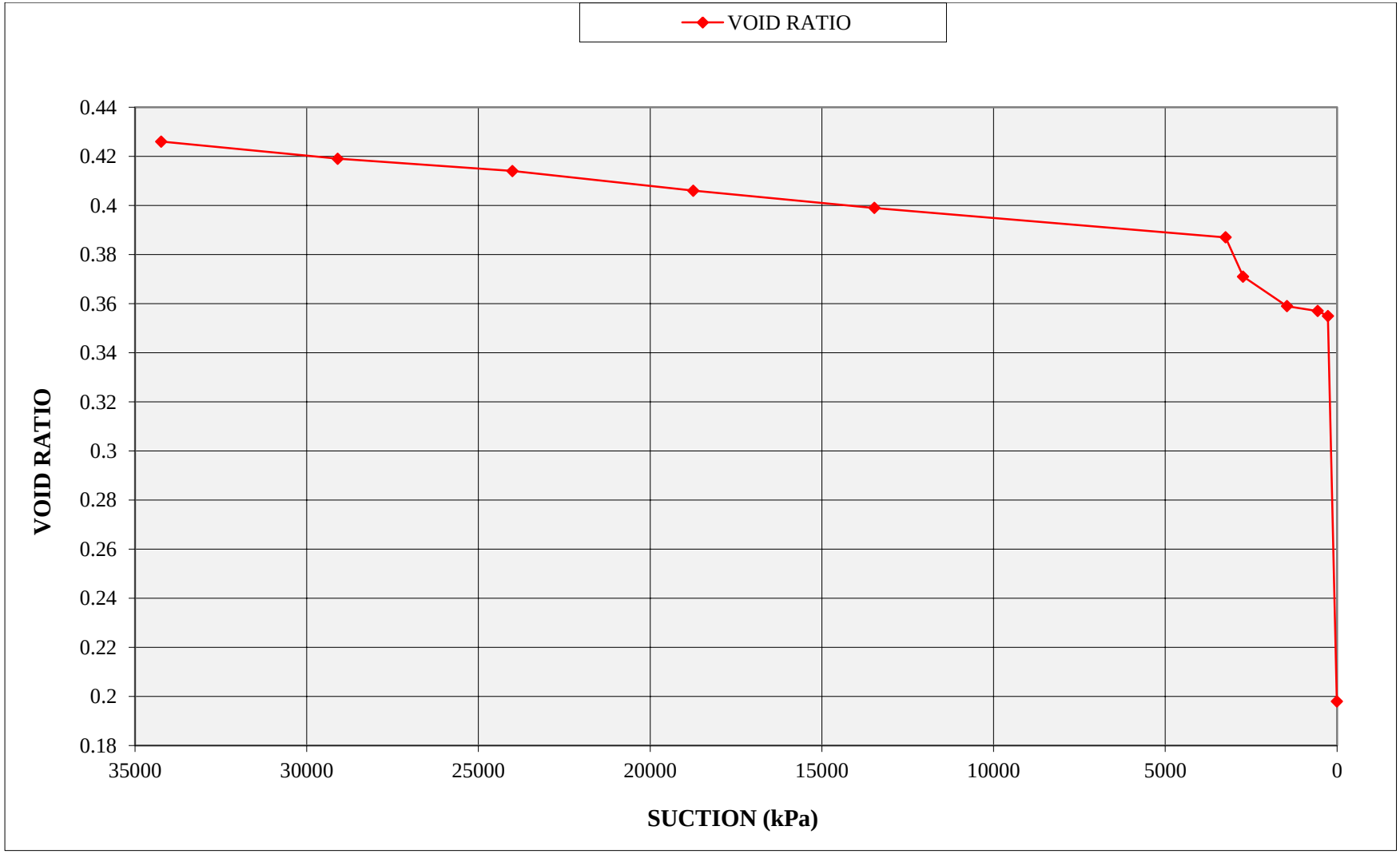

Figure 59: Relationship between consolidation and soil suction pressures with increasing moisture content - Magaliesberg colluvium

From Table 26 and Figure 59 it is evident that the overall void ratio of the aeolian material decreases as the suction pressures in the material decrease during the increase in moisture content of the material. This relationship between void ratio and suction pressures can be expressed in terms of two phases (Figure 60).

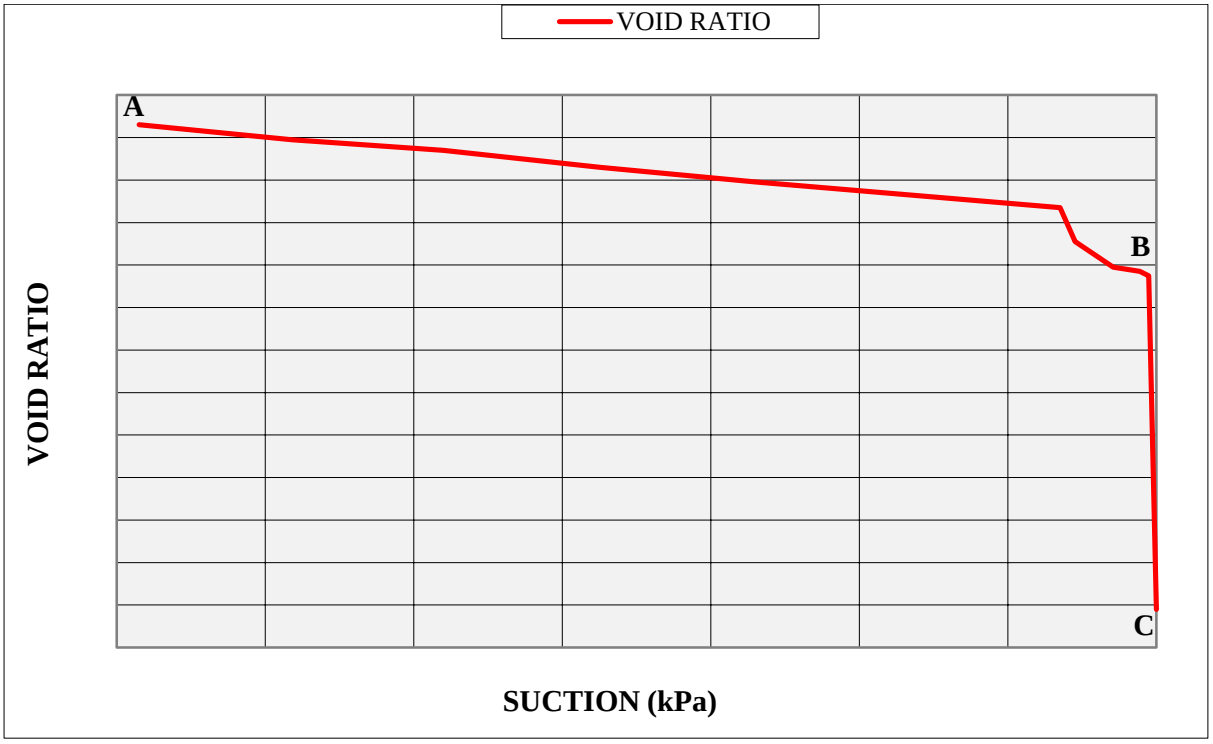

Figure 60: Two-phase behaviour between suction pressures and void ratio at a constant load of 200 kPa - Magaliesberg colluvium

During the first phase (A-B) both the void ratio and the suction pressures of the material decrease steadily with increase in moisture content. The void ratio decreases from its initial value (consolidated at 200 kPa) of 0.426 to 0.357 and suction pressures from 34240 kPa to 559 kPa with an increase in the natural moisture content of the material from 5.59 % to 9.7 %.

The second phase (B-C) is characterized by a significant drop in the void ratio of the material, dropping from 0.357 to 0.198. Suction pressures continue to decrease, but the decrease is much less significant when compared to the decrease in suction pressures during the first phase.

It can therefore be argued that the void ratio and suction pressures will decrease steadily as the moisture content is increased (A-B) up to a **critical point** (Point B) where suction pressures have decreased sufficiently to trigger collapse (B-C) and a subsequent sudden decrease in void ratio.

5.**4**.6 Relationship between effective stress and soil collapse

The total effective stress is assumed to be the sum of the applied stress (total stress) and the pore water suction pressures. The change in the void ratio of the material with a change in the effective stress state of the residual granitic material is plotted on a log-scale illustrated in Figure 61.

The intrinsic consolidation curve, representing the consolidation properties of the material independent of the natural state of the material is also indicated in Figure 61.

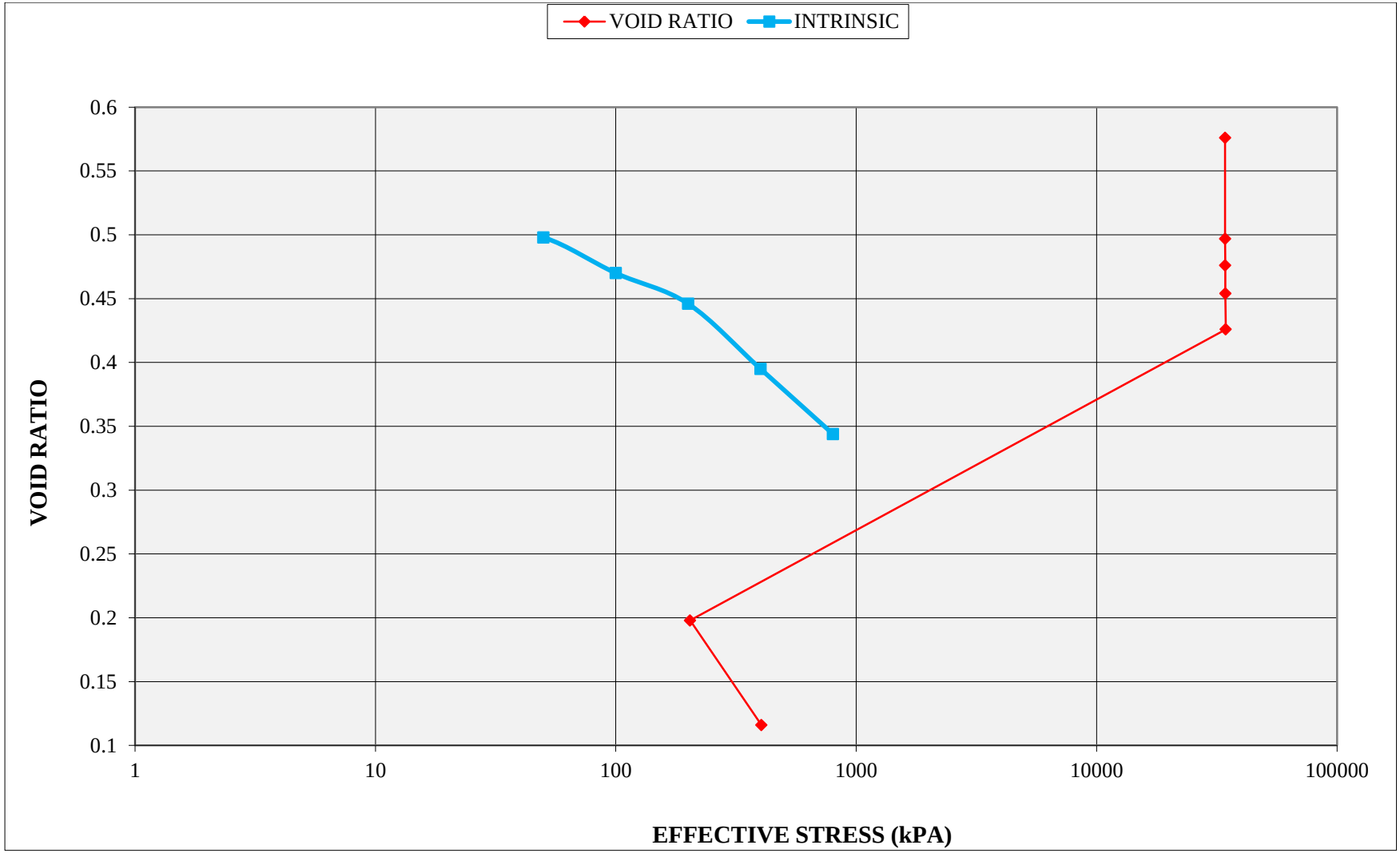

Figure 61: Effect of change in effective stress state on consolidation - Magaliesberg colluvium

It is clear that the effective stress state of the material is controlled by the magnitude of the pore water suction pressures at lower moisture contents. Initially the void ratio decreases as the effective stress increases with an increase in the applied stress up to 200 kPa. At this stage the influence of the applied stress on the overall effective stress and consolidation behaviour is minimal due to the magnitude of the suction pressures influencing the effective stress state. However, as soon as additional moisture is introduced to the material at 200 kPa and the "critical" moisture content is reached, the pore water suction pressures and subsequently the effective stress decreases dramatically. It should be appreciated that this is an immediate change in the effective stress state that occurs as soon as the material has reached the particular "critical" moisture content and suction pressures decrease. Once this point is reached, the influence of the applied stress becomes the predominant influence on the consolidation behaviour of the material.

The void ratio of the colluvium material decreases up to its final value of 0.116 as the effective stress state of the material increases, almost exclusively now due to the influence of the increase in applied stress and the effect of suction pressures being considered negligible.

When comparing the consolidation of the material after the drop in effective stress (and thus after collapse) with the intrinsic compressibility of the material, it can be seen that there is some variation between the samples. As mentioned in Section 5.4.3 the final void ratio of the tested sample is uncharacteristically low and can be blamed on testing error or disturbance of the test apparatus. It is expected that the decrease in void ratio once the incremental increase in moisture is completed and the sample load increased will rather be the same or very similar to the intrinsic compressibility of the reconstituted sample.

5.5 Summary

5.5.1 Relationship between matrix suction pressures and soil collapse

From the available data, the relationship between matrix suction pressures and soil collapse can be described in terms of two phases. During the first phase (Phase A-B) both the void ratio and the suction pressures of the material decrease steadily with increase in moisture content.

The second phase (B-C) is characterized by a significant drop in the void ratio of the material. Suction pressures continue to decrease, but the decrease is much less significant when compared to the decrease in suction pressures during the first phase.

It is therefore argued that the void ratio and suction pressures will decrease steadily as the moisture content is increased (A-B) up to a **critical point** (Point B) where suction pressures have decreased sufficiently to trigger collapse (B-C) and a subsequent sudden decrease in void ratio.

5.5.2 Effective stress and soil collapse

The effective stress state of the material is assumed to be the sum of the matrix suction forces and the applied stresses.

It is evident that the effective stress state of the material is governed largely by the suction forces which are significantly greater than the applied stresses at the natural moisture contents of the materials. The effective stress state of the residual granite material from Tzaneen, which has a high natural moisture content, is much less affected by the pore water suction pressures and subsequently mainly influenced by the applied stresses.

Initially, as the applied stress and thus effective stress is increased, the void ratio of the materials decreases steadily. As additional moisture is introduced and the moisture contents of the materials incrementally increase, a sudden and dramatic decrease in effective stress and void ratio occurs as suction forces decrease. Collapse settlement of the material is associated with this sudden decrease in effective stress. For the Tzaneen material the decrease in effective stress, and subsequently the magnitude of collapse, is much less pronounced and the matrix suction forces are already low at the natural moisture content of 18 %.

After surpassing the critical moisture content causing matrix suction forces to decrease, the effective stress and consolidation behaviour of the material is largely governed by the applied stress.

5.5.3 Collapse and intrinsic compressibility

The intrinsic compressibility of reconstituted samples of each material was plotted against the consolidation behaviour of the material in its natural state for each of the samples. This was done in effort to evaluate the effect of the soil structure on the consolidation behaviour of the material, particularly after collapse has taken place.

For the majority of the materials the consolidation behaviour of the material after collapse has occurred correlates very closely to the consolidation behaviour of the reconstituted material at similar effective stresses, implying that the remnant soil structure, if any, has very little influence on the remaining consolidation behaviour of the material after collapse has occurred.

5.5.4 Optical microscope analysis

Optical microscope analysis has been performed on all the materials before and after the materials have been subjected to consolidation testing. From the microscope analysis and photographs a definitive change in structure was noticed after consolidation for all of the material. The most noticeable is that in all the materials there is a significant decrease in the **number** of voids in the material after consolidation has taken place, with the average void **size** remaining constant. This suggests that volume change through collapse settlement in the material is governed by the total loss in volume of some voids whilst other remain unchanged with an increase in moisture content or applied stress.

6. CONCLUSIONS AND RECOMMENDATIONS

From the available data and discussions the following conclusions can be made:

i. Matrix suction pressure is the driving force behind the soil collapse phenomenon. At lower moisture contents and degrees of saturation, suction pressures are several orders of magnitude larger than any applied stress to the material through structural loading. As the moisture content/degree of saturation of the material increases the suction pressures steadily decrease, until a critically low matrix suction pressure is reached. Once this critical point is reached there is a large and sudden decrease in void ratio (collapse). Matrix suction pressures thus decrease (as moisture content is increased) to a critical point where collapse settlement is triggered and the applied stress becomes the predominant influence on the effective stress state of the material.

ii. From the microscope analysis, it can be concluded that the change in the overall void ratio of the material through collapse settlement is a product of the complete collapse of some voids while others remain intact. In other words, even though the AVERAGE void ratio of the material decreases, settlement due to collapse is not caused by the collapse of all of the available voids in the material, but rather by the complete collapse of some voids while the rest remain unchanged. This implies that in order to achieve the full collapse potential of the material several collapse "events" might be necessary and that after consolidation in the odometer the material might still have a remnant potential to collapse.

iii. It is evident that the geological origin of the material plays a role in its collapse behaviour. The transported materials have higher dry densities and lower initial void ratios than the residual materials. However, after the materials have been subjected to the full range of stresses and moisture content changes it is obvious that the transported soils experience a similar or even greater decrease in void ratio than the residual material. This is likely due to the remnant structure in the residual materials contributing to the strength of the material and, to a lesser extent, the grain shape of the transported materials allowing for a closer packing of grains under an applied stress. This implies that a residual soil and transported soil with the same initial void ratio will not experience similar amounts of collapse and that the transported material will in all likelihood have a greater reduction in void ratio. The residual material will however still have a remnant collapse potential.

It should thus be emphasised that, when analysing the collapse behaviour and potential for collapse of a material, the geological origin of the material should be taken into account.

It is recommended that in future more research is dedicated to the behaviour of collapsible soils and the influence of matrix suction pressures on the collapse behaviour. A particularly interesting addition to the topic might be the relation of the material stiffness before and after additional moisture is added and how this relates to the amount of collapse that takes place.

7. REFERENCES

Barden, L., McGown, A. and Collins, K. (1973). *The Collapse Mechanism in Partly Saturated Soil*. Eng. Geol., Volume 7, pp. 49-60.

Booth, A.R. (1977). *Collapse Settlement in Compacted Soils*. CSIR Research Report 324, Council for Scientific and Industrial Research, Pretoria, South Africa.

Brink, A.B.A. (1979). Engineering Geology of Southern Africa, Volume 1, Building Publications, Pretoria.

Brink, A.B.A. (1983). Engineering Geology of Southern Africa, Volume 3, Building Publications, Pretoria.

Brink, A.B.A. (1985). Engineering Geology of Southern Africa, Volume 4, Building Publications, Pretoria.

Brink, A.B.A., Partridge, T.C. and Williams, A.A.B. (1982). Soil Survey for Engineering, Oxford University Press.

Brink, A.B.A. and Kantey, B.A. (1961). *Collapsible Grain Structure in Residual Granite Soils in South Africa*. Proceedings, 5th International Conference SM and FE, Paris, pp.611-614.

Bulut, R., Lytton, R. L., and Wray, W. K. (2001). *Suction Measurements by Filter Paper.* Expansive Clay Soils and Vegetative Influence on Shallow Foundations, ASCE Geotechnical Special Publication No. 115 (eds. C.Vipulanandan, M. B. Addison, and M. Hasen), ASCE,Reston, Virginia, pp. 243-261.

Burland, J.B. (1990). *30th Rankine Lecture - On The Compressibility And Shear-Strength Of Natural Clays*. Geotechnique, Vol40, pp.329-378, ISSN: 0016-8505

Cerato, A.B. and Lutenegger, A.J. (2002). *Determining the Intrinsic Compressibility of Fine-grained soils*. University of Oklahoma. Available from: faculty-staff.ou.edu/C/Amy.B.Cerato

Chandler, R.J. and Gutierrez, C.I. (1986). *The Filter Paper Method of Suction Measurement*. Geotechnique, Volume 36, No 2, pp.265-268.

Dudley, J.H. (1970). *Review of Collapsing Soils*. Journal of the Soil Mechanics and Foundation Division, ASCE, Volume 96, SM3, pp. 925-947.

[DM] Department of Mines (RSA) (1973). 1:50 000 *Rietvleidam 2528 CD* geological sheet. Printed and published by The Government Printer.

[DME] Department of Minerals and Energy (RSA) (1993). 1:250 000 *Ellisras 2326* geological sheet. Printed and published by The Government Printer.

[DME] Department of Minerals and Energy (RSA) (1986). 1:250 000 *Barberton 2530* geological sheet. Printed and published by The Government Printer.

[DME] Department of Minerals and Energy (RSA) (1985). 1:250 000 *Tzaneen 2330* geological sheet. Printed and published by The Government Printer.

Errera, L.A. (1977). *Stress Paths and Collapsing Soils*. MSc Thesis, Department of Civil Engineering, Cape Town.

Fredlund, D.G. and Gan, J. K-M. (1995). *The Collapse Mechanism of a Soil Subjected to One-Dimensional Loading and Wetting*. In: Derbyshire, E., Dijkstra, T. and Smalley, I.J. (eds.) (1995). Genesis and Properties of Collapsible Soils, NATO ASI Series, Kluwer Academic Publishers, pp. 173-205.

Fredlund, D. G. and Rahardjo, H. (1993). Soil Mechanics for Unsaturated Soils, NewYork: John Wiley & Sons, Inc.

Hamblin, A.P. (1981). *Filter-paper method for Routine Measurement of Field Water Potential*. J. Hydrol., 53: 355-360.

Handy, R.L. (1973). *Collapsible Loess in Iowa*, Soil Sci. Soc. Am. Proc., Volume 37, pp.281-284.

Jennings, J.E. and Knight, K. (1957). *The Additional Settlement of Foundations Due to Collapse of Structure of Sandy Subsoils on Wetting*. Proceedings of the Fourth International Conference on Soil Mechanics and Foundation Engineering, London, Volume 1, pp.316-319.

Jennings, J.E. and Knight, K. (1975). *A Guide to Construction On or With Materials Exhibiting Additional Settlement Due to Collapse of Grain Structure*, Proc. Sixth Regional Conference for Africa on Soil Mechanics and Foundation Engineering, Durban, South Africa, pp. 99-105.

Jennings, J.E. and Brink, A.B.A. (1978). *Application of Geotechnics to the Solution of Engineering Problems – Essential Preliminary Steps to Relate the Structure to the Soil Which Provides the Support*, Proceedings, ICE, Volume 64.

Knight, K. (1961). *The Collapse Structure of Sandy Subsoils Upon Wetting*. Phd Thesis, University of Witwatersrand.

Loubser, M and Verryn S. (2008). *Combining XRF and XRD analyses and sample preparation to solve mineralogical problems*. South African Journal of Geology, 111, 229 - 238.

LSM Analytical Services. (2011). Brochure: LSM Analytical Services – The Cost Effective Solution. http://www.lsmanalytical.com/index.htm Date of access: 10 April 2011.

Mohamed, T.A., Ali, F. H., Hashim, S. and Huat, B.B.K. (2006). *Relationship Between Shear Strength and Soil Water Characteristic Curve of an Unsaturated Granitc Residual Soil*. American Journal of Environmental Sciences, Science Publications, 2 (4): pp. 142-145

Robb, L.J., Brandl, G., Anhaeusser, C.R. and Poujol, M. (2006). Archaean Granitoid Intrusions. In: Johnson, M.R., Anhaeusser, C.R. and Thomas, R.J. (eds.). *The Geology of South Africa*. Geological Society of South Africa, Johannesburg / Council for Geoscience, Pretoria. pp. 57-93.

Rogers, C.D.F. (1995). *Types and Distribution of Collapsible Soils*. In: Derbyshire, E., Dijkstra, T. and Smalley, I.J. (eds.) (1995). Genesis and Properties of Collapsible Soils, NATO ASI Series, Kluwer Academic Publishers, pp. 173-205.

Rust, E., Heymann, G. and Jones, G. A. (2005). *Collapse potential of partly saturated sandy soils from the east coast of Southern Africa*. Journal of the South African Institution of Civil Engineering, Vol 47, no 1, pp. 8 - 14.

Schwartz, K. (1985). *Collapsible Soils: Problems of Soils in South Africa, state-of-the-art.* The Civil Engineer in South Africa, 27, pp. 379-393.

Schwartz, K. and Yates, J.R.C. (1980). *Engineering Properties of Aeolian Kalahari Sands*. Proceedings of the Seventh International Conference on Soil Mechanics and Foundation Engineering, Accra.

Sultan, H.A. (1969). *Collapsing Soils*, Proc. Seventh International Conference on Soil Mechanics and Foundation Engineering, Speciality Session No. 5, Mexico City.

Van Schalkwyk, A. And Vermaak, J.J.G. (1998). *The Relationship Between the Geotechnical and Hydrogeological Properties of Residual Soils and Rocks in the Vadose Zone*. Draft Final Report to the Water Research Comission, University of Pretoria.

Wagener, F von M. (1976). *Contribution to Forum on Engineering Problems Associated with Lavas in the Pretoria-Witwatersrand Complex.* Geotechnical Division, SAICE.

Walsh Sparks, A.D. (1963). *Discussion in Section A, Expansive and Collapsing Soils and Soil Moisture*, Proceedings 3rd Regional Conference for Africa SM and FE, Salisbury.

Weinert, H.H. (1980). The Natural Road Construction Materials of Southern Africa. H&R Academica, Cape Town, ISBN 0 86874 047 0, pp.231-238.

Weston, D.J. (1980). *Compaction for Collapsing Sand Roadbeds*, Proceedings 7th Regional Conference for Africa SM and FE, Accra.